THE UNIVERSITY OF CHICAGO

THE DISTRIBUTION OF *MYTILUS CALIFORNIANUS* IN THE STRAIT OF JUAN DE FUCA

A DISSERTATION SUBMITTED TO
THE FACULTY OF THE DIVISION OF THE BIOLOGICAL SCIENCES
AND THE PRITZKER SCHOOL OF MEDICINE
IN CANDIDACY FOR THE DEGREE OF
DOCTOR OF PHILOSOPHY

DEPARTMENT OF ECOLOGY AND EVOLUTION

BY
AARON S. KANDUR

CHICAGO, ILLINOIS
DECEMBER 2014

ProQuest LLC.
789 East Eisenhower Parkway
P.O. Box 1346
Ann Arbor, MI 48106 - 1346

To Margaret Elise Bishop

ACKNOWLEDGEMENTS

I would like to thank my advisors John T. Wootton and Catherine Pfister, as well as the other members of my committee Greg Dwyer, David Jablonski, Scott Lidgard, and Leigh Van Valen. Thanks to my parents Robert Kandur, Laurie Patrick, and Marylou Kandur, and thanks to Charles and Margaret Bishop. Thanks to my lab mates especially Sophie Mccoy, Will Tyburczy, Courtney Stepien, Mark Novak, Ole Shelton, and Erin Grey. Thanks to Thomas H. Suchanek and Robert Paine for access to data and Trevor Price for help with Chapter 1. Thanks to the Makah Tribe for access to their beautiful land.

TABLE OF CONTENTS

LIST OF FIGURES

LIST OF TABLES

CHAPTER 1
INTRODUCTION

The distribution of individuals across the landscape is a fundamental aspect of all species ecology. Intraspecific patterns of distribution along with demographics largely define the physical reality underlying the population concept. Patterns such as aggregation edges, changes in density (of individuals or aggregations), and large scale range limits sometimes have obvious or well recognized causes, but in many instances little is known about the specifics of distribution determination. Most empirical models correlate population density with one or a few environmental predictors, while theoreticians have developed complex models including competition, predation, gene flow, and metapopulation dynamics. Simple models based on diffusion or automata are capable of reproducing distributional patterns observed empirically. This and the patchy nature of some species distribution suggest they are partially contingently determined, in the sense that random abiotic processes can strongly constrain population size, for example biologically decoupled geologic processes can determine habitat area.

Human population growth and accelerating climate change is increasing the relevance of these theoretically significant topics. Ecosystems around the world are being destroyed, causing extinctions and declines in ecosystem function. Effective management and prediction of the implications of human actions will aid efforts to develop a balance between human beings and the ecosystems that sustain us. Accurate models capable of predicting the dynamics of changes in distribution as a function of changes in the environment are potentially powerful management tools.

I investigated the determinants of distributional patterns in the mussel *Mytilus californianus* in the Strait of Juan de Fuca in Washington State. A three pronged approach including evolutionary, geomorphological, and population ecology research methods elucidated processes determining the density and distribution of the species

as well as forces impacting its future trajectory. Primary conclusions include: 1. Changes in aerial temperatures in Washington State in the near future are unlikely to dramatically influence the abundance and distribution of *Mytilus californianus*. 2. The interaction of sea level rise with the geomorphological features of rocky coasts has the potential to dramatically change the distribution and abundance of shallow water depth restricted species like *Mytilus californianus*. 3. Distributional patterns of *Mytilus californianus* occurring at multiple spatial scales are a result of the integration of population vital rates as determined by environmental gradients, and variation in vital rates are sometimes scale dependent (growth and recruitment rates) and sometimes not (survival rates). 4. Mussel populations were most sensitive to variation in growth rates, least sensitive to variation in recruitment rates, and intermediately sensitive to variation in survival. 5. *Mytilus californianus* density is unlikely to be primarily controlled by variation in growth rate or recruitment rate.

CHAPTER 2
ADAPTATION AT A RANGE LIMIT IN THE MUSSEL *MYTILUS CALIFORNIANUS*: NO ROLE FOR GENE FLOW DISRUPTION OF LOCAL ADAPTATION

2.1 Introduction

Anthropogenic climate change is modifying environments at an accelerating rate, and ecologies around the world are being affected (IPCC 2007). Extinctions and range shifts due to changes in weather patterns have the potential to severely impact humans in a variety of ways including irreversible losses of biodiversity, range shifts of pathogens and pests, and shifts in the productivity of fisheries or agricultural regions (Martens et al. 1999; Walther et al. 2002; Parmesan and Yohe 2003; Parmesan 2006). These issues demand human development of strategies to both predict and ameliorate the negative consequences of climate change. A fundamental component of this goal is development of accurate theory concerning what dynamics determine range limits, why, and when they change (Beale, Lennon, and Gimona 2008). This goal is currently impeded by a conspicuous lack of consensus regarding whether or not evolutionary processes need to be included in causal accounts describing range limits (Pearson and Dawson 2003; Roy et al. 2009). Niche modelers (empiricists) often make predictions of range shift with measured parameters describing the fundamental niche and the predicted environmental state (bio-climatic envelope models), without reference to population structure, immigration/emigration dynamics, and trait demography (Huntley, Bartlein, and Prentice 1989; Huntley et al. 1995; Berry et al. 2002; Mbogga, Wang, and Hamann 2010). Theoreticians have shown accurate predictions may require inclusion of these more complex features of populations in order to be accurate (Mayr 1954; Haldane 1956; Gaines and Bertness 1992; Kirkpatrick and

Barton 1997; Case, Taper, et al. 2000; Goldberg and Lande 2006; Filin, Holt, and Barfield 2008).

Mayr (1954) and Haldane (1956) proposed the hypothesis that range limits could be enforced by reduction of peripheral population growth rate caused by maladaptation due to the swamping of selection in the range periphery. Maladaptation was hypothesized to be caused by excessive gene flow from central populations existing in environments selecting for alternative phenotypes. The distinguishing feature of this hypothesis is that the constraint causing maladaptation in such a peripheral population includes population structure and its interaction with environmental gradients, rather than simply environmental gradients and a static set of conditions in which the species is viable. Such gene flow disruption of local adaptation (hereafter GFDLA) has been a popular topic recently, and has spawned numerous models showing the mathematical plausibility of such dynamics.

There are multiple examples of GFDLA maintaining maladapted phenotypes at small spatial scales in patchy environments, but we are aware of no certain examples of GFDLA enforcing a range limit (Camin and Ehrlich 1958; Blondel et al. 1992; Dias and Blondel 1996). Sanford et al. (2006) gave a suggestive example in which a northern fiddler crab range limit may be set by local maladaptation due to gene flow, but they provide no evidence showing that the optimal phenotype is obtainable by the focal species in the absence of such gene flow. The lack of examples at larger scales could result from inadequate sampling due to the increased difficulty of empirically interrogating population dynamics at larger scales, or because at larger spatial scales the phenomena becomes less common. The models do provide novel and plausible explanations for some population dynamic phenomena (rapid range contractions and expansions) but their empirical voracity is entirely unknown (Kirkpatrick and Barton 1997).

Recently the importance of including the added complexity of GFDLA dynamics in models of range limits has been questioned. Price and Kirkpatrick (2009) developed a model of range limits disregarding GFDLA in favor of a simpler competition based framework. Barton (2001) showed that gene flow could in principle facilitate local adaptation via delivery of genetic variance which was lacking, a possibility that has

been supported by the empirical example provided by Bridle, Gavaz, and Kennington (2009) in rain forest *Drosophila*. The present example was chosen initially because it appeared to be an ideal situation to find and empirically document the GFDLA phenomena at a range limit scale. The population under study is small, situated at a range limit, and receives substantial immigration from nearby large populations in a different environment. Despite this situation it is as locally adapted as large populations throughout the species range. Its failure to exhibit maladaptation highlights the possibility that GFDLA models may rarely be applicable to the determination of range limits, despite the empirical support they enjoy at smaller scales. Support for this conclusion is proportional to the degree of correspondence between the given example and a theoretically ideal situation for the GFDLA mechanism. If the example corresponds well to the theoretical ideal and few species appear more likely to exhibit GFDLA, the probability of GFDLA's ubiquity and association with range limits is reduced.

2.1.1 Study System

Mytilus californianus is an intertidal mussel with a nearly one-dimensional (coastal) range extending from Isla Socorro to the Aleutian islands (Coan, Scott, and Bernard 2000). In the central part of the range it is a competitively dominant space holder in the mid to low intertidal (Paine 1974; Dayton 1971). In the northern portion of its range, it is limited by predation in the low intertidal, and by thermal stress and exposure time in the upper intertidal (Dayton 1971; Paine 1974; Suchanek 1981). In California Robles, Sweetnam, and Eminike (1990) showed lobster predation to play a role in density regulation across the mussel bed. Reproduction is via broadcast spawning with a relatively long planktotrophic phase greater than 7 days (Strathmann 1987). Addison et al. (2008) found no measurable population structure from southern Alaska to Baja, but recent work by Logan, Kost, and Somero (2012) shows phenotypic variation across this region, which could be the result of developmental plasticity or undiscovered genetic variance. It is possible that future surveys utilizing larger numbers of loci and more intensive sampling will find population structure as has

happened in ecologically similar species such as *Balanus glandula* (Sotka et al. 2004). Even if population structure is present, it appears likely that the species is panmictic over relatively large spatial scales if not its entire range. Though mean dispersal distance is not known for *Mytilus californianus* an estimate exists for the ecologically similar species *Balanus glandula* of 60 km, both species are planktotrophic, have similar durations of planktonic development, and frequently exist in association with one another (Sotka et al. 2004). The magnitude of this estimate makes the assumption of panmixis at the scale of at least 100's of kilometers a conservative one. The natural history of the species is also well characterized and it is a good experimental species in that it tolerates transplant well, is readily marked, and is easy to locate at any point in its range if present. Most importantly, it exists in a situation that appears to make GFDLA at a range limit likely.

The main range of *Mytilus californianus* is along the Pacific coast of N. America, but it also extends into the Strait of Juan de Fuca between Vancouver Island and Washington State (Coan, Scott, and Bernard 2000; Morris, Abbott, and Haderlie 1980; Harley and Helmuth 2003). The Strait is an approximately 20 kilometer wide body of water extending 150 kilometers inland from the outer coast. Population density on the Washington side of the Strait is comparable to that of the outer coast: for the first 80 kilometers inland, high density mussel beds exist with comparable biomass to outer coast beds (A. Kandur, unpublished data). Observatory Point is the last major population on the Washington coast, but near the eastern edge of the Strait a final tiny high-density population exists at Port Townsend (48 8' 38.37 N, 122 46' 38.67 W). This population consists of two large boulders, each less than 20 m^2, capped with mussels. Thus the population is orders of magnitude smaller than those on the western end of the Strait and the outer coast. Based on the comparative sizes of the populations, the strong currents through the Straits that can move larvae quickly, and the long planktotrophic phase of mussel larvae (at least 7 days), it is unlikely that local reproduction at Port Townsend sustains the population. At the eastern terminus of the strait suitable substrate (rock benches) exists especially on the South West coast of Fidalgo Island, but *Mytilus californianus* is almost completely absent represented by rare lone individuals often spaced meters apart.

The thermal environment in the intertidal zone along the Strait varies strongly, with increasing mean and maximum temperatures as one moves from the outer coast inland, with an especially marked increase in temperatures 60 kilometers west of Port Townsend at Observatory point (figure 2.1) arising from a combination of decreasing wave intensity, decreasing fog, and the timing of low tides (Harley and Helmuth 2003). The result is that mussels in Port Townsend exist in a substantially hotter environment then the populations they are likely derived from, those at or west of Observatory Point. A similar increase in mean temperatures is achieved by traveling on the outer coast at least as far south as Boiler Bay Oregon a distance of 400 kilometers (figure 2.2). In the southern portion of the range viable populations exist in substantially warmer conditions than the Port Townsend site or Oregon.

Taken together the situation of the Port Townsend *Mytilus californianus* population seems like a likely candidate to exhibit gene flow disruption of local adaptation. It is a small population receiving immigrants from larger populations in substantially different thermal conditions, an environmental variable known to be important to this species (Roberts, Hofmann, and Somero 1997; Helmuth and Hofmann 2001). If other populations exist in thermally similar circumstances as Port Townsend and they are locally optimized for this thermal regime, then according to the hypothesis that gene flow can restrict local adaptation it is expected that Port Townsend mussels will be measurably maladapted to their environment. Such maladaptation could also account for the low observed population density found on the west coast of Fidalgo Island the eastern range limit of the species in the Strait of Juan de Fuca.

2.1.2 Empirical Strategy

In order to test the hypothesis that Port Townsend mussels are maladapted relative to other populations it is necessary to show a relationship between thermal environment and a phenotypic state such as thermal tolerance, and that Port Townsend mussels depart from this relationship by being less thermally tolerant than predicted. Given this information a complimentary field common garden experiment reciprocally transplanting individuals between Port Townsend and the near cold adapted popu-

lations elucidates which adaptive mechanisms (phenotypic plasticity or genetically based variance) account for the observed adaptation or lack thereof.

2.2 Methods

2.2.1 Mussel Thermal Response

Mussels were collected from the mid intertidal at wave-exposed locations at seven sites along the West Coast of North America: Punta Morro Mexico (ca. 31° 51' 41.16"N, 116° 40' 4.11"W), Santa Barbara (ca. 34° 24' 21.33"N, 119° 52' 40.31"W, CA), Hopkins Marine Station (ca. 36° 37' 19.96"N, 121° 54' 14.46"W, CA), Bodega Bay (ca. 38° 19' 3.85"N, 123° 4' 26.61"W, CA), Boiler Bay (ca. 44° 49' 48.44"N, 124° 3' 40.64"W, OR), Tatoosh Island (ca. 48° 23' 30.89"N, 124° 44' 27.07"W, WA), and Port Townsend (ca. 48° 8' 38.65"N, 122° 46' 38.41"W) (Fig 2.2). Following 6 months of common garden conditions, 10 mussels from each site were removed from mesh bags and placed in small plastic crates (21x7x4.5 cm). At this time, thermocouples were inserted into the valves of four additional mussels that would later be connected to a temperature controller unit to control the rate of heating. Mussels remained in the crates in ambient seawater tanks for approximately two hours before the experiment. Meanwhile, two large Styrofoam boxes (30x35x85cm) were prepared for heat ramp experiments in air. These were set-up inside a cold room (4°C) to allow better control of the temperature ramp rate. The Styrofoam boxes were equipped with an Omega rubber heating mat (Model SRMU020230, 120 Volts, 1.25 Amps, 2X30in.) and a controller unit (Omega Autotune Temperature Controller CSC32). Mussels from three sites were placed in one box, and mussels from the other four sites were placed in another. Several preliminary runs were performed to ensure that the ramp rate was identical between boxes. Lids were placed on the boxes and the heat ramp began with mussel temperatures starting at 12-13°C. Mussels were ramped at a rate of 8°C h^{-1} to 36°C, held for one hour at 36°C and then quickly returned to flow-through seawater tanks at ambient temperature (12-13°C). After the experiment, mussel mortality was assessed daily by squeezing the valves together and looking for

movement or closure. Mussels were marked as alive if they closed easily, moribund if they were slightly gaping but would not close, or dead if they were gaping > 1cm.

In order to calculate a response variable based on the assay for correlation with collection site temperatures, time series of the number of surviving mussels were used to calculate mean per day rates of population decline for each sample. For each day of the study the logarithm was taken of the ratio of number living on day t divided by the number living on day t-1, the mean of these values provides an estimate of rt, the exponential rate of population decline. This rate reflects differences in the tolerance for high temperature events among the different groups of mussels, and is referred to hereafter as the thermal tolerance phenotype.

2.2.2 Measurement of Thermal Environment

Data describing the mussel-specific thermal environment at each collection site were obtained from http://climate.biol.sc.edu/data.html, an online data base of Robo Mussel time series from around the world. Robo mussels are bio-mimetic temperature loggers that approximate the internal thermal state of middle sized mussels (Helmuth 2002). There are a multitude of temperature statistics which could be expected to covary with the thermal tolerance phenotype, those that emphasize the upper range of experienced temperatures are particularly appropriate since the assay exposed mussels to temperatures near the maximum mussel temperature experienced across the West Coast. Three different temperature statistics which have high support are shown: 1. Mean daily maximum temperature for the hottest two months at each site. 2. Mean daily maximum temperature during the summer (May to August). 3. The mean of temperatures greater than seawater temperature during the summer (figure 2.3). For statistic three, seawater temperature was approximated by smoothing of the Robo mussel temperature time series with the R (Version 2.12.0) function LOWESS, with a smoother span of f=0.01. Other statistics show positive relationships between thermal tolerance and increasing aspects of temperature, the presentation of multiple statistics is intended to show that the relationship is robust and not due to an arbitrary and misleading choice of statistic. Statistics were not calculated on a full year basis

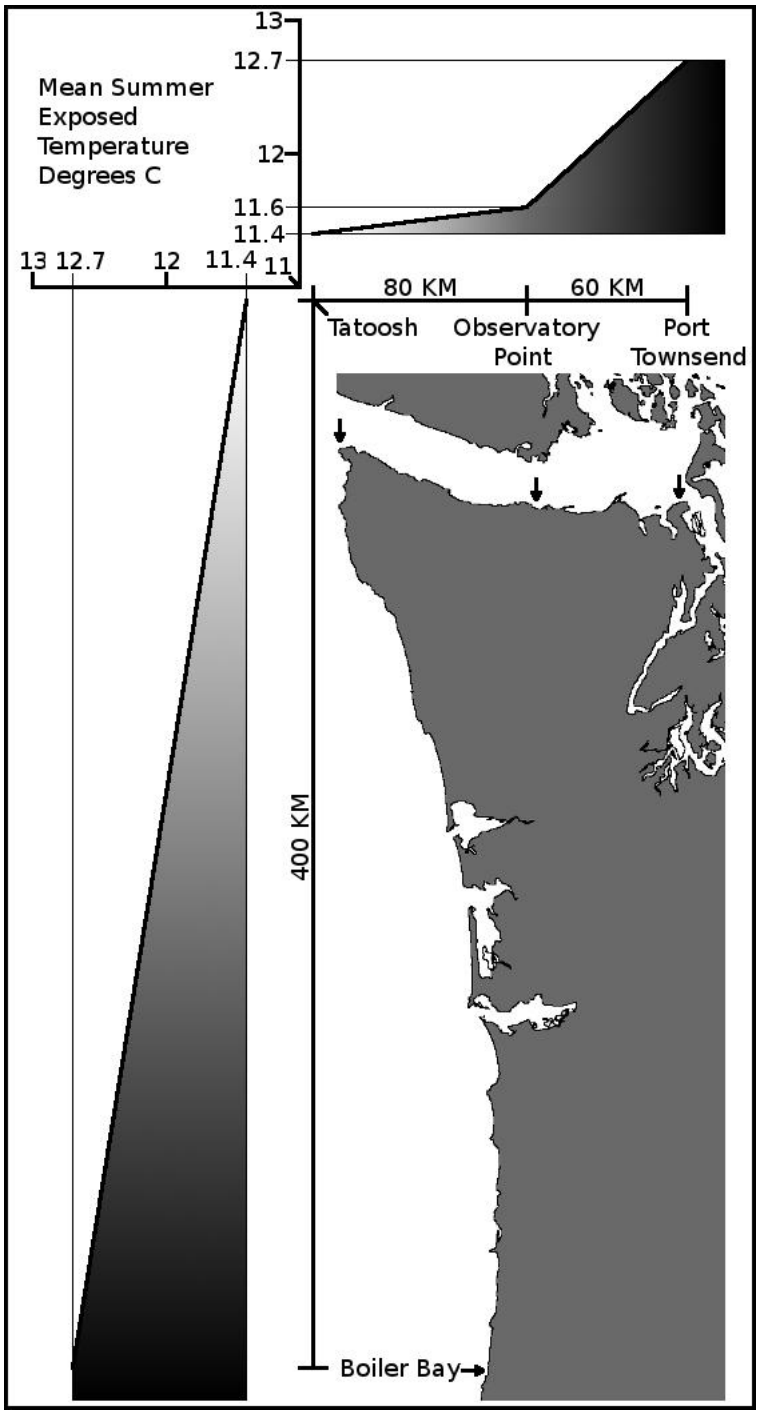

Figure 2.1: The steep gradient in mean summer time exposed temperatures C across the Strait of Juan de Fuca relative to the shallower outer coast gradient.

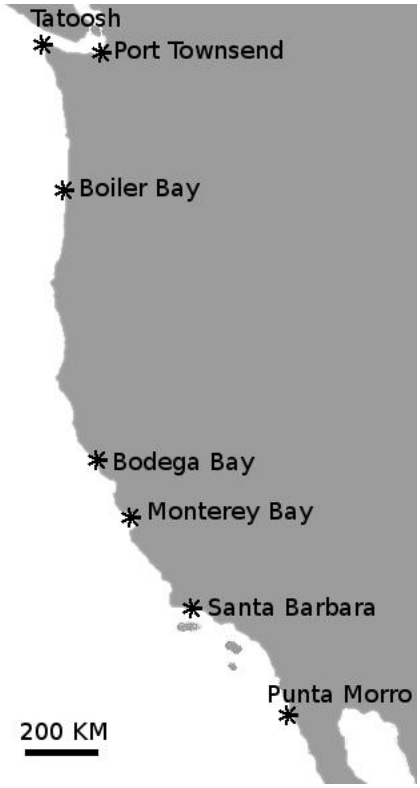

Figure 2.2: Map of collection sites used for the measurement of the thermal tolerance phenotype.

because robo-mussel data was only available from Port Townsend and Boiler Bay mid level wave exposed mussels from late May to the end of August. For statistic 1 the hottest two months were calculated as the months in which the greatest number of temperature records above 20° C occurred. The incomplete Robo-mussel temperature record at Boiler Bay was compensated for by utilizing a contiguous greater than year long time series of mid level Robo-Mussel data for a site at Boiler Bay with intermediate wave exposure. At Port Townsend the hottest two months were calculated with reference to a contiguous year long HOBO (Onset Computer Corp.) temperature logger data set. HOBO's as non bio-mimetic sensors do not perfectly approximate mussel temperatures but they do show elevated temperatures when Robo's do, and correlations between paired Robo mussels and HOBO's show highly significant linear relationships for multiple temperature statistics including means, variance, and summed degree's (see appendix 7.1).

2.2.3 Common Garden Experiments

At Port Townsend and Tatoosh, common gardens were set up at the upper and lower margins of the mussel bed. A completely reciprocal design was used: each site received transplants from the other three sites and a local reciprocal transplant. Juvenile non-reproductive mussels were used to reduce the probability that developmental plasticity could have already acted to adapt individuals and to avoid effects of gamete release that might confound measures of growth. Sixteen to 18 individuals were used in each of the 16 treatments. Length and width measurements were taken at the time of initial collection and individuals were placed in individual cells of clear plastic tackle boxes with quarter inch plastic mesh lids, which were bolted to the rock at each location. HOBO (Onset Computer Corp.) temperature loggers were placed at each site and Robo Mussels were placed at three of the four sites, as no more were available at the time of experiment initiation. Tide heights were measured at Tatoosh with a laser level referenced to landmarks of known height. At Port Townsend, tide heights were measured on a calm day at a specific time and calculated with reference to the NOAA maintained tide gauge there. The experiment was initiated in late June 2010

and ended in late August 2010, when all individuals were removed from the study sites, assessed to be alive or dead, and measured for final length and width. In the following description of the experiment the term target will be used to refer to the site where mussels in a treatment were transplanted, and origin used to denote where the mussels in a treatment came from. In this notation there are 4 reciprocal transplants treatments where target and origin are the same (home mussels) and 12 treatments where target and origin differ (away mussels).

Lengths of mussels were converted to estimated biomass via a regression obtained from Suchanek (1979). This was done because reproductive output is known to vary directly with biomass in broadcast spawners such as mussels (Suchanek 1979). The mean initial size of individuals collected across all treatments was not equal (ANOVA $p < 0.05$) and analysis at the end of the experiment pooling all individuals showed a significant trend of increasing absolute growth in biomass with decreasing initial weight (linear model $p < 0.05$). To account for this relationship and to permit calculation of the growth of a typical mussel, in each treatment, the following method was used. Individual absolute growth of surviving mussels was regressed against initial estimated biomass, a linear model was fit and an AIC value calculated for the linear model and the simpler model of constant (mean) rate of growth across all individuals in the treatment. The model with the lower AIC value was chosen and used to calculate the expected growth rate in that treatment of a mean sized mussel for the entire experiment (see appendix 7.2).

A generalized linear model was fit to test for a significant relationship between survival and initial size. The model was non-significant ($p = 0.22$) so no size correction was used to calculate survival probabilities in the different treatments. Instead survival was calculated as the percentage of individuals surviving at the end of the experiment. An estimate of expected individual fitness in each treatment was calculated as the product of treatment survival probability and estimated treatment-specific growth. This product gives the expectation of surviving biomass at the end of the experimental period per treatment, a reasonable proxy for potential reproductive output in a broadcast spawning bivalve (Suchanek 1979; Nakaoka 1995).

Analysis of treatment-specific fitness was analyzed with both an ANOVA and a

linear model in R using the functions lm() and aov(). ANOVA was used to test for local adaptation to site and height, the linear model was then used to explore the environmental factors underlying the determination of fitness. Categorical variables for the ANOVA included Target Height, Target Place, Origin Height, Origin Place, and all two way interactions. Interactions between origins and targets would indicate local adaptation. Stepwise model reduction via comparison of AIC values was used to arrive at the minimal model. In the linear model several explanatory variables were expected to influence fitness, previous work has identified the importance of temperature and submergence time to this species, making their inclusion obvious (Roberts, Hofmann, and Somero 1997; Somero 2002; Harley and Helmuth 2003). The goal of the common garden experiment was to investigate the mechanism of adaptation and the degree to which local phenotypic optimization occurred. To do this, testing for the influence of origin submergence time and temperature as well as target submergence time and temperature is necessary, with the expectation that local adaptation would cause significant interactions between origin and target conditions. It was unclear which temperature metric best represents the action of temperature on mussel fitness, so mean temperature, summed degrees, and max temperature were all explored. A final explanatory variable, summed unexpected exposure time, was calculated as the time a mussel is exposed when it would have been submerged at its origin place. This variable accounts for the fact that mussels may develop rhythms of when to feed and when to stay closed to avoid dessication, and the fact that they may not be able to modify this pattern instantly when transplanted (Rao 1954).

The temperature variables were calculated with temperature time series from Robo Mussels at three of the sites. At the fourth site, predicted Robo Mussel values for the statistics mentioned above were obtained by using a HOBO (Onset Computer Corp.) temp logger and a regression between 5 co-located HOBO and Robo Mussel temperature loggers, arrayed across the intertidal at Tatoosh and Port Townsend. Adjusted R^2 for these regressions are high (all > 0.95) and the values for the missing site fall within the range of the five known points (see Appendix 7.1). Temperature variables and submergence times were normalized via subtraction of the mean and division by a standard deviation.

Submergence times were calculated with the measured tide heights of the sites using NOAA measured tidal dynamics at Port Townsend. Currently there is no tidal observation station at Tatoosh and the nearest one at Neah Bay is too far to be used without correction so the program XTide (http://www.flaterco.com/xtide/) was used to predict tidal dynamics at Tatoosh. Predictions are slightly less accurate than directly-measured levels because variation in wind direction and velocity as well as atmospheric pressure impact tides, but comparisons between predictions and measurements at sites such as Port Townsend show that predicted values are highly accurate, at least when weather is not extreme.

2.3 Results

Mussel tolerance to heat stress in the lab was associated with increasing environmental heat stress in the six sites along the Pacific coastal gradient (i.e., not including Port Townsend). Linear regressions between the three temperature statistics and the thermal tolerance phenotype (exponential rate of population decline post heat stress) are significant or nearly so with p-values of 0.02, 0.06, and 0.1 respectively (table 2.1). AIC comparison of the linear models to a three parameter asymptotic function chose the more complex model in all three cases (tables 2.1 and 2.2). The Port Townsend site, located on a much steeper temperature gradient, did not depart from the relationships found for the other locations and, if anything, appears to be better adapted than expected given its origin thermal environment, as indicated by its point appearing above the linear regressions and the asymptotic functional forms (figure 2.3). Therefore there is evidence of mussel adaptation to thermal regime, but a maladaptation hypothesis for range limit enforcement is not supported.

The common garden experiment was first analyzed with an ANOVA to test for local adaptation, the ANOVA included the categorical variables of Origin Place, Origin Height, Target Place, Target Height, and all two way interactions. Local adaptation would be expected to cause interactions between Origin Height and Target Height as well as Origin Place and Target Place. Stepwise AIC comparisons were used to reduce the model and the minimal model supports a local adaptation hypothesis (table 2.3).

Table 2.1: Estimated parameter values for linear regressions of the form: Thermal Tolerance Phenotype $\sim a * Temp\ Statistic + b$.

AIC	Model	Estimate	Std. Error	t-value	Pr(> |t|)
-14.75	Intercept	-0.397	0.093	-4.258	0.013*
	Mean Hottest 2 Months Mean Daily Max °C	0.013	0.003	3.749	0.02*
-10.31	Intercept	-0.390	0.158	-2.462	0.0695
	Mean Summer Exposed Temperature °C	0.021	0.010	2.145	0.0985
-11.79	Intercept	-0.380	0.125	-3.041	0.0384*
	Mean Summer Daily Max °C	0.014	0.005	2.65	0.057

Table 2.2: Estimated parameter values for non-linear regressions of the form: Thermal Tolerance Phenotype $\sim a - b * e^{-c * Temp\ Statistic}$.

AIC	Temp Statistic	Parameter	Estimate	Std. Error	t-value	Pr(> |t|)
-35.68	Summer Mean Daily Max °C	a	-0.006	0.005	-1.159	0.330
		b	-62.71	44.39	-1.413	0.253
		c	-1.026	0.129	7.981	0.0041**
-35.65	Mean Summer Exposed °C	a	-0.007	0.005	1.486	0.234
		b	34970000	80790000	-0.433	0.694
		c	0.473	0.123	3.838	0.312
-31.81	Mean Summer Daily Max °C	a	-0.005	0.007	-.652	0.561
		b	-135.4	156.2	-.866	0.450
		c	0.859	0.185	-4.644	0.0188*

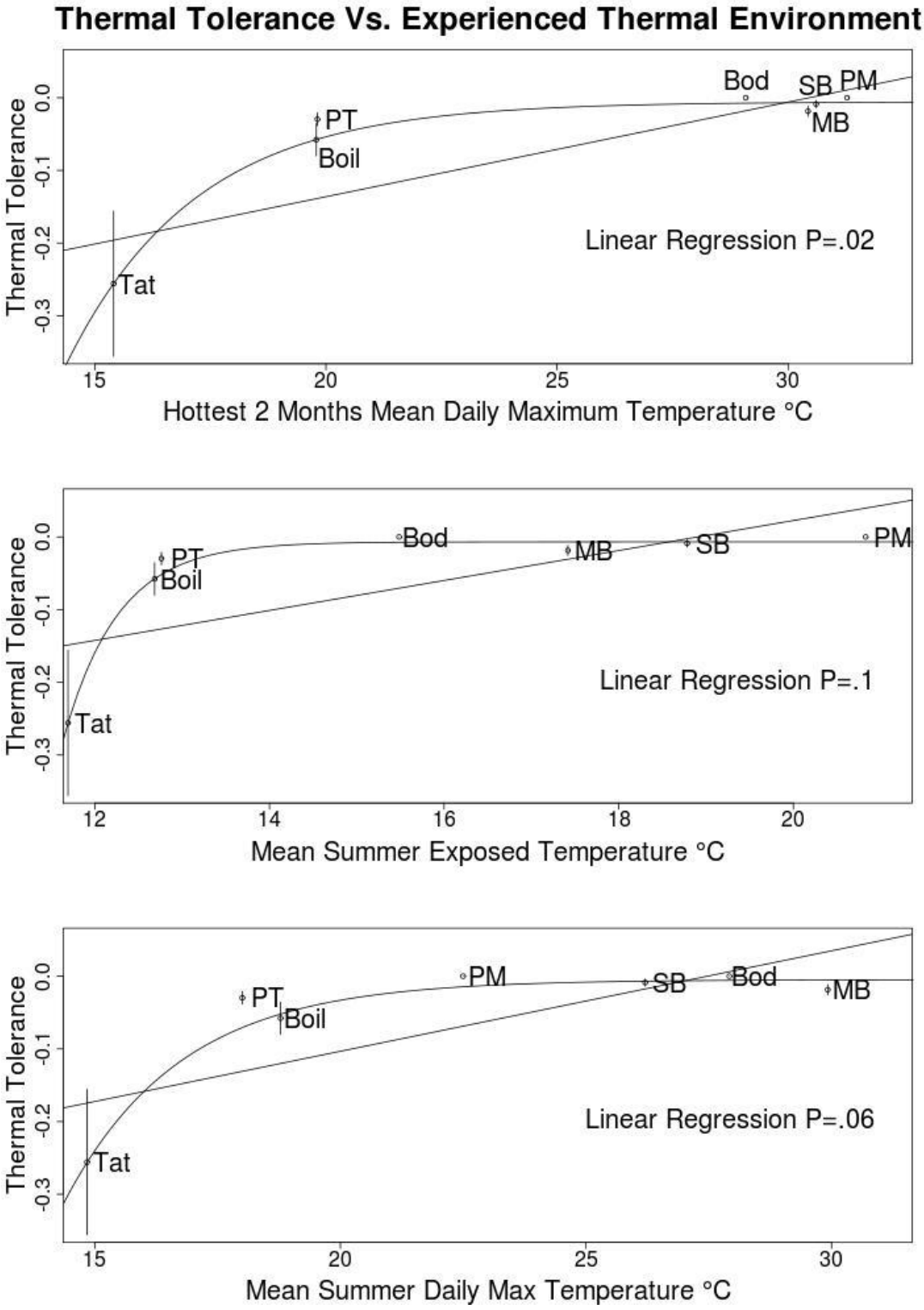

Figure 2.3: Regressions between the thermal tolerance phenotype and three temperature statistics.

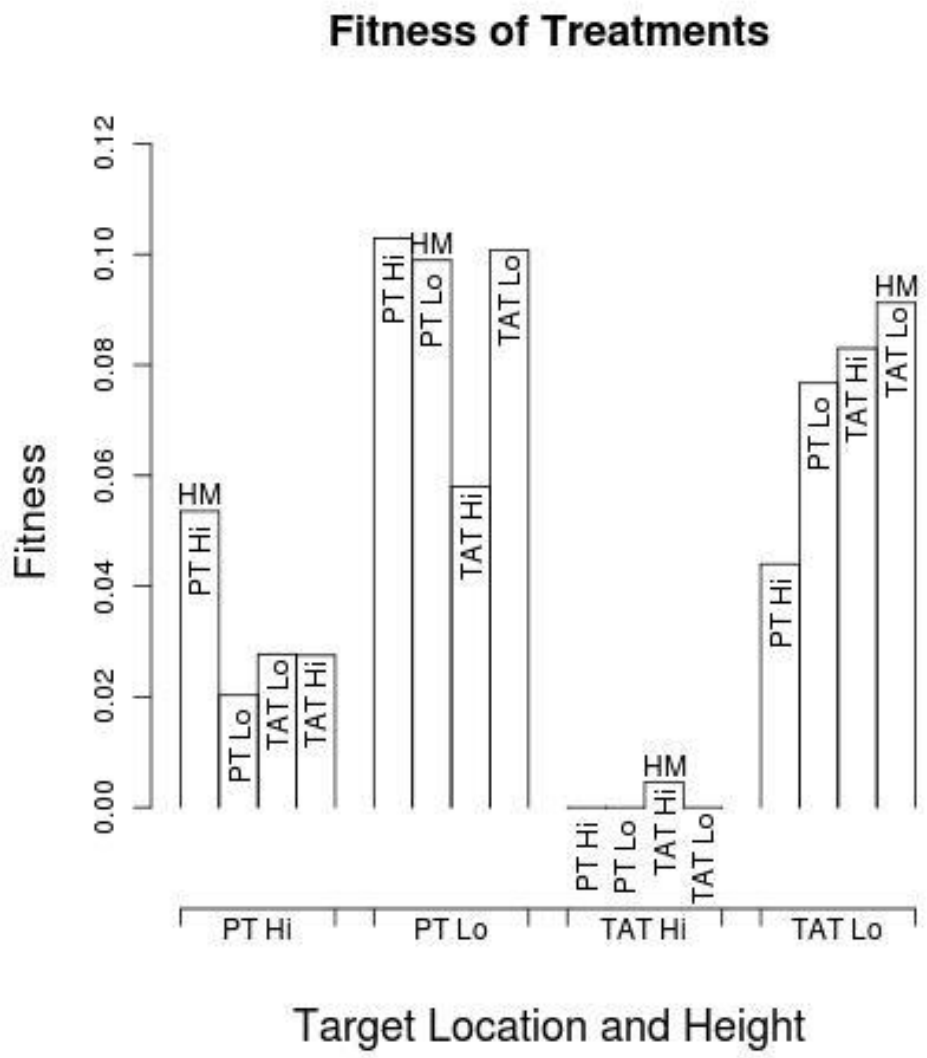

Figure 2.4: The fitness of all treatments, vertically written labels indicate the origin location and height of the treatment, the x-axis label indicates the target location of the treatment. HM labels indicate the home (reciprocally transplanted) treatment in each group.

Table 2.3: Tables summarizing the local adaptation ANOVA. The marginally significant underlined interaction affects indicate local adaptation.(residual standard error=0.0135).

Description	DF	Sum Sq	Mean Sq	F Value	Pr(>F)
Origin Place	1	<0.0001	<0.0001	0.0047	0.9471
Origin Place	1	0.00011	0.00011	0.6088	0.4577
Origin Place	1	0.0022	0.0022	12.41	0.0078**
Origin Place	1	0.0170	0.0170	93.48	<0.0001***
Origin Place x Target	1	0.0009	0.0009	4.9196	0.0573
Origin Height x Target Height	1	0.0009	0.0009	4.7197	0.06159
Target Place x Target Height	1	0.0002	0.0002	1.19	0.3067
Residuals	8	0.0015	0.0001		

Table 2.4: Tables summarizing the local adaptation linear model. The marginally significant underlined interaction affects indicate local adaptation.(adjusted R^2=0.85). SD refers to "summed degrees". "Tar" refers to target (the location of transplant), "Origin" refers to initial location.

Coefficient	Estimate	Std. Error	t-value	Pr(> |t|)
(intercept)	0.04983	0.00367	13.57900	>.0001***
Tar SD	-0.0293	0.00367	-5.46	0.00014***
Origin SD	-0.0013	0.0037	-0.352	0.732
Tar % Time Submerged	0.0273	0.00383	7.123	>.0001***
Tar SD x Origin SD	0.00906	0.00391	2.3190	0.04283*
Tar SD x Tar % Time Submerged	0.0158	0.00773	2.053	0.06714

Local adaptation would also be indicated if Home mussels (those that were reciprocally transplanted) outperform the transplanted Away mussels within each treatment. In three of the four treatments Home mussels outperformed the other three transplanted sets in the treatment, in the one instance in which Home mussels do not beat all of the locally transplanted mussels it outperforms one clearly, and is marginally worse than the two treatments it loses to (figure 2.4).

In order to ascertain which factors underlay the differential success suggesting local adaptation a linear model with multiple continuous environmental variables was fit. The minimal linear model for the common garden experiment shows that the most important determinant of fitness is the percentage time submerged and summed de-

grees of a treatments target location, indicating that environmental affects dominate the determination of fitness in this case (table 2.4). However the significant interaction between origin summed degrees and target summed degrees provides evidence for adaptation to the thermal regime in which individuals were derived. The interaction shows that it is worse than expected to be transplanted to a hotter environment than you came from, based on the environmental effect alone. A significant interaction between target summed degrees and target percentage time submerged, shows that it is particularly bad to be both at a hot site and exposed to air. The categorical variables of origin place, target place and home or away did not improve model fit indicating that the continuous environmental variables accounted for the observed between-site differences.

In order to test the assumption that developmental plasticity did not have time to act in the young individuals utilized in the experiment, the linear model analysis was repeated after the data was split into two groups. In one group, the largest half of individuals were taken from each treatment, and the other group consisted of the smaller half of all individuals from each treatment. If developmental plasticity was active in the size range of the individuals in the experiment it would be expected that the group comprised of older larger individuals would be better adapted. This could be due to either the cumulative impact of developmental plasticity or selection acting through this life stage. Either of these mechanisms would be manifested by stronger target-by-origin interaction effects (indicating local adaptation) in the larger older group. The smaller sample size in each group reduced the significance of the models but the minimal models for each sub group are similar to that of the complete data set (Appendix 7.1 and 7.2). Most importantly there is no evidence that larger older individuals show increased origin by target interaction effects as compared to the smaller younger group indicating that the mechanism of local adaptation was active at an age less than that of the experimental individuals and was not continuing to act at the time of manipulation. This result indicates that either developmental plasticity had acted and ceased by the time of experiment or that selection or self segregation occurred between the time of settlement and before experiment initiation.

2.4 Discussion

Theory suggests that maladaptation of marginal populations can limit the range of species where steep environmental gradients exist relative to dispersal distance, but there has been little empirical testing of this hypothesis (Mayr 1954; Haldane 1956; Holt and Gaines 1992; Kirkpatrick and Barton 1997; Case, Taper, et al. 2000; Goldberg and Lande 2006; Filin, Holt, and Barfield 2008). The natural history and population distribution of *Mytilus californianus* corresponds to a theoretically ideal situation for the operation and testing of this mechanism. The focal population is small and largely sustained by immigration from a differently adapted population, increasing the probability of swamping of local selection. The environmental gradient (temperature) is of known importance to the niche of the organism, is almost an order of magnitude steeper than that of the large coastal populations (figure 2.1), and populations across the range show phenotypic variation associated with the gradient (figure 2.3). Finally large southern populations exist in conditions hotter than the focal population, and are phenotypically more heat tolerant than Port Townsend's environment would select for, proving the capability to adapt should it have been found that Port Townsend mussels were maladapted. Despite the correspondence to ideal conditions for GFDLA (relatively large quantity of gene flow into populations on a steep environmental gradient), the results show no evidence for maladaptation and therefore no evidence for control of the range limit.

The common garden experiment and size split analysis instead support the interpretation that maladaptation is prevented by the existence of sufficient local genetic variance in the focal trait of thermal tolerance to allow for phenotypic optimization in a marginal population. This conclusion is supported by the recent work of Denny et al. (2011) showing the large range of small scale temperature variation and thermal tolerance in this species. The failure of the proposed mechanism means that population structure mediated constraints on adaptation probably play a minor role in setting range limits in this species, and supports the conclusion of Denny et al. (2011) that the species is relatively well buffered from the affects of increasing temperatures in the northern portion of its range.

The intellectual support for the hypothesis that gene flow dynamics often contribute to the enforcement of range limits has been solely theoretical thus far (Kirkpatrick and Barton 1997; Case, Taper, et al. 2000; Goldberg and Lande 2006; Filin, Holt, and Barfield 2008). At small scales, theory and empirical examples agree that the mechanism often plays a role in determining population density. As a first test of the theory at large scales, the *M. californianus* system calls into question the long-held theoretical intuition that gene flow dynamics often set range limits. The study system was chosen because of its relative likelihood of exhibiting the predicted behavior but failed to find any support for it. The generality of this result remains to be determined, and will require identifying other situations where species ranges correspond to environmental gradients of variable steepness.

Finding situations where the theory holds may be challenging for several reasons. First many species do not disperse over long distances and therefore do not receive gene flow from populations sufficiently distant to exist in selectively different environments. Species that reproduce locally are less likely to be affected by GFDLA because small scale population structure allowing local optimization is achievable. Geographic existence in association with appropriately steep gradients may be rare. Species possessing significant developmental plasticity or who often participate in assortative mating, increase the availability of phenotypic variance, enlarging our expectations for their adaptability reducing the probability of GFDLA.

It is possible that this system is unique and that further investigation in other taxa will show the hypothesis to be more widespread than it appears based on this example. In particular two features of the described population might reduce the affects of maladaptation in this situation. The Port Townsend population has a uniquely large size structure compared to the Western Strait populations, probably because of a relatively reduced amount of wave-induced disturbance at Port Townsend. The large size of individuals reduces the variance requirements for effective local adaptation because fewer genetically suitable (thermally tolerant) juveniles need to be delivered to achieve comparable quantities of biomass at Port Townsend. Another possibility is that even though the outer coast populations can be shown to be cold adapted they may harbor an uncommonly large quantity of phenotypic variance in the relevant

trait as compared to other taxa in other environmental contexts.

The conspicuous lack of empirical examples at range limit scales despite the long existence of the hypotheses, rigorous theoretical treatments of them, interest in these dynamics, and the described example hints that perhaps the GFDLA phenomena is not common at large scales. Further empirical investigation in other species is needed to ascertain the generality of this conclusion. The practical implication of this interpretation is that models of range limits and range shift in species similarly or apparently less likely to exhibit the hypothesized mechanism than *Mytilus californianus* need not include evolutionary dynamics. Specifically taxa that reproduce locally or that do not exist on steep gradients are probably not affected by gene flow mediated maladaptation.

Summarizing: 1.) The studied population exists in an ideal state to exhibit gene flow disruption of local adaptation. 2.) The species natural history and distribution is particularly predisposed to GFDLA. 3.) Many species and populations are less likely than this one to exhibit GFDLA. 4.) This species and population does not exhibit GFDLA. Which leads us to conclude: A.) For this species predictions of future range limit change need not include gene flow disruption of local adaptation. B.) The theoretical impetus for increasing the complexity of models of range limits to GFDLA needs further empirical (any) support if it is to be broadly accepted and integrated into models used to predict range shift. C.) There are many species which can a priori be ruled out from requiring consideration of this mechanism for accurate prediction of range shifts.

The disconnect between workers who consider GFDLA dynamics causal to the determination of range limits and those that do not must be resolved if ecology is to move forward, and become capable of making reasonable recommendations for how best to live with and through the biotic changes induced by climate change. In order to achieve this goal a first step will be to find empirical examples in which GFDLA sets or contributes to range limits if they exist. The key difficulty in providing such an example is to find maladaptation at the edge of one portion of a species range which cannot be explained by an intrinsic inability to adapt. This can be proven if in another part of the range where similar environmental conditions predominate in

the absence of the swamping affect, the apparently optimal phenotype is achieved. If examples can be found and it becomes obvious that for some populations inclusion of GFDLA dynamics is necessary a next step is the development of heuristics capable of quickly determining which populations are most likely to require this added level of complexity for accurate treatment. An essential question to be answered is: What is the minimum amount of population level data and natural history information required to a priori include or exclude GFDLA dynamics from a predictive model of how a range limit will be affected by environmental change? Once a sample of populations have been tested for GFDLA dynamics it will become possible to generalize about which specific conditions are necessary for the functioning of the mechanism, improving our capacity to predict, prepare, and ameliorate the biotic consequences of climate change. The increasing tractability of these questions is hopeful and should lead to further empirical investigation which will resolve the tacit debate concerning whether evolutionary dynamics need to be included in models of range limits, this will be aided by careful choice of model systems (especially those with one dimensional ranges), the increasing availability of relevant remotely sensed data, and collaboration among research groups.

CHAPTER 3
SEA LEVEL RISE, SHORE MORPHOLOGY, AND THE DISTRIBUTION OF *MYTILUS CALIFORNIANUS*

3.1 Introduction

Sea level is predicted to rise between 0.5 and 1.90 meters by 2100 (Nicholls and Cazenave 2010; Schaeffer et al. 2012; Vermeer and Rahmstorf 2009). Along rocky coasts where erosion of the rocky substrate is slow, this rise might dramatically change the surface area between high and low tide as a result of submergence or emergence of shore platforms which develop over long periods. Such changes in habitat area could cause shifts in productivity and community composition along rocky coasts which account for 33-80% of world coastlines (Emery and Kuhn 1982; Jackson and McIlvenny 2011; Johnson 1988; Vaselli et al. 2008).

The population distribution of intertidal species is known to be affected by many different factors, but the effect of shore morphology is poorly understood. Patterns of zonation in many intertidal species are driven by physiological tolerances at upper limits and species interactions such as predation and competition at lower limits (Connell 1961; Paine 1966; Paine 1976; Somero 2002). Space is often a primary limiting resource for the crowded and species rich shoreline in temperate rocky habitats (Dayton, 1971; Paine, 1976). The angle of the shore relative to the plane of the sea surface between critical upper and lower tide heights determines the surface area of benthic habitat, imposing an upper ceiling on the potential population size of species limited by space within a restricted tidal zone (see Fig 3.1).

Shallowly sloping shore platforms or intertidal terraces are common features of rocky coasts around the world, which often account for a great deal of intertidal habitat area (Dasgupta 2010; Trenhaile 1980). The development and altitudinal distribution of shore platforms is complexly determined, incompletely understood, and

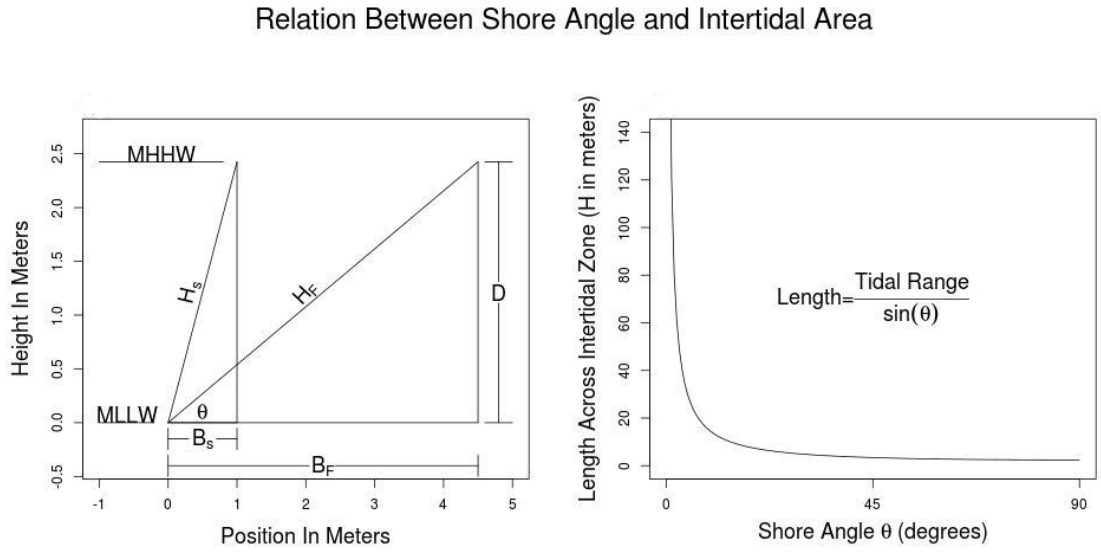

Figure 3.1: The geometry of shore angle is shown, the segment H represents the distance across the intertidal zone along the profile of the rock (subscripts refer to steep (S) or flat (F) profiles). The hyperbolic relation between and H is shown, when is small the distance across the intertidal is large when it is near 90 the distance across the intertidal is equal to the tidal range.

thought to be the result of the combined interaction of erosion due to wave action, historical sea levels, local tidal dynamics, local bathymetry, rates of geodetic change, and erosion from weathering of rock caused by repeated wetting, drying, and/or freeze-thaw cycles (Dasgupta 2010; Stephenson 2000; Trenhaile 1980; Trenhaile 2001). The interaction of sea-level rise with shore platforms may drive rapid changes in habitat area for intertidal species because of the slow rates of platform development which span at least thousands of years (Stephenson et al. 2010).

Generalization of how sea-level rise will affect rocky intertidal zones around the world in terms of total area may be difficult, but recent investigations predict reduced intertidal habitat area as a result of sea level rise along rocky coasts, in estuaries, and within deltas (Day et al. 1995; Fish et al. 2005; Fujii and Raffaelli 2008; Galbraith et al. 2002; Jackson and McIlvenny 2011; Vaselli et al. 2008). At local scales, increases in sea level will be variable relative to the global mean because of small scale variation in rates of geodetic change, of proximity to ice sheets and their changing gravitational pull as they lose mass, and of changes in ocean circulation, winds, and

barometric pressure. On rocky shores the change in habitat area will depend on the variable distribution of shore angles with increasing altitude (Jackson and McIlvenny 2011; Vaselli et al. 2008). Similar effects will also arise in soft-sediment habitats. For example in some estuaries, sea level rise will inundate formerly intertidal sand or mud flats as water depth out-paces accretion rates or because man-made structures such as sea walls block mud or sand flat expansion to higher regions. Such changes will modify benthic communities and may reduce foraging opportunities for dependent species such as shore birds (Fujii and Raffaelli 2008; Galbraith et al. 2002). Oceanic populations have been affected by similar processes. For example Pyenson and Lindberg (2011) hypothesize that changes in the availability of continental shelf habitat driven by sea level variation caused dramatic changes in biomass of the grey whale *Eschrichtius robustus* during the past 500,000 years.

There are many potential ecological impacts of changes to the distribution of shore angles, but the most important is the potential for dramatic increases or decreases in habitat area which will drive rapid changes in population sizes. The competitive hierarchy of intertidal species is modified on vertical substrates because of the inability of detached mussels to settle, and bird predators to feed on vertical walls (Wootton 1993). Predation by species requiring subtidal or low intertidal refuges may also be impacted via shifts in mean feeding rate due to changes in travel time from refuge regions to higher intertidal areas where prey are abundant. Variation in the angle of insolation caused by variation in shore shape could impact both primary producers and thermally sensitive species (Harley and Helmuth 2003; Wethey 1983). Recruitment dynamics could be modified by reduction in the ease of settlement on steep substrates or by larval preferences for specific attributes of settlement areas directly or indirectly related to shore angle.

To evaluate how sea-level rise will impact shoreline communities in the context of variable shore morphology, I developed a methodology to quantify how sea-level rise will change the abundance of *Mytilus californianus*. The method uses survey data to specify how abundance and biomass vary with shore angle and tide height and then uses these relationships to project biomass onto 3D representations of shore platforms generated with aerial and satellite imagery. The method is general and

could be applied to other similar species, or scaled up to construct accurate range wide predictions of the effect of sea-level rise. The local and regional results obtained suggest that sea-level rise will dramatically change the abundance and distribution of *Mytilus californianus* within the next century. Ecologically similar and associated species are predicted to be similarly affected.

3.2 3D Mapping Methods

I generated topographic maps of two intertidal terraces on the coastal shores of Washington State. Strawberry Point on Tatoosh Island (48.3918 N, 124.7351 W) and Tongue Point (48.1669 N, 123.7072 W) located 80 kilometers inland from Tatoosh on the southern shore of the Strait of Juan de Fuca. I used the maps in concert with relationships linking tidal height and submergence time to biomass per unit area to predict how population density will change in these locations with increases in sea-level of the order predicted during the next century (see Figs. 3.2 and 3.3).

3.2.1 Tidal Height and Submergence Time

Tidal height, expressed as height above mean lower low water (MLLW), is often used as an explanatory variable in intertidal experiments (Denny and Gaines 2007). The primary functional significance of tidal height is its direct relationship to the proportion of time an organism spends submerged in water or exposed to air (Dehnel 1956; Harley and Helmuth 2003). For these reasons actual submergence times are calculated from tidal height, tested as explanatory variables, and utilized in models describing how sea level rise will impact mussel biomass, to maximize the specificity of predictions and geographic generality. Submergence time was defined as the proportion of time a location is submerged by the tide for an integer number of years.

I measured tidal heights of sample sites, mussel bed limits, and mussel bed thickness with a laser level referenced to landmarks of known tide height relative to MLLW. Submergence time, the proportion of time a given tidal height is under water was calculated from January 2008 to December 2010 across the tidal range at the two primary study sites Strawberry Point on Tatoosh Island and Tongue Point as well as at two

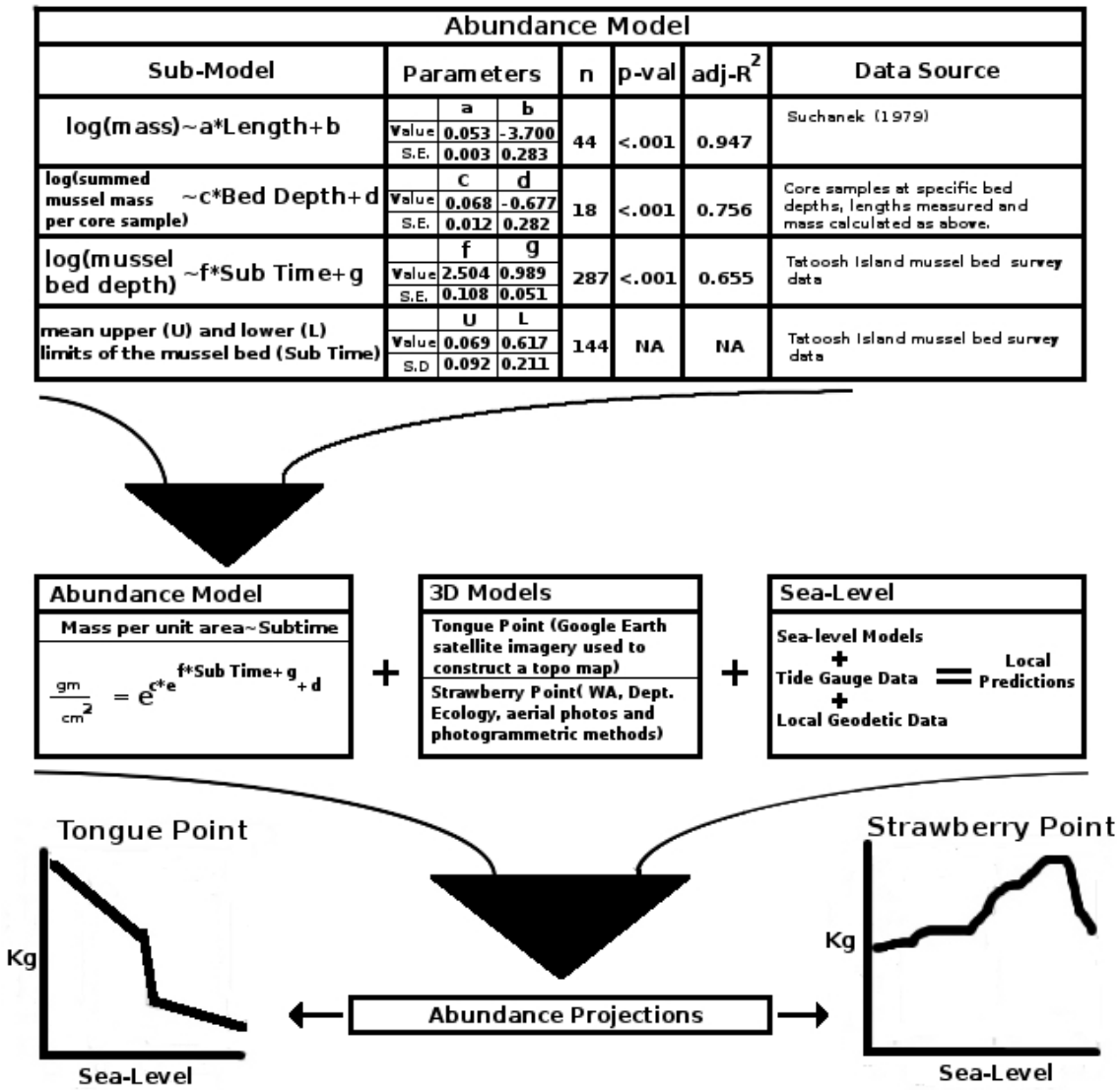

Figure 3.2: A flow Chart showing the process used to arrive at abundance projections.

Figure 3.3: Locations of the two case studies are shown (Strawberry Point on Tatoosh Island, and Tongue Point) along with locations of sites used to compare variation in submergence time at identical tide heights(Port Townsend and Deception Pass).

other sites Port Townsend, WA (48.1172° N, 122.7592° W) and Deception Pass, WA (48.4072° N, 122.6447° W). I calculated submergence times for the latter two sites to probe variation in submergence time at identical tidal heights. Minute scale tidal height predictions for this period for all sites were obtained from a web-based tide calculator (http://tbone.biol.sc.edu/tide/). To confirm that submergence times were stable with regard to the temporal window chosen (2008-2010) I checked whether observations over shorter intervals gave the same proportional submergence times.

3.2.2 Development of 3D Maps of Terraces

I used two methods to develop accurate 3D maps of the terraces treated in the case studies. For Strawberry Point photogrammetry was utilized. Photogrammetry uses multiple photographs of an object to calculate a representation of its three dimensional shape. Identical locations are tagged in multiple images offset a few degrees from one another, enabling the triangulation of camera positions using geometry and linear algebra. For Tongue Point images taken from Google Earth, the Washington State Department of Ecology's Coastal Atlas, and amateur photographs available on Flikr showing the point during multiple phases of tide were used to develop a topographic map. Photogrammetric methods could not be used at Tongue point because available photographs were insufficiently detailed and offset from one another.

3.2.3 3D Topographic Map of Tongue Point

Satellite derived images of Tongue Point showing the terrace at multiple phases of tide were taken from Google Earth. Because the specific time of image capture is not available for Google Earth images tide heights were approximated using time stamped images from the Washington State Department of Ecology and amateur photographs available on Flikr. For each Google Earth image a time stamped image was found showing a similar state of emergence. Then the tide height at the time of image capture was found using a web based tide calculator (http://tbone.biol.sc.edu/tide/). The water line which defines a contour of known height shown in each Google Earth image was then traced using Image J, and the contours subsequently graphed together

in R (Ver. 2.14.1) to create a topographic map of the terrace (see figure 3.4).

I divided the terrace into a series of 37 transects each 7.8 meters wide running perpendicular to its long axis, and calculated tidal heights along each transect by interpolating between intersecting contour lines. If contiguous transect points intersected the same contour line, the segment was assumed flat. The tidal heights along each transect were calculated for 10 centimeter long sections, submergence time for each section was then calculated based on tidal predictions for 2008-2010.

3.2.4 3D Map of Strawberry Point

The-open source photogrammetric program insight3d (http://insight3d.sourceforge.net/) was used to develop the 3D map of Strawberry Point. Images used for the reconstruction were downloaded from the Washington State Department of Ecology's Coastal Atlas: https://fortress.wa.gov/ecy/coastalatlas/Default.aspx.

I used three aerial images of Strawberry Point to develop the maps utilized in the sea level rise calculations. Once camera positions had been calibrated, points tracing key topographic features of the terraces were matched and triangulated producing a 3D point cloud. Tagged points were then manually connected into a set of triangles defining the surface of the terrace. A data file encoding the 3D coordinates of each triangular surface was then imported into R (Ver. 2.14.1) for further manipulation.

The XYZ coordinate system developed by Insight 3D is arbitrarily scaled and oriented, necessitating its transformation to provide distances in terms of an appropriate distance unit (m) and to orient the Z axis so that it is normal to the surface of the water. This was accomplished using custom scripts in R (Ver.2.14.1) and is explained in appendix 7.4.

Discretization of 3D Surface

Once the coordinates in the datafile defining the triangular surfaces that approximate the surface of Strawberry Point were appropriately transformed and scaled, each triangle was broken into a discrete number of 225 cm^2 square fragments of known tide height and submergence time in R (Ver. 2.14.1) 3.6. The procedure used to

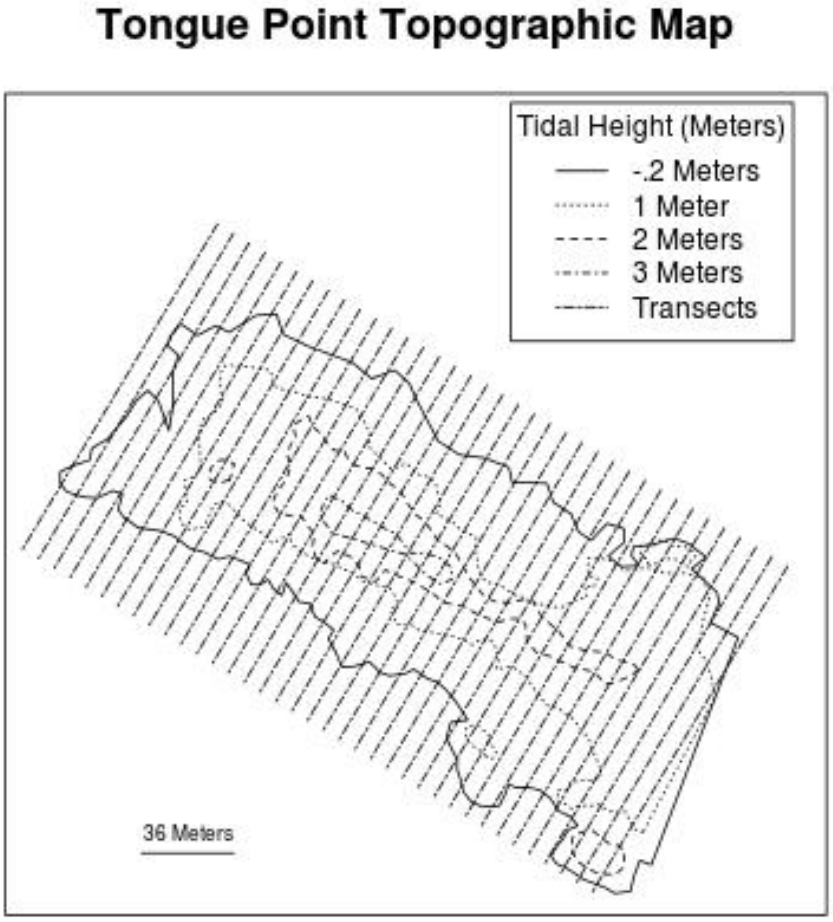

Figure 3.4: The topographic map of Tongue Point. The map was created using multiple images of the point available on Google Earth at different phases of tide.

Figure 3.5: Strawberry Point is the terrace shown in the foreground. The dark fringe meeting the water line on the end of the point is the mussel bed, the lighter band above it is composed of lighter colored (unwetted) higher intertidal mussels, the lightest and highest band is composed of barnacles. Above the barnacles is bare space. (Photo credit Robert Paine)

accomplish this is described in appendix 7.5.

3.2.5 Size Structure Samples, Mussel Bed Thickness, and Vertical Limits of the Mussel Bed

Size structure samples were collected along with bed thickness values from 18 locations on Tatoosh Island. Size structure samples were collected by hand removal of all mussels within a 15x15 cm quadrat placed on the mussel bed. To quantify the relationship between mussel bed thickness and submergence time a survey of mussel bed thicknesses at specific tidal heights (enabling submergence time calculation) was completed during the summer of 2010. A total of 285 points across mussel beds around Tatoosh Island were measured with a laser level referenced to landmarks of known tidal height. Bed thicknesses were measured by hammering a steel spike perpendicularly into the mussel bed and recording the length of penetration. Upper and lower limits of the of the mussel bed were measured at 144 locations around the island with a laser level and landmarks of known height above MLLW to quantify the mean and variance of bed limits. Locations were chosen to provide a diversity of exposures and shore morphologies.

3.2.6 Mussel Mass and Shell Length

Suchanek (1981) quantified the relationships among total mussel mass, reproductive mass, and shell length via direct measurement of 44 mussels length, total weight, and dissected reproductive mass. Image J was used with a scanned image of figure 1 from Suchanek (1981) to obtain data points. Linear regressions among the log of total mussel mass, the log of mussel reproductive mass, and shell length were then performed in R (Ver. 2.14.1) using the function lm().

3.2.7 Calculation of Mussel Mass As a Function of Sea Level

Once the 3D reconstructions of Tongue Point and Strawberry Point were decomposed into uniform sized sections (7800 cm^2 at Tongue Point, 225 cm^2 for Strawberry Point)

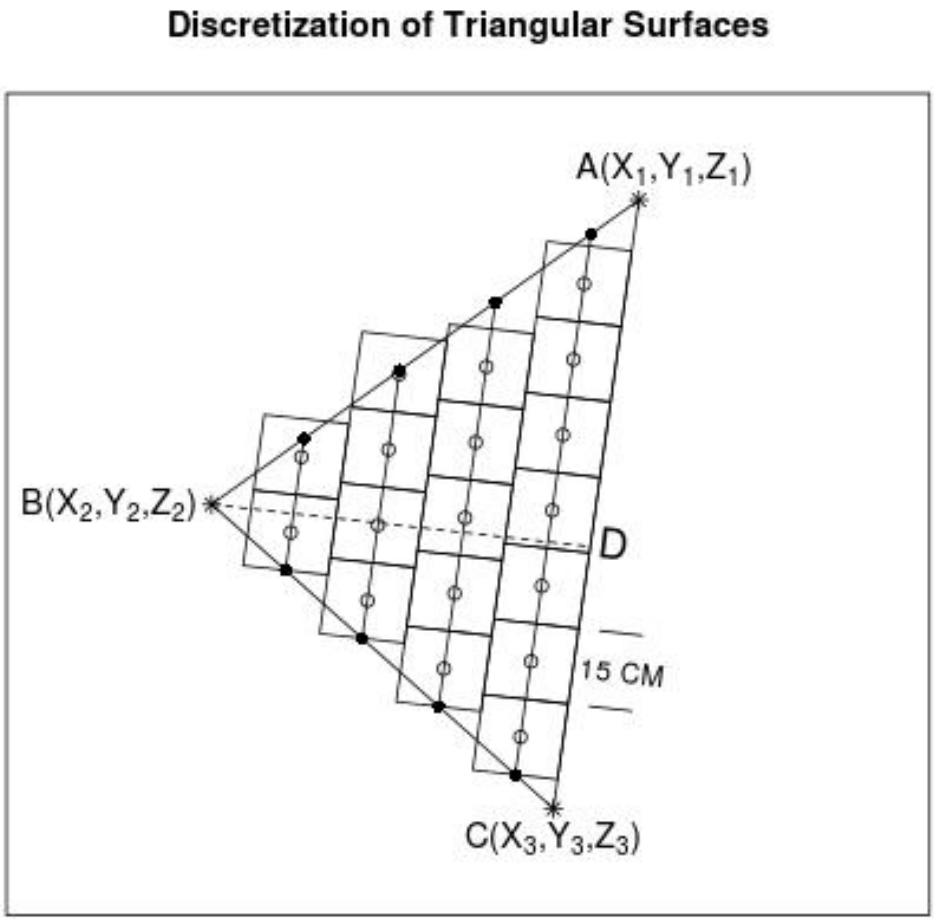

Figure 3.6: The discretization method for triangles composing the 3D surface approximating Strawberry Point. The tidal height and submergence time for the center point for each square was calculated, submergence time was then used to calculate mussel bed thickness, which was used to calculate mussel mass per square centimeter, this number was then multiplied by the area of a square (225 $cm^2$3D

of known tide height, submergence times were calculated using tidal predictions from 2008-2010 for each location using an on line tide predictor (http://tbone.biol.sc.edu/tide/). Mussel total mass and reproductive mass were calculated for each section based on regressions predicting mass as a function of submergence time. An estimate of total mass was calculated by summing all sections and the procedure was then repeated iteratively after tidal heights of all sections in each location were decreased by 1 cm increments to give predictions of mass change across the range of predicted sea levels.

3.2.8 Sea Level Rise Predictions

Globally, sea level is predicted to rise by 18-59 cm by 2100, based on the conservative IPCC (2007) report. Subsequently development of semi-empirical models and more refined projections of the contribution due to melting of the West Antarctic and Greenland ice sheets have increased projections (Brysse et al. 2013; Nicholls et al. 2011; Schaeffer et al. 2012). For 8 scenarios of global greenhouse gas emissions, median predictions for each model ranged from 59 cm to 102 cm by 2100, with minimum and maximum 90% confidence intervals for all models ranging from 40 to 139 cm by 2100 (Schaeffer et al. 2012). The most pessimistic scenario analyzed was based on the Copenhagen Accord and Cancun agreements, which have been criticized as being insufficiently ambitious in terms of emissions reductions to plausibly achieve the stated goal of preventing a global mean temperature increase of more than 2°C (Rogelj et al., 2010). The IPCC (2007) report projects global surface temperatures to exceed 4°C by the end of the century. Nicholls et al. (2011) collected sea level rise predictions based on this projection and found a model median range of 74-160 cm by 2100 for 7 models with minimum and maximum projections of 50-190 cm by 2100.

Although global sea-level rise is a critical aspect in determining relative shore exposure, accurate local predictions also require accounting for changes in relative sea level arising from geological processes such as uplift, subduction, and isostatic rebound. I accounted for these using NOAA calculated water level trends derived from tide gauges near Tatoosh Island (Neah Bay, Wa; station id: 9443090) and Tongue Point (Port Angeles, Wa; station id: 9444090) and geodetic trends quantified

by the Pacific Northwest Geodetic Array station located in Neah Bay, Washington (station id: MKAH).

The nearest actively maintained tide gauge to Tatoosh Island, at Neah Bay approximately 10 kilometers east of the island, indicates a long-term rate of relative sea level change of -1.63±0.36 mm/yr for the period from 1934-2006. This drop in sea level is driven by the long term trend of geodetic uplift in the region, a result of subduction of the Juan de Fuca plate under the North American Plate, changes in the gravitational pull of melting ice sheets, and post-glacial rebound (NRC 2012; Peterson et al. 2012). The rate of geodetic rise for the area has been estimated at 3 mm/yr since 1996, approximately equal to the recent satellite based estimate of global sea-level rise of 3.3±0.4 mm/yr calculated for the period 1993-2009 (NRC 2012; Nicholls and Cazenave 2010). The recent trend of increasing rates of sea level rise matches the prediction of increasing rates through the next century. Even highly conservative scenarios assuming zero emissions by 2016 predict rates of sea level rise by 2100 of 5 mm/yr, and more likely scenarios predict rates between 9 and 18 mm/yr by 2100 (Schaeffer et al. 2012). If geodetic rates remain constant at approximately 3 mm/yr displacement due to this component will be +27 centimeters by 2100, subtraction of this quantity from the range of predicted sea level rise by 2100 (50-190 cm, from Nicholls et al. 2011) yields a relative sea level increase for Tatoosh between 23 and 163 cm by 2100.

The nearest tide gauge to Tongue Point is approximately 20 km east in Port Angeles. The estimated trend in sea-level change from data at Port Angeles is 0.19 1.399 mm/yr for 1975 to 2006. The difference in the local rate of sea level rise from Neah Bay to Port Angeles is likely due to the lower rate of uplift at Port Angeles. Mazzotti, Jones, and Thomson (2008) predicted a relative sea level rise for Port Angeles of 12 cm by 2100 but based their prediction on the highly conservative estimates given in the IPCC (2007) report. Relative sea level rise at Tongue Point and Port Angeles is likely to be greater than for Neah Bay but also less than the global mean prediction. Assuming that the absolute sea level change equals that of Neah Bay (1.35 mm/yr) and that decreased geodetic rise at Port Angeles causes the variation in measured sea level between the locations, geodetic rise at Port Angeles

can be calculated as the absolute rate (1.35 mm/yr) less the relative rate measured in Port Angeles (0.19 mm/yr), giving an estimated geodetic rise in Port Angeles of 1.16 mm/yr. Assuming this rate stays constant until 2100, Port Angeles area will be expected to rise by 10.3 cm. Reducing the global mean prediction for sea level rise by 10.3 cm gives a range for local relative sea level rise at Tongue Point of 39.7-179.7 cm by 2100.

3.3 Results

3.3.1 Submergence Time and Tidal Height

The relation between tidal height and submergence time is non-linear, and variable at a spatial scale of tens of kilometers because of variability in local bathymetry. For example at an identical tidal height of 2 meters at Tongue Point and Port Townsend there is a nearly four-fold difference in the amount of time submerged. Annual intervals or aggregated multi-year periods yield almost identical submergence times when calculating submergence times for each tide height (see fig. 3.7).

3.3.2 Mussel Mass and Submergence Time

To quantify how mussel biomass per unit area depends on submergence time I used three regressions. First I estimated the mass of each mussel in the core samples using equation 3.1 in figure 3.2 and then calculated the log summed mussel mass per core sample. Next I correlated the estimated log summed mass per core sample with mussel bed depth. Finally, I related mussel bed depth with submergence time (see equations 3.2 and 3.3 in figure 3.2 and figures 3.9 and 3.8). By combining these regressions, I estimated the relation between mass per unit area and submergence time (equation 3.4 in figure 3.2).

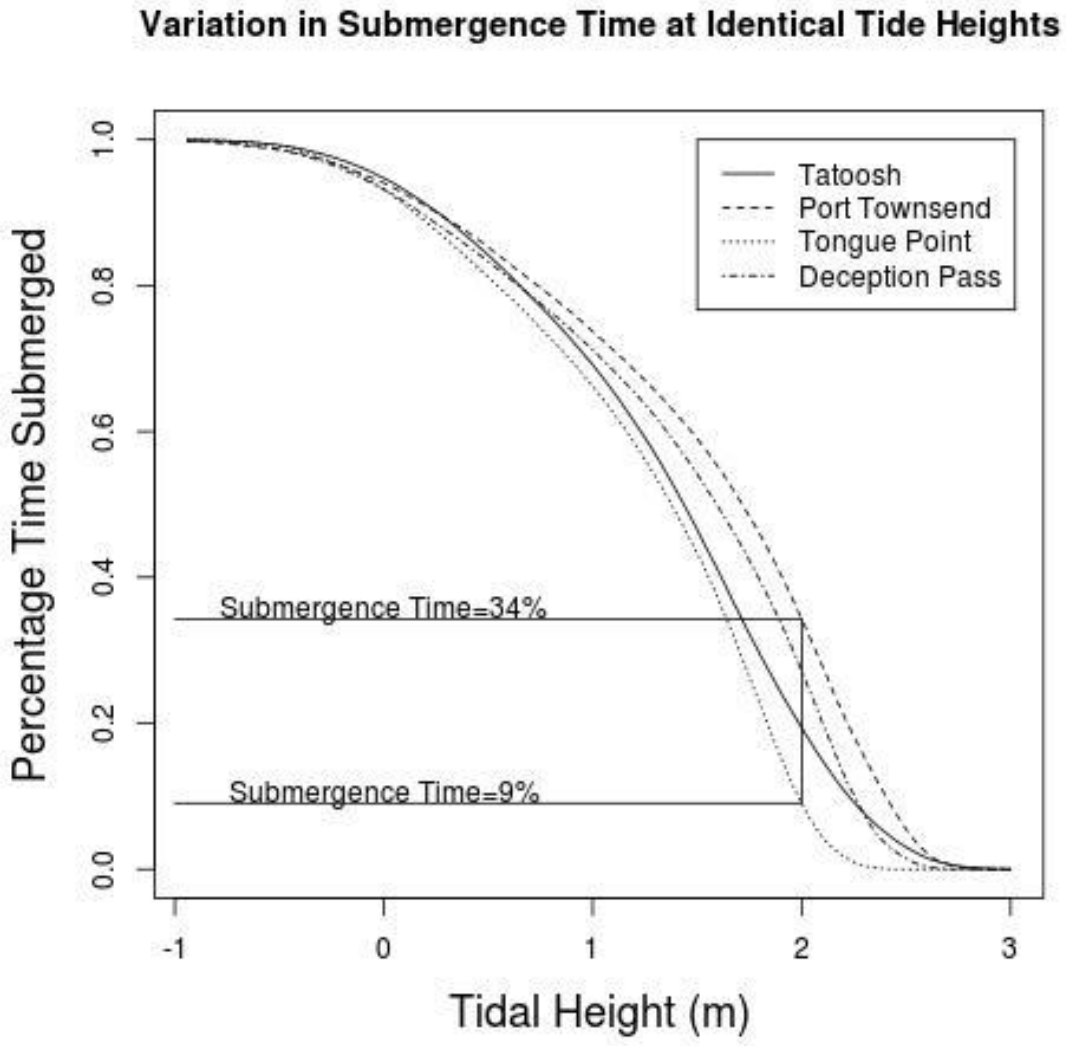

Figure 3.7: Variation in percentage time submerged at identical tide heights is shown for Tatoosh Island, Tongue Point, Port Townsend and, Deception Pass. Port Townsend and Tongue Point vary 4-fold in submergence time at a tide height of 2 meters.

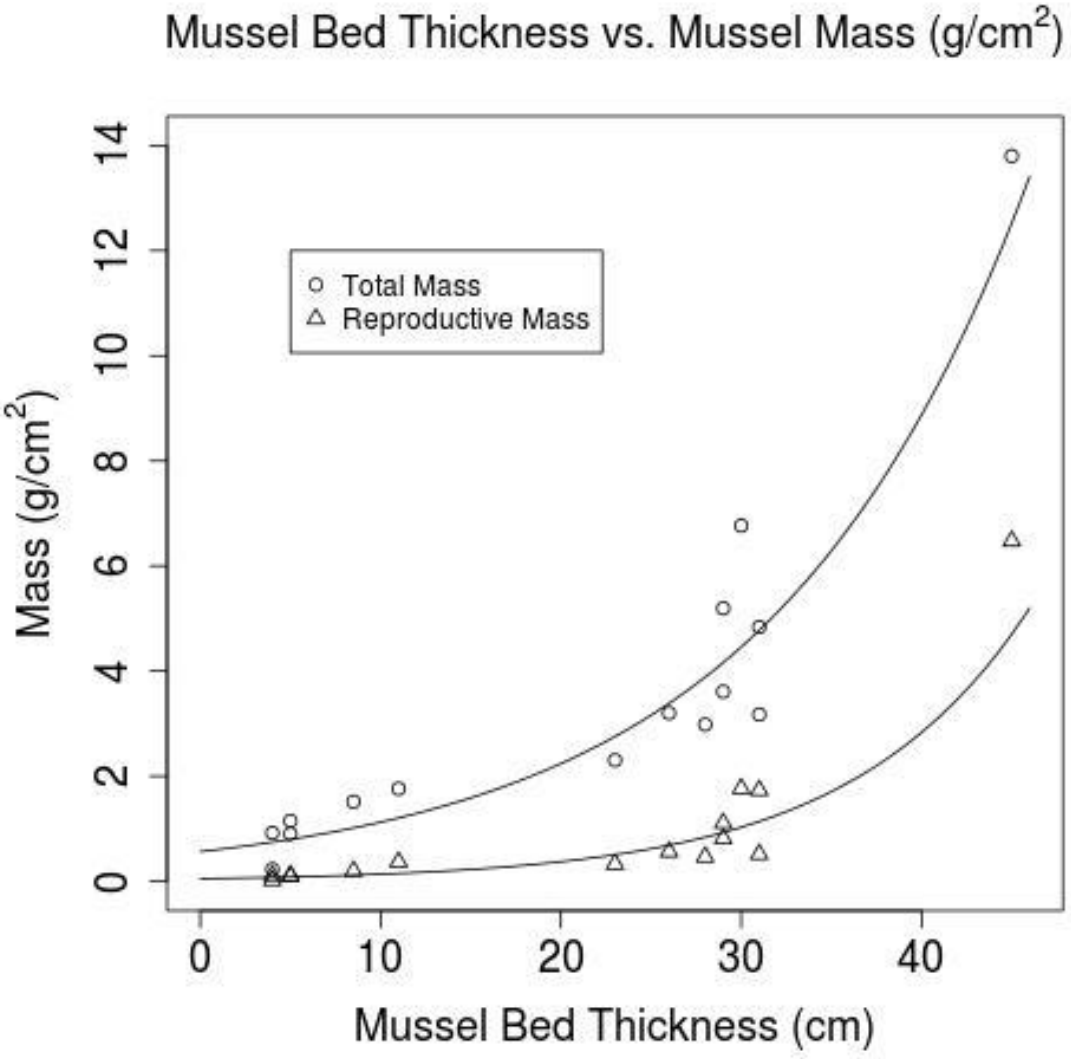

Figure 3.8: Regressions between total and reproductive mussel mass of size structure samples vs mussel bed thickness. (Total Mass: $p<0.001$,Adjusted $R^2=0.756$, n=18; Reproductive Mass: $p<0.001$,Adjusted $R^2=0.807$, n=18).

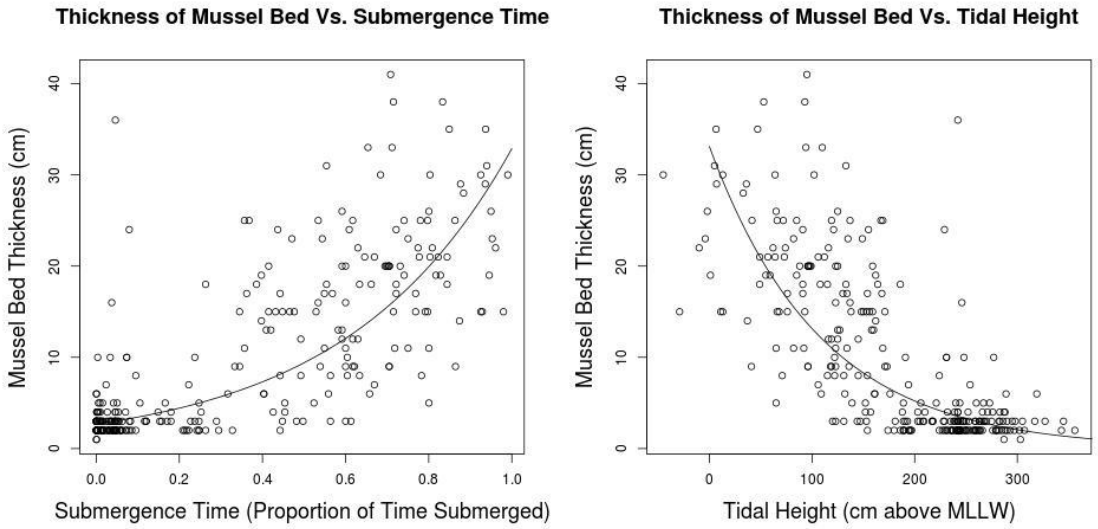

Figure 3.9: Regressions between mussel bed thickness, tidal height, and submergence time. Submergence times were calculated using tidal predictions for Tatoosh Island from 2008-2010.(Mussel Bed Thickness Submergence Time: $p<0.001$, Adjusted $R^2=0.655$, n=287, Mussel Bed Thickness Tidal Height: $p<0.001$, Adjusted $R^2=0.617$, n=287)

3.3.3 Upper and Lower Limits of the Mussel Bed

Mussels span a wide range on Tatoosh on average more than half of the intertidal zone is dominated by mussels (see table 3.1). The heights in table 3.1 were used as limits of the mussel bed in the subsequent calculation of mussel mass at Strawberry Point. No survey data describing upper and lower limits were available for Tongue Point. A date and time stamped photograph of Tongue Point showing the water level equal to the lower limit of the mussel bed along the southwest corner of the point indicates a lower limit of 95 cm giving a submergence time of 67%. Furthermore, measurements from Observatory Point, located 5 km east of Tongue Point, found an upper bed limit of 208 cm, and a lower limit of 74 cm, with locally calculated submergence times of 74% and 5% respectively. In light of the similarity between these points and the more extensive measurements found for Tatoosh, I used the mean submergence times of upper and lower bed limits on Tatoosh to estimate upper and lower tide heights of the Tongue Point Mussel bed.

Table 3.1: Upper and lower limits of the mussel bed on Tatoosh Island. Tide heights are in meters.

Description	Submergence Time	s.d.	Tide Height	s.d.
Upper Mussel Bed Limit	0.069	0.092	2.48	38
Lower Mussel Bed Limit	0.61	0.21	1.10	58

3.3.4 Dependence of Biomass on Shore Angle

To calculate the dependence of biomass per length of shoreline M on shore angle, it is necessary to integrate along the profile of the mussel bed. I used equation 3.1 from figure 3.2 to calculate mass per cm^2. Position p corresponds to the horizontal distance from MLLW (figure 3.10). $T(p, \theta)$ defines the line representing the surface of the rock underlying the mussel bed.

$$M(\theta) = \int_L^U e^{c*e^{f*S(T(p,\theta))+g}+d}\, dp \tag{3.1}$$

t=tide height

s=submergence time

p=position

t_U=tide height submerged 6.9% of the time (upper limit of mussel bed)

t_L=tide height submerged 61.7% of the time (lower limit of mussel bed)

$S(t)$=submergence time at tide height T

$T(p,\theta)$=tan(θ)*p

$P(t, \theta)$=$\frac{T}{\tan(\theta)}$

$U = P(t_U, \theta)$

$L = P(t_L, \theta)$

$M(\theta)$=mass of mussels per cm of shoreline given θ

$T(p, \theta)$ defines the tide height at a given distance p from the intersection of rock and MLLW given θ. $P(t, \theta)$ defines the distance p as a function of t and θ. U and L are the limits of integration and are equal to p at the upper and lower limits of the mussel bed respectively.

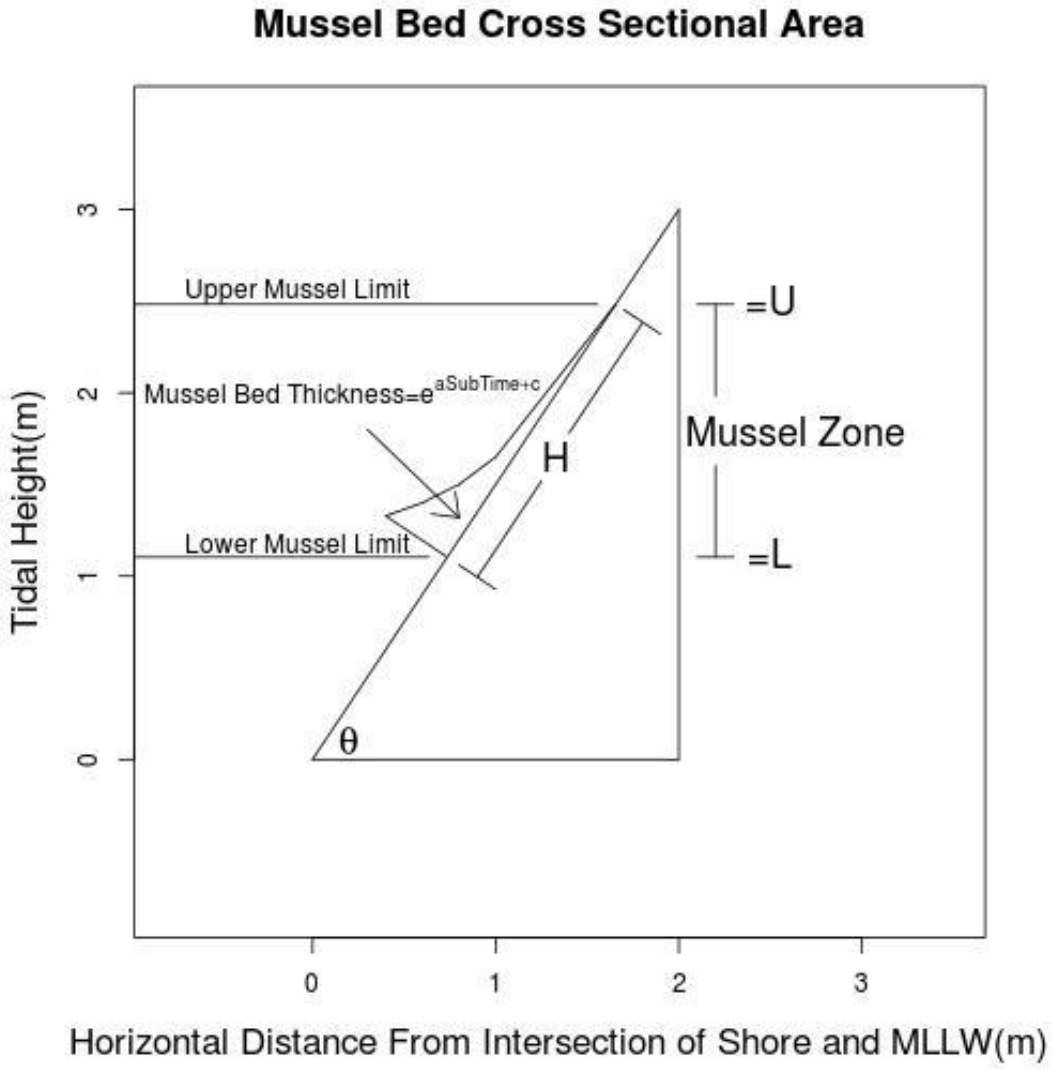

Figure 3.10: Diagram showing features used in equation 3.1 which describes the dependence of mussel bed mass on shore angle θ, p corresponds to the x-axis.

3.3.5 Case Study 1. Tongue Point

As sea level rises, the topography of Tongue Point is predicted to cause an almost monotonic loss of habitat area between high and low tide driving a rapid decline in biomass and reproductive output(figure 3.11). A drop in mussel biomass of 13150 kg (15%) is predicted for the minimum estimate of relative sea level rise. An increase of up to 90 cm will cause an almost linear decline in mussel mass. Beyond this level the rate of decline increases dramatically as the majority of platform area is brought below the mussel zone causing a 77% decline in population size at a relative sea level rise of 100 cm. The maximum predicted rise in sea level by 2100 would result in an 87% decline in population size at Tongue Point.

3.3.6 Case Study 2. Strawberry Point

In contrast to Tongue Point as relative sea level rises habitat area will increase at Strawberry Point as the currently emergent terrace becomes submerged. A monotonic increase in population size and reproductive output is predicted (figure 3.12). The minimum expected relative sea level rise is predicted to cause an increase in population mass of 225 kg or 3.5%. The maximum expected relative sea level rise is predicted to increase population mass by 3385 kg or 53%. As on Tongue Point, on Strawberry Point a critical region exists at intermediate rises in sea level in which the rate of change of population size increases dramatically. In this case, the rise drives rapid population expansion as the flat region of the platform becomes dominated by mussels. Beyond 2100 sea level is predicted to continue to rise possibly for several centuries. At Strawberry Point population size would reach a maximum at a relative sea level rise of 255 cm, beyond which population size is predicted to decline rapidly as shore angle in the mussel zone again steepens, reducing habitat area.

3.3.7 Mussel Abundance and Shore Angle

Mussel populations respond in a highly non-linear manner to changes in sea level as a result of strong non-linearity in relationships among mussel growth, submergence

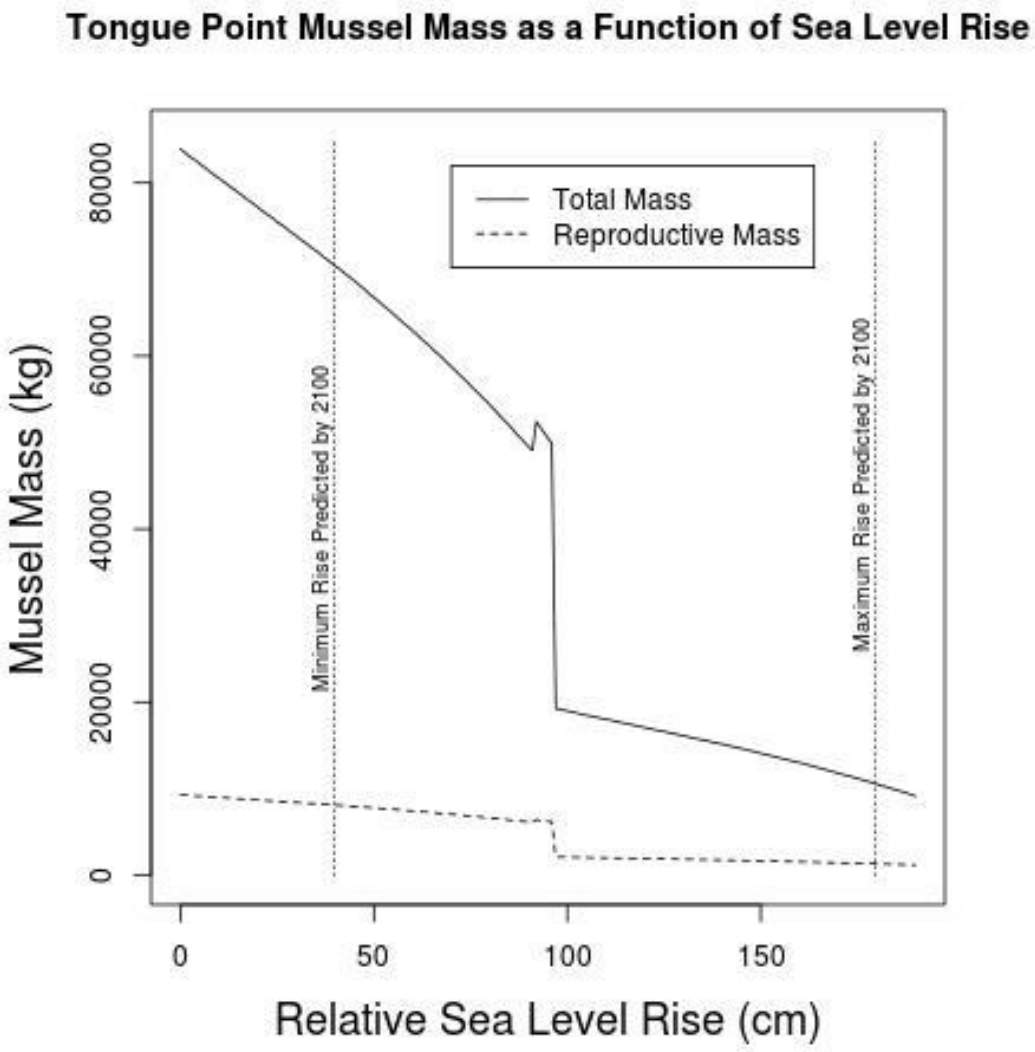

Figure 3.11: The predicted change in mussel total and reproductive mass is shown for Tongue Point. Vertical lines indicate minimum(39.7 cm) and maximum(179.7 cm) predicted relative sea level rise accounting for local geodetic rates of rise.

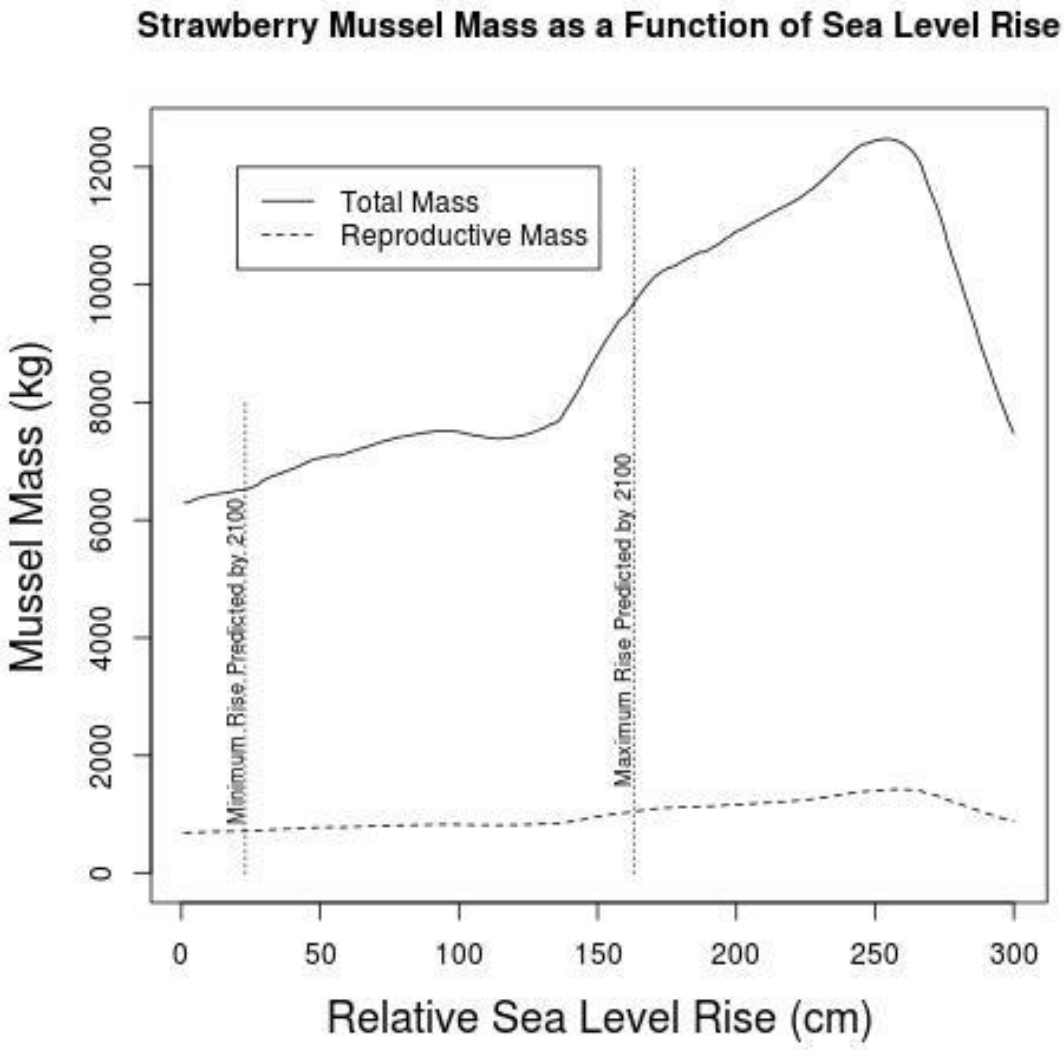

Figure 3.12: The predicted change in mussel total and reproductive mass is shown for Strawberry Point. Vertical lines indicate minimum (23 cm) and maximum(163 cm) predicted relative sea level rise accounting for local geodetic rates of rise.

time, and incident angle of the rock (figure 3.13). This non-linearity makes mussel populations extremely sensitive to changes in the availability of habitat that is formed by low shore angle, which probably accounts for a large proportion of regional biomass, individuals, and reproductive output. My results demonstrate that mass per unit area is an exponential function of mussel bed depth. Mussel bed depth in turn is an exponential function of submergence time. This relation taken with the exponential increase in mussel mass with bed depth yields an exponential relation between submergence time and both mussel total mass and reproductive mass per unit area. The surface area of rock between high and low tide or between mussel bed upper and lower limits is a hyperbolic function of shore angle (θ in figure 3.10). The exponential relation between submergence time and mussel mass per unit area coupled with the hyperbolic relationship between shore angle and habitat area combine to form an even more hyperbolic dependence of mussel mass on shore angle.

The secular increase in sea level predicted by climate models and confirmed by modern observations will interact with the extreme sensitivity of mussel populations to changes in the availability of low shore angle habitat, which itself is a function of tidal height (Cazenave and Nerem 2004; Church and White 2006; Schaeffer et al. 2012). In the case of Tongue Point sea level rise of the order predicted (39.7-179.7 cm by 2100) will reduce the area of intertidal habitat in the mussel zone potentially causing a substantial decrease in population size in one of the largest mussel populations in Washington State. At Strawberry Point on Tatoosh Island, the current topography of the near-shore means that predicted increases in sea level (23-163 cm by 2100) will have an effect opposite to that at Tongue Point, with intertidal habitat area increasing to drive population expansion. Thus shore morphology is a critically important factor at the local scale.

3.3.8 Sea-Level Rise Beyond 2100

The Tongue Point and Strawberry Point case studies highlight the fact that even conservative forecasts of sea level rise will dramatically change local abundances of mussels in the near future. Several recent publications have suggested predictions

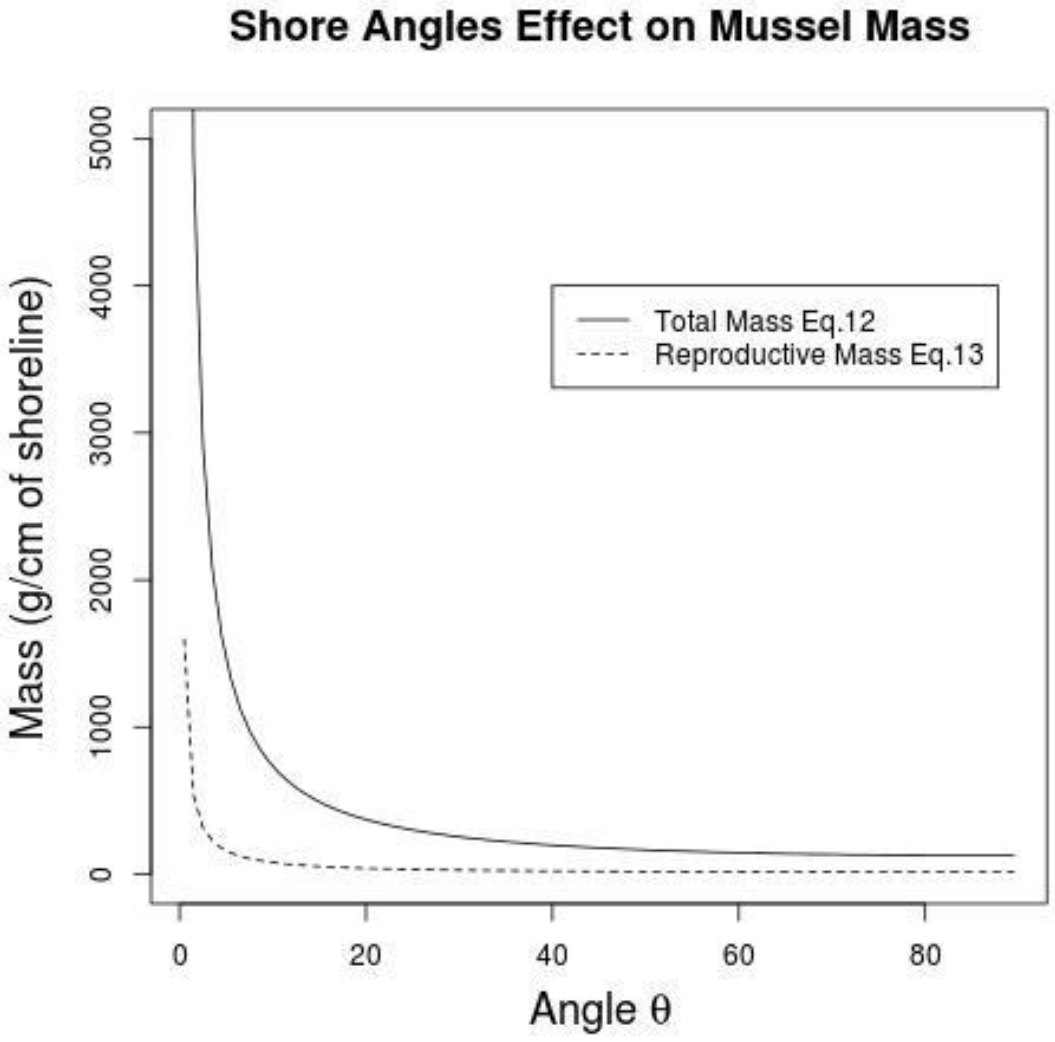

Figure 3.13: The hyperbolic relation between mussel bed mass and shore angle θ.

of future sea level rise have been chronically underestimated, making scenarios at the higher range of predictions appear more likely (Brysse et al. 2013; U.S. Climate Change Science Program; National Research Council 2009; Rahmstorf et al. 2007). Climate models predict that sea level rise will continue through 2300 achieving global mean levels substantially higher than predicted through 2100, possibly beyond 3 meters (Schaeffer et al. 2012). A rise of this magnitude would reverse the predicted increase in mussel mass at Strawberry Point driving a decline similar to that of Tongue Point predicted for this century (Schaeffer et al. 2012).

Sea level may also be impacted in this region by coseismic subsidence events caused by the accumulation and eventual release of inter-seismic strain, a process driven by the subduction of the Juan de Fuca Plate (NRC 2012; Long and Shennan 1994; Peterson et al. 2012). The sediment record of low-lying Neah Bay wetlands contains evidence for four such events in the last 1300 years during which geodetic height fell by 50-100 centimeters in short periods of time instantly raising relative sea levels (Peterson et al. 2012). These subsidences were separated by intervals of 200-400 years, and the last occurred around 300 years ago, implying the possibility of such an event during the next century.

3.3.9 Variation in Shore Morphology

Regionally, shore platforms often occur at similar heights with similar slopes because of regional scale consistency in the factors leading to their development such as rock strength, wave regime, tidal range, and rates of uplift. Around Tatoosh Island and the adjacent mainland of Cape Flattery, most platforms exist at a similar height to Strawberry Point near mean higher high water (Bird and Schwartz 2000). Because of this regional consistency in platform height, sea level rise will probably cause a local expansion in the population size of mussels until these higher platforms become permanently submerged below the mussel zone, as may occur beyond 2100. In the southern portion of its range which extends to Baja California *Mytilus californianus* and other depth sensitive species may be more strongly impacted because relative sea level rise will be greater due to the the lack of geodetic uplift that reduces relative

sea level rise in Washington State (NRC 2012; Soot-Ryen 1955).

3.3.10 Timescale of Platform Development

My results show that a critical feature of the ecological response of rocky coast organisms to sea level change is the dependence of shore morphology on tidal height. Because shore platforms regionally co-occur at common heights, rapid changes in sea level relative to the development time of platforms are likely to cause dramatic shifts in habitat area at specific tide heights. The process and rate of platform development is still debated by experts but measurements of modern erosion rates indicate that terraces develop over at least thousands of years (Stephenson et al. 2010). Dasgupta (2010) collected down-wearing erosion rates for platforms around the world and reported a range of 0.004 -3.65 mm/yr with a mean of 1.07 mm/yr when rapidly eroding chalk cliffs were excluded. Downwearing at Tatoosh Island has been estimated at 0.97 (s.d. 0.08) mm/yr based on the relative height above the rock surface of 6 stainless steel bolts initially installed flush to the surface in 1974 and measured for their extension above the rock in 2004 (R.T. Paine unpublished data). Choi et al. (2012) used cosmogenic ^{10}Be to date Korean shore platforms composed of slightly metamorphosed sandstone similar to the rock composing Tatoosh Island, and found surface exposure ages across terraces of 4-148 ka, indicating initial development occurred at least 148 ka ago (Choi et al. 2012). The long minimum estimates of time required for platform evolution in hard rock cliffs (thousands of years), which require stable sea levels, indicate that predicted rates of sea level rise will outstrip formation of new platforms. This discrepancy in rates makes intertidal habitat area almost independent of erosion rates in resistant substrates for the timescale of predicted sea level rise.

3.4 Discussion

Mytilus californianus is both a competitive dominant and a foundation species that creates habitat (the mussel bed) for the diverse community living within the bed (Dayton 1971; Paine and Levin 1981; Suchanek 1979). The mussel is a major occupier of space in the mid intertidal in much of its range, which extends from Isla Socorro off

the coast of Baja California to the Aleutian Islands (Coan, Scott, and Bernard 2000). Mussels interact strongly with many other species and provide nutrient resources to associated primary producers (Paine and Levin 1981; Pfister 2007; Wootton 2001). The effects of probable changes in *Mytilus californianus* density may be large and multiple in localities losing or gaining large amounts of mussel mass. Several species are partially or largely dependent on *Mytilus californianus* as a prey item, including the starfish *Pisaster ochraceous*, multiple species of predatory snails, and spiny lobsters (*Panulirus interuptus*) in the southern portion of the range (Paine 1966; Paine 1976; Robles, Sweetnam, and Eminike 1990). Wootton (2010) investigated the impact of long term removal of *Mytilus californianus* from the community and found that temporal variation in common co-occuring species was reduced due to the absence of mussel bed disturbance events, while other metrics of community dynamics remained similar to controls (Wootton 2010). Changes in sea level will affect the habitat area for the entire mid intertidal community in contrast to the deletion of a single species, but if reduction in recruit production caused local declines in mussel population density the community might be shifted to the more temporally stable state predicted.

As a planktotrophic broadcast spawner, *Mytilus californianus* spends weeks in the water column before settlement, so that reproduction is often not local and juveniles often settle kilometers or more from home populations (Becker et al. 2007; Carson et al. 2011; Strathmann 1987). The metapopulation and evolutionary dynamics of such a population can be complex, with marginal habitat areas possibly being subsidized by larger populations and widely separated populations being connected by substantial gene flow due to the long potential distance of dispersal (Addison et al. 2008; Carson et al. 2011). These processes could be rapidly modified by changes in the population size of this species throughout its range as a result of its sensitivity to changes in sea level at local scales. Populations could blink on or off in the next 100 years as a result of sea level rise, significantly modifying the connectivity and evolutionary trajectory of the species.

I have shown that populations of *Mytilus californianus*, a major constituent of the North American West coast rocky intertidal fauna, will be extremely sensitive to changes in sea level. The factors responsible for the sensitivity of *Mytilus californi-*

anus to changes in sea level are: 1. Its general restriction to a narrow depth zone relative to predicted changes in sea level. 2. The exponential increase in mussel density with decreasing tide height and increasing submergence time. 3. The common existence and concentration of population density on intertidal terraces of low shore angle which are variably distributed relative to sea level. Terraces are common features of rocky shores around the world and many species are restricted to the region between low and high tide or to particular depths in the shallow subtidal (Denny and Gaines 2007). These species share the potential for dramatic changes in population distribution as a result of human caused sea level rise. In order to assess the potential impacts of this process on shore populations around the world an integrated assessment of the changes in habitat area for different scenarios of sea level rise is required. Remote sensing coupled with continued ecological investigation of the determinants of species distributions is needed to make accurate predictions of the impacts on coastal populations.

CHAPTER 4
DEMOGRAPHIC AND VITAL RATE VARIATION OF *MYTILUS CALIFORNIANUS* IN THE STRAIT OF JUAN DE FUCA

4.1 Introduction

Anthropogenically induced climate change and environmental degradation are causing extinctions, range shifts, and range contractions across the planet (Parmesan and Yohe 2003; Sagarin et al. 1999; Helmuth 2002; Harley 2011). Therefore the determinants of spatial distributions of species are of increasing relevance to conservation and management goals. I investigated the determinants of spatial distribution in the mussel *Mytilus californianus*, an important member of the north east Pacific intertidal zone. I quantified variation in growth, survival, and recruitment across environmental gradients and several distributional limits in the Strait of Juan de Fuca in order to elucidate processes underlying the determination of population density. Parameter values and functional forms of minimal models describing growth and survival were subsequently used to parameterize the integral projection model described in Chapter 5.

4.2 Study Organism

Mytilus californianus a competitive dominant on non-vertical rock benches in the intertidal zone along the West Coast of North America (Suchanek 1979; Paine 1966; Paine 1974; Paine 1976; Wootton 1993; Singh et al. 2013). Along the Pacific coast of North America, mussels occupy a wide band of the intertidal, often spanning more than 50% of the tidal range, and sometimes occupying nearly the entire range of the tide on the ends of wave beaten points. Where geological processes have left large

debris-free rock benches within the species vertical range, large mussel beds (100's of m^2) often exist, monopolizing space. The beds average 20 cm deep or more in the low intertidal, occasionally achieving depths of 45 cm. Such depths represent kilograms per m^2 of biomass (see fig.3.8). An important aspect of the species ecology is its susceptibility to wave disturbance during winter storms (Paine and Levin 1981; Wootton and Forester 2013). Mussels filter large amounts of plankton from the water, excrete large quantities of nutrients utilized by the associated algae and microbial community, spawn massive numbers of gametes, provide habitat for more than 300 associated species, and consume oxygen (Bayne and Scullard 1977; Suchanek 1981; Pfister 2007; Pfister, Gilbert, and Gibbons 2014). The species is an important prey item in the diets of multiple species including starfish, snails, sea otters, crabs, and the spiny lobster *Panulirus interruptus* in the southern portion of the range (Robles 1987; Robles, Sweetnam, and Eminike 1990; Sanford et al. 2003; Sanford et al. 2006; Sanford and Worth 2009). In general *Mytilus californianus* is an important community member which interacts strongly with many other species (Wootton 1994); across a large range which extends latitudinally from Isla Socorro off the coast of Mexico to the Aleutian Islands (Coan, Scott, and Bernard 2000).

4.3 Spatial Distribution of *Mytilus californianus* in Washington State

It is important to consider disributional patterns and potential biotic and abiotic determinants along a continuum of scales since discernible patterns exist across at least 3 spatial scales. In Washington State *Mytilus californianus* is common on the outer coast where immobile rock formations exist in the intertidal zone. Mussel beds are generally restricted vertically to the intertidal zone. On Tatoosh Island the mean lower and upper limits of the mussel bed are respectively 1.1 and 2.5 meters above MLLW (see section 3.2.5). Classically the upper limit has been hypothesized to be determined by increasing gradients of physiological stress relating to the frequency and duration of emergence which results in decreased feeding time and greater exposure to high and low temperature extremes (Connell 1972; Bayne et al. 1976; Somero 2002;

Harley and Helmuth 2003). Usually mussel beds are thickest and most extensive on the ends of wave beaten points and in areas where shallow shore angles result in large amounts of habitable area between the upper and lower limits (see chapter 3). In Washington State, experiments show that the lower limit of the mussel bed is largely determined by predation of mussels by the starfish *Pisaster ochreaceous* (Paine 1966). The vertical limits of the mussel bed comprise the smallest scale distributional pattern investigated in the present study, depending on the angle of the shore the upper and lower limits of the bed may be as little as tens of centimeters wide or as much as tens of meters wide.

At a small scale along the shore, mussel bed width often decreases as one moves from more wave exposed to less wave exposed parts of a bench or headland. Often the seaward ends of benches possess shallower shore angles as compared to the more protected regions far from the ends of points, making the disentanglement of causes of the restriction of mussel bed extent potentially complex. Less is known about this pattern than about the causes of the vertical limits of the mussel bed. Effective Shore Level (ESL), defined by Harley and Helmuth (2003) as the height above MLLW of the water level when a location is first washed by waves during an incoming tide, explains some of the variation in the upper limit of the mussel bed as one moves towards more wave protected areas. Even less is known about the apparent increase in the lower limit of the bed as one moves away from exposed regions. The spatial scale of the along-shore decline in the extent of mussel beds usually takes place across a hundred or a few hundred meters.

At the scale of kilometers mussel populations are concentrated on rocky headlands which in Washington State are generally a few tens of kilometers in extent, and are comprised of rock benches or intertidal platforms separated occasionally by small keyhole beaches. Between such headlands, beaches kilometers to tens of kilometers in extent composed of sand, gravel, and/or cobbles separate headland complexes and offer little or no viable habitat except the occasional massive immobile boulder. Thus the population is highly discontinuous and primarily dependent on the availability of immobile rock surfaces at appropriate tide heights.

At the extreme eastern edge of the Strait of Juan de Fuca near Deception Pass, ge-

ologically suitable habitat exists but mussels are orders of magnitude less dense than they are at more western sites with appropriate substrate. Harley (2011) showed that in the eastern Strait, increasing thermal stress experienced by sessile invertebrates driven by changes in the timing of low tides and decreasing wave exposure decreases upper vertical limits, without reducing the foraging height of the predator *Pisaster ocraceous*. Caging experiments showed that in the absence of predation several species of sessile invertebrate would extend their vertical range downward, potentially increasing population size. *Mytilus californianus* however did not recruit into the predator free cages, in contrast to the situation on the outer coast. This result suggests that recruitment limitation, in addition to a lack of predator free space, may cause the local absence of *Mytilus californianus* in the eastern Strait.

4.4 Methods

4.4.1 Field Sites

Research was conducted on Tatoosh Island at the mouth of the Strait of Juan de Fuca, and at 5 sites spanning the longitudinal extent of the Strait: Cape Flattery (48.3869° N, -124.7245° W), Freshwater Bay (48.1509° N, -123.6361° W), Port Townsend (48.1172° N, 122.7592° W), and Coffin Rocks (48.4129° N, -122.6620° W). On Tatoosh, monitoring was conducted within two separate micro-sites Strawberry Point (48.3918° N, 124.7351° W) and The Finger (48.393979°,-124.7393°). At both micro-sites 12 plots were created within which growth, survival, recruitment, temperature, and size structure data were collected. Within each micro-site the plots were arrayed in a grid spanning the horizontal (along-shore) and vertical extent of the mussel bed. At Cape Flattery, Freshwater Bay, Port Townsend, and Coffin Rocks four plots were monitored identically, and were situated so as to span the vertical extent of the mussel bed where it was most extensive.

The Cape Flattery site, which is adjacent to Tatoosh on the mainland, and the Freshwater Bay site, which is approximately 80 kilometers east of Tatoosh, are characterized by intertidal rock benches on which extensive mussel beds exist. At Port

Figure 4.1: The locations of field sites across the Strait of Juan de Fuca.

Townsend, plots were located on a mussel capped boulder less than 100 meters from shore which was partially exposed during low tides. The adjacent shoreline is composed of sand and cobble beaches which offer no suitable habitat for *Mytilus californianus*; one other mussel capped boulder exists approximately 1.6 kilometers west along the shore. Coffin Rocks is a small intertidally-exposed reef approximately 300 meters from shore just north of Deception Pass. A bed of *Mytilus edulis* caps the reef, and very low densities ($<1/m^2$) of lone moderately sized (<10 cm) *Mytilus californianus* are present on the reef and the adjacent shoreline which is characterized by extensive rocky benches which appear to offer suitable habitat similar to the intertidal benches of Tatoosh. Deception Island which is approximately 1 km from shore near Coffin Rocks is fringed by intertidal benches, and harbors similarly low densities of *Mytilus californianus*, many of which are large (>10 cm).

4.4.2 Measurement of Environmental Parameters

Environmental conditions within each experimental plot were monitored with temperature loggers (Hobo Pendant loggers, Onset Computer Corp., Bourne, MA) every 5 to 15 minutes depending on the length of the deployment. At Tatoosh, tide height within each plot was measured with a laser level and referenced to landmarks of known tide height. At the other sites, multiple observations of the height above current water level were used in conjunction with tide tables to estimate tide height. Tide data were obtained from the "WWW Tide and Current Predictor" (http://tbone.biol.sc.edu/tide/). Several environmental descriptors related to tide height were calculated and correlated with rates of growth, survival, and recruitment. Submergence time, defined as the percentage of time a plot is submerged was calculated with estimated tide heights and tidal predictions for 2008-2010 downloaded from the "WWW Tide and Current Predictor" (http://tbone.biol.sc.edu/tide/).

Effective shore level (ESL), the mean tide height when a plot is first inundated by waves during an incoming tide, accounts for the effects of wave splash's ameliorating immersion effects and was calculated following the methods of Harley and Helmuth (2003) using tide height data and the temperature time series collected for each plot during 2008-2010. "Submergence time effective shore level" (SESL) a metric developed by Blanchette, Helmuth, and Gaines (2007) is the percentage time submerged, at a plot's ESL. On Tatoosh the distance from each plot to the end of the nearest exposed point, was measured using a measuring tape.

4.4.3 Estimation of Mussel Growth Rates

To estimate mussel growth and survival rates, adult mussels were transplanted from a single location (the north end of "the Glacier") in the mid intertidal on Tatoosh Island into each experimental plot. Mussels were held in plastic mesh cages bolted to the rock with wall anchors, individuals were numerically marked via engraving with a Dremel tool, and lengths were measured prior to final placement. Initially mussels were measured and checked for survival every few weeks, however the trauma of removal from cages appeared to harm individuals excessively, so the frequency of

measurement was reduced to the beginning and end of each summer field season. Initial transplants took place in June 2008 and were monitored through the next two field seasons until the end of August 2010. Initially 16-18 mussels were placed in each plot. During the first winter a number of cages were lost to storms and replacements derived from the same location on Tatoosh were transplanted in April 2009. Ten mussels were included in each replacement package. At non-Tatoosh sites all plots, even those retaining their original mussels, received new transplants in June 2009. A total of 1460 adult mussels were ultimately transplanted and used in the growth analysis; their mean length was 5.7± 1.4 cm (s.d.). Only mussels surviving when remeasured were included in the growth analysis, and data from the first few months of summer 2008 were left out because of the detrimental effect of repeated measurement and disruption of byssal threads. For each individual, only the longest interval between living measurements was utilized.

Growth data were fit to a number of models that included dependence on multiple environmental gradients and geographic locations. The basic growth form was a non-asymptotic, monotonic, decelerating, logarithm-based function defined to be equal to the size of a new settler at time 0. The length at age is given by:

$$L_{(t,E,G)} = a_{(E,G)} * log(b * t + 1) + L_{min} \tag{4.1}$$

$L_{(t,E,G)}$ is the length at time t given environmental conditions E and geographic location G, b is a free parameter describing the incremental affect of elapsed time on growth, t is the elapsed time in days, and L_{min} is the size of a recruit at settlement. Changes in growth rate driven by variation in environmental gradients or location enter the model as modifications of $a_{(E,G)}$ the environmentally dependent growth rate function. Various versions of $a_{(E,G)}$ were developed including different combinations of environmental gradients (horizontal position, ESL, SESL, submergence time, and their logarithms) and geographic factor aggregations (site, place, region, and "not Coffin Rocks"). Site, the finest geographic factor tested, included a separate factor for Strawberry Point and The Finger on Tatoosh as well as a factor for each mainland location. Place aggregates the Tatoosh micro-sites into a single factor, and contains

a factor for each mainland location. Region aggregates Tatoosh with Cape Flattery, and has separate factors for all other locations. "Not Coffin Rocks" aggregates all locations excluding Coffin Rocks, creating a binary factor. The models assumed environmental dependence of the functional form of $a_{(E,G)}$ was linear. For example assuming growth was dependent on submergence time, horizontal position, and place, $a_{(E,G)}$ would be:

$$a_{(E,G)} = cE_{st} + dE_{hp} + G_{Tatoosh} + f \tag{4.2}$$

where c and d are fitted coefficients, E_{st} is the submergence time, E_{hp} is the horizontal position, $G_{Tatoosh}$ is a Tatoosh specific fitted coefficient, and f is a fitted intercept term. Equation 4.1 can be solved for t to give age at length instead of length at age:

$$T_{(L_t,E,G)} = b^{-1}e^{\frac{L_t - L_{min}}{a_{(E,G)}} - 1} \tag{4.3}$$

Equations 4.1 and 4.3 can then be used together to predict change in length or final length given initial size and a time increment:

$$L_{(t_2,E,G)} = a_{(E,G)}log(b(T_{(L_{t_1},E,G)} + t_2 - t_1) + 1) + L_{min} \tag{4.4}$$

$$\Delta L = a_{(E,G)}log(b(T_{(L_{t_1},E,G)} + t_2 - t_1) + 1) + L_{min} - L_{t_1} \tag{4.5}$$

To fit the model, likelihood functions were derived for each potential version. I assumed ΔL was a normally distributed random variable whose variance was constant or a linear function of initial size, time increment, or position on environmental gradients. The negative log-likelihood function (NLL) was expressed as:

$$NLL = \sum \frac{log(2(\Delta L_i))}{2} + \frac{(\Delta L_i - E(\Delta Li))^2}{2var(\Delta L_i)} \tag{4.6}$$

where ΔL_i is the change in length of individual i over the time increment, and $E(\Delta L_i)$ is given by equation 4.5. An example variance function $var(\Delta L_i)$ would be:

$$var(\Delta L_i) = g\Delta t_i + fE_{st_i} \tag{4.7}$$

where Δt_i is the time increment between the i^{th} individual's measurements, E_{st_i} is the individuals submergence time, g and f are fitted coefficients. Fifteen versions of the model were fit using the optim() function in R ver.3.1.1 with the "Nelder-Mead" minimization routine. AICc values and relative likelihoods were then calculated and compared to assess model fit. Standard errors for the parameters describing growth were calculated by boot-strapping; 50% of the data was randomly sampled without replacement and the model refit 1000 times.

4.4.4 Estimation of Survival Rates

Adult survival rates were modeled using the Tatoosh transplant data excluding the first few months of summer 2008 to remove mortality that occurred as a result of transplant. The survreg() function in R ver. 3.1.1 fit survival models with constant and variable hazard functions to the censored transplant data in each plot. I then compared the fit of models using AICc for constant and more complex hazard functions. Next I related plot level rate parameters to the environmental parameters tide height, horizontal position, submergence time, ESL, and SESL to develop an environmentally dependent survival function on the basis of comparison of relative Likelihoods. ANCOVA tested for variation in survival rates across the Strait once important environmental gradients were accounted for.

Elsewhere (Chapter 2) I demonstrated local adaptation in juvenile mussels, suggesting that mussels transplanted to environmental conditions different than those in which they developed may show declines in performance relative to locally developed individuals. I therefore incorporated the strength of local adaptation in survival into the model using the data in Chapter 2. The changes in the arcsine root transform of submergence time ($asin(\sqrt{E_{st}})$) of transplanted mussels were regressed against the difference in the log mean time to death ($ln(\mu)$) of reciprocally transplanted mussels and those transplanted from other locations. The proportional nature of submergence time drove the decision to use the arcsine root transform. There were 5 plots of 18 mussels which were transplanted to lower submergence times. Their survival rates were compared to the survival rates of reciprocally transplanted mussels to calculate

how much prior habitat impacted transplant to more emergent locations as a function of difference in submergence time for the source population used in the growth study.

4.4.5 Estimation of Tuffy Recruitment Rates

Mussel recruitment was monitored by censusing Tuffy™scouring pads placed in each experimental plot for two weeks, which were subsequently replaced every two weeks during summer field seasons (2008-2010). Tuffy's™act as a good settlement substrate for *Mytilus californianus* and have been used in numerous studies tracking its recruitment dynamics (Connolly, Menge, and Roughgarden 2001). After initial collection, Tuffy's™were frozen at -20° C and stored before being rinsed and counted under a dissecting microscope.

I used ANCOVA to analyze variation across sites, along environmental gradients related to tide height, and with horizontal position (distance to nearest exposed point) of Tatoosh plots. Relative likelihoods were used to compare models predicting survival rates.

4.4.6 Size Structure Sampling

Size structure samples were collected adjacent to experimental plots in summer 2009 and 2010. Each sample included all mussels identifiable with the naked eye inside 225 cm^2 core samples. Samples were either counted and measured immediately or frozen at -20° C and counted at a later date.

4.4.7 Coffin Rocks

At Coffin Rocks, mussels were too rare for size structure samples to be collected, so a correlation between mean individual age and submergence time derived from the Tatoosh size structure samples was used to estimate the number of iterations. No detailed measurements of population density were made at Coffin Rocks, but densities were observed to be < 1 individual per m^2. Thirty individuals were measured to obtain an estimate of the size of the sparsely distributed population (mean 8 $\pm$ s.d. 2 cm).

Table 4.1: AICc comparison of models predicting growth rate of mussels across the Strait of Juan de Fuca. NP=number of fit parameters, NLL=negative log-likelihood, LW=likelihood weight. c_j and g_k are location coefficients, c_j had two categories one for Coffin Rocks and one for all other sites, g_k had 4 categories one for Cape Flattery/Tatoosh, Freshwater Bay, Port Townsend, and Coffin Rocks.

$a \sim$Explanatory var.	variance model	NP	NLL	AICc	LW
none constant a	constant variance	3	426.86	859.78	<0.0001
none constant a	variance$\sim \Delta T$	3	428.75	863.58	<0.0001
none constant a	variance$\sim \Delta T + E_{st}$	4	424.38	856.87	<0.0001
$log(E_{st})$	constant variance	4	425.06	858.23	<0.0001
$log(E_{st})$	variance$\sim \Delta T$	4	485.29	978.70	<0.0001
$log(E_{st})$	variance$\sim \Delta T + E_{st}$	5	453.77	917.71	<0.0001
$log(E_{st}) + log(E_{hp})$	constant variance	5	417.61	845.38	<0.0001
$log(E_{st}) + log(E_{hp})$	variance$\sim \Delta T$	5	426.10	862.36	<0.0001
$log(E_{st}) + log(E_{hp})$	variance$\sim \Delta T + E_{st}$	6	420.54	853.31	<0.0001
$log(E_{st}) + log(E_{hp}) + c_j$	constant variance	7	393.35	800.80	0.08
$log(E_{st}) + log(E_{hp}) + c_j$	variance$\sim \Delta T$	7	395.39	805.08	0.009
$log(E_{st}) + log(E_{hp}) + c_j$	variance$\sim \Delta T + E_{st}$	8	390.18	796.75	0.61
$log(E_{st}) + log(E_{hp}) + g_k$	constant variance	8	393.09	802.56	0.033
$log(E_{st}) + log(E_{hp}) + g_k$	variance$\sim \Delta T$	8	395.46	807.32	0.003
$log(E_{st}) + log(E_{hp}) + g_k$	variance$\sim \Delta T + E_{st}$	9	390.01	798.50	0.25

The model was fit assuming a density of one 8 cm mussel per m^2or 0.0225 eight cm individuals in the area of one 225 cm^2 core sample, the plot size used at all other sites.

4.5 Results

4.5.1 Growth

Three model versions had high likelihood weights. Each included ln(submergence time), ln(horizontal position), and a site specific coefficient (either c_j for "Not Coffin Rocks", or g_k for Region, see table 4.1) in the determination of growth parameter a. The variance model was constant in the 3^{rd} highest relative likelihood model, and included the length of time between measurements and submergence time for the top two models.

Table 4.2: Parameter values of $a_{(E_{st},E_{hp},c_j)}$, b, and $var(L_{t_2})$ used in the IPM. Standard errors were calculated via boot-strapping (see methods).

Coefficient Description	Parameter	Value	standard error
Submergence Time	m	0.23	0.072
Horizontal Position	d	-0.06	0.034
Coffin Rocks	c_1	0	NA
All other locations	c_2	-1.23	0.224
Intercept	f	5.22	0.264
Effect of elapsed time	b	.003	0.0001
Variance model time coefficient	g	0.0006	0.0001
Variance model submergence time coefficient	h	0.256	0.084

4.5.2 Survival

The log of the mean time to death $\ln(\mu)$, the parameter which determines survival rate, was best predicted by $ln(asin(\sqrt{E_{st}}))$ across all plots. Models including geographic variation or dependence on other environmental variables had lower relative likelihoods and included more parameters (see table 4.3). Comparison of models with constant or more complex hazard functions showed that the constant models outperformed models assuming variable survival with age.

4.5.3 Recruitment

The log number of recruits per Tuffy™per two weeks was directly related to submergence time, and negatively related to horizontal position. Tuffy™recruitment rate varied geographically, Cape Flattery had the highest recruitment rate followed by Tatoosh and Freshwater Bay which had similar recruitment rates. Port Townsend and Deception Pass had the lowest recruitment (see tables 4.5 and 4.6).

4.6 Discussion

4.6.1 Spatial Variation in Vital Rates

Growth rates were variable across all spatial scales (meters, 10's of meters, 10's of kilometers). In contrast survival was singularly determined by submergence time

across the Strait of Juan de Fuca. Tuffy™measured recruitment also varied across scales, and was dependent on region (variable across 10's of kilometers), submergence time, and horizontal position. Density dependent processes may play an important role in population dynamics, the decline in growth observed horizontally along the shore could be caused by upstream filtering of food, similarly the high rates of growth observed at Port Townsend and Coffin Rocks could be driven by the absence of large nearby food competing mussel beds. The observed difference in variability across vital rates suggests a potentially multi-causal determination of distributional limits across scales.

Future work incorporating linkages between population dynamics models and spatially-dependent vital rates documented here could help elucidate these linkages and provide a better understanding of adult-recruitment linkages and spatial scales of dispersal. The analyses highlights that different aspects of the environment affect different demographic parameters. Therefore, to fully understand determinates of species distributions, models integrating these relationships will be required (Chapter 5).

Table 4.3: AICc comparison of models predicting log mean time to death of mussels across the Strait of Juan de Fuca. NP=number of fit parameters, LW=likelihood weights, Subtime=submergence time.

$log(\mu)$ ~Explanatory var.	NP	AICc	LW
none constant μ	1	37.28	<0.0003
ESL^3	2	7.29	0.021
ESL^2	2	9.07	0.0085
ESL	2	16.29	<0.00036
$Subtime$	2	13.29	0.001
$SESL$	2	12.90	0.001
$log(Subtime)$	2	2.46	0.23
$ln(asin\sqrt{Subtime})$	2	1.56	0.36
$ln(asin\sqrt{Subtime}) + log(HP)$	3	3.09	0.17
$ln(asin\sqrt{Subtime}) + ND$	3	3.63	0.13
$ln(asin\sqrt{Subtime}) + Site$	7	8.48	0.01
$ln(asin\sqrt{Subtime}) + Place$	6	8.06	0.01
$ln(asin\sqrt{Subtime}) + Region$	5	6.31	0.03

Table 4.4: Model predicting $log(\mu)$ as a function of $ln(asin(\sqrt{E_{st}}))$. Adjusted-R^2 =0.68, n=32.

	Estimate	Std. Error	t value	Pr(>|t|)
(Intercept)	8.3442	0.2108	39.58	0.0000
$log(asin(\sqrt{E_{st}}))$	1.2452	0.1506	8.27	0.0000

Table 4.5: AICc comparison of models predicting log number of recruits per tuffy every two weeks across the Strait of Juan de Fuca. NP=number of fit parameters, LW=likelihood weight.

$R \sim$Explanatory var.	NP	AICc	LW
$Subtime$	2	-6.72	0.0007
ESl	2	4.68	0.0007
$SESL$	2	3.05	0.0007
$Subtime + Site$	7	-24.21	0.0007
$Subtime + Place$	6	-22.78	0.0007
$Subtime + Region$	5	-12.14	0.0007
$Subtime + Site + HP$	8	-35.67	0.156
$Subtime + Place + HP$	7	-38.85	0.789
$Subtime + Region + HP$	6	-33.32	0.047

Table 4.6: ANCOVA predicting the log number of recruits per two weeks per tuffy, Cape Flattery, which had the highest recruitment, is the reference factor with a coefficient was 0. All other sites had lower recruitment as indicated by the negative coefficients. Adjusted-R^2 =0.87, n=39.

	Estimate	Std. Error	t value	Pr(> |t|)
(Intercept)	2.2879	0.2813	8.13	0.0000
Coffin Rocks	-2.4360	0.3919	-6.22	0.0000
Port Townsend	-2.3568	0.4118	-5.72	0.0000
Freshwater Bay	-0.8607	0.3841	-2.24	0.0321
Tatoosh	-0.8648	0.3095	-2.79	0.0087
Subtime	4.1890	0.2810	14.91	0.0000
HP	-0.0110	0.0025	-4.49	0.0001

CHAPTER 5
AN ENVIRONMENTALLY DEPENDENT INTEGRAL PROJECTION MODEL OF *MYTILUS CALIFORNIANUS* IN WASHINGTON STATE

5.1 Introduction

Spatial distributions are fundamental aspects of a species ecology, but much uncertainty remains concerning how distributional limits across multiple spatial scales are mediated, especially along continuous environmental gradients (Brown, Stevens, and Kaufman 1996; Parmesan et al. 2005; Holt and Keitt 2005; Roy et al. 2009). In recent years, ecologists have attempted to model these systems and the roles of various forcing factors, but the empirical difficulty of parameterizing more complex models has slowed progress. Here I test an environmentally dependent Integral Projection Model (IPM), which predicts patterns of size distribution across multiple spatial scales across the Strait of Juan de Fuca (Easterling, Ellner, and Dixon 2000). The model makes accurate predictions across a range of locations and environmental conditions, and suggests a complex determination of size structure mediated by different suites of causes at each spatial scale. Parameterization of the model was aided by the the nearly one dimensional (intertidal) range of *Mytilus californianus*, and the plethora of prior investigations of the species ecology.

Many models describe spatial distributions with varying degrees of complexity, the simplest models of species ranges, "bioclimatic envelope models", correlate population density with a small number of environmental predictors (Araújo and Peterson 2012). These models have often been parameterized and can predict distributional limits for some species. In other situations more complex models potentially including demographic dependence on environmental variables, scale dependent dynamics, species interactions, and evolutionary dynamics may be required to make accurate

predictions (Angert and Schemske 2005; Holt 2003). Few of the more complex models including demographic or evolutionary interactions have been parameterized, therefore it is unclear how complex models of range limits need to be.

A vigorous debate exists between proponents of "Top Down" and "Bottom Up" controls on community organization. Recently syntheses have been proposed which incorporate both kinds of factors to explain community structure (Menge 2000; Robles and Desharnais 2002). Most of the work supporting the bottom up paradigm has been correlative; investigations show correlations between metrics of community structure or community representation without proposing or testing models that make explicit quantitative connections between bottom up effects and the determination of population density. The IPM allows dissection of the importance of each vital rate across environmental contexts, this makes it possible to test the demographic relevance of observed variation in growth, recruitment, and survival rates. Thus analysis of the model can be used to test an important tacit assumption of many investigations which support strong "Bottom Up" controls on community structure, that observed variation in growth rates or recruitment rates between areas of hi and low mussel density are sufficient to cause observed demographic variation.

The IPM was developed and tested in order to answer the following four questions bearing on the determination of size structure across environmental gradients and location: 1. What is the minimum set of ecological factors needed to predict the presence or absence of the species across the landscape? 2. Are distributional limits and changes in population density caused by modification of single or multiple population vital rates? 3. Are distributional patterns apparent at multiple spatial scales mediated by identical processes? 4. Does a sensitivity analysis of the model suggest that the bottom up effects of variation in food supply or recruitment rate strongly influence the population density of mussels given the variation in growth and recruitment observed?

5.2 Methods

The model was parameterized on Tatoosh Island and at four sites spanning the Strait of Juan de Fuca using data collected during 2008-2010 (see Chapter 5). A penalized likelihood method was used to arrive at minimal models of mussel growth and survival rates. Comparison of parameter estimates explored the determination of population density and distributional limits across multiple scales. Sensitivity analysis elucidated the relative importance of variation in growth, survival, and recruitment to determination of population density.

5.2.1 Model Overview

The model was a modified version of the integral projection model or IPM described by Easterling, Ellner, and Dixon (2000). The number of individuals at time t_2 of size y given an initial size distribution $N(x, t_1)$ is described by the equation:

$$N(y, t_2) = \sigma + \int_{L_{min}}^{L_{max}} S(x, T)G(x, y, T)N(x, t_1)\ dx \tag{5.1}$$

$T = t_2 - t_1$ (14 days)
$S(x, E_{st}, T)$ = the probability of individuals of size x surviving the interval T
$G(x, y, E_{st}, E_{hp}, c_j, T)$ = the probability of being size y at time t_2 given initial size
L_{max} =maximum length
L_{min} = the length of a newly settled recruit(0.039 cm)

There are several differences between the original Easterling, Ellner, and Dixon (2000) model and this model. The fecundity term was removed from within the integral and replaced with the recruitment term σ, which was defined to be independent of the state of the population and was modeled as a constant influx. At the beginning of each iteration, a constant number of recruits (σ) were added to the first size class. Additionally the growth and survival models depended on environmental variables and the location's local growth regime. The growth, survival, and recruitment functions are described below in the Results section.

In practice the model is not solved analytically but is discretized and approximated in order to simulate the changes in population density through time. A projection matrix composed of probabilities of transitioning between any initial and final size is defined across the size range of the species. This matrix can then be multiplied by a vector of current sizes of mussels $N(x, t_1)$ to obtain a prediction of the new size distribution. Necessitating the choice of a parameter n defining the number of size classes used in the discretization (the dimension of the matrix): n=1200 was chosen. Simulations performed with larger values showed similar results; smaller values of n eventually result in a breakdown of model function and the accuracy of results. Coan, Scott, and Bernard (2000) reported the maximum size of *Mytilus californianus* as 25 centimeters, 30 cm was used in the model as a conservative value. An realization of the model represented 14 days, the mean deployment time of Tuffy™recruitment collectors.

The model was fit to the size distribution data of all plots leaving only σ as a free parameter using optim() in R Ver. 3.1.1. The number of iterations was set to the mean age plus one standard deviation of mussels in the size structure sample. Ages were calculated based on the empirically estimated growth curves. Simulations began with zero population density and grew only with the bi-monthly addition of recruits. The sum of squared errors between the predicted and empirical size distributions of individuals greater than 1 cm was used as the objective function in model fitting. Juvenile mussel survival was assumed equal to literature estimates for planktonic larvae at settlement, (since no estimates exist for settled recruits) and then rises linearly to the adult value by a size of 1 cm (Becker et al. 2007). Once estimates of recruitment rates were obtained by fitting, the estimates of σ were compared to the Tuffy™measured rates across the Strait, and an ANCOVA was performed on the mean fitted σ of each plot, for comparison to the recruitment estimates for Tuffy's™in Chapter 4.

5.2.2 Mussel Growth Model

In the IPM, the growth function G was based on the model version with the lowest AICc (see equations 5.2-5.6 in chapter 5). It was similar to the other two supported models, of intermediate complexity, and had the lowest error of all models. The variance model was dependent on initial length and submergence time (see table 4.2 for parameter values). The probability of growth to another size y given initial length x and time interval T was calculated (as equation 5.6). Final length was assumed to be a normally distributed random variable with expectation L_{t_2}, standard deviation $\sqrt{var(L_{t_2})}$, and cumulative distribution function Φ.

$$a_{(E_{st},E_{hp},c_j)} = m * ln(E_{st}) + d * ln(E_{hp}) + c_j + f \tag{5.2}$$

$$var(L_{t_2}) = g\Delta t + hE_{st} \tag{5.3}$$

$$L_u = y + \frac{L_{max} - L_{min}}{2 * n} \tag{5.4}$$

$$L_l = y - \frac{L_{max} - L_{min}}{2 * n} \tag{5.5}$$

$$G(x, y, T) = \Phi_(x_{t_2}, \sqrt{var(L_{t_2})})|_{L_u} - \Phi(x_{t_2}, \sqrt{var(L_{t_2})})|_{L_l} \tag{5.6}$$

5.2.3 Mussel Survival Model

Local adaptation repressed survival rates in transplanted juvenile mussels (see Chapter 2). When mussels were transplanted to lower submergence times than they developed in the difference between survival rates was predicted by the change in submergence time (ΔE_{st}) (see appendix 7.3 and figure 5.1). A model describing this relation (figure 5.1) was combined with a model predicting $log(\mu)$ as a function of $ln(asin(\sqrt{E_{st}}))$ of transplanted adult mussels to develop the local adaptation corrected μ_{Adult} function used in the IPM (see figure 5.2). Equation 5.9, which was used

to predict adult μ in the IPM, combines equations 5.7 and 5.8 (see tables 7.3 and 4.4 for parameter values).

No data describing juvenile (<1 cm) survival were collected and few data exists in the literature; Becker et al. (2007) estimated a mean time to death of 1.90 days for pre-settlement juveniles. No good estimates were available of post-settlement individual survival so juvenile mean time to death μ was assumed to rise linearly from 1.90 to μ_{Adult} at a length of 1 cm (see figure 5.3 and equation 5.10). Survival rate assuming constant size was calculated as shown in equation 5.11. The probability of survival through time was approximated as follows: 1. The predicted size of a growing individual was calculated for each day of the time interval using equation 4.4. Survival probabilities ($S(x, E_{st})$) were then calculated for each day based on the predicted size and the product of these used to calculate a probability of survival for the entire interval (equation 5.12).

$$\mu = e^{p*ln(asin(\sqrt{E_{st}}))+q} \tag{5.7}$$

$$\Delta ln(\mu) = r\Delta asin(\sqrt{E_{st}}) \tag{5.8}$$

$$\mu_{Adult} = e^{p*asin(\sqrt{E_{st}})+q+\Delta ln(\mu)} \tag{5.9}$$

$$\mu_{All} = \mu_{Adult} \qquad if(x >= 1)$$

$$\mu_{All} = \frac{\mu_{Adult} - 1.90}{1 - .039}(x - .039) + 1.90 \qquad if(x < 1) \tag{5.10}$$

$$S(x, E_{esl}) = e^{\frac{-1}{\mu_{All}}} \tag{5.11}$$

$$S(x, T) = \prod_{d=1}^{T} S(x_d, E_{esl}, d) \tag{5.12}$$

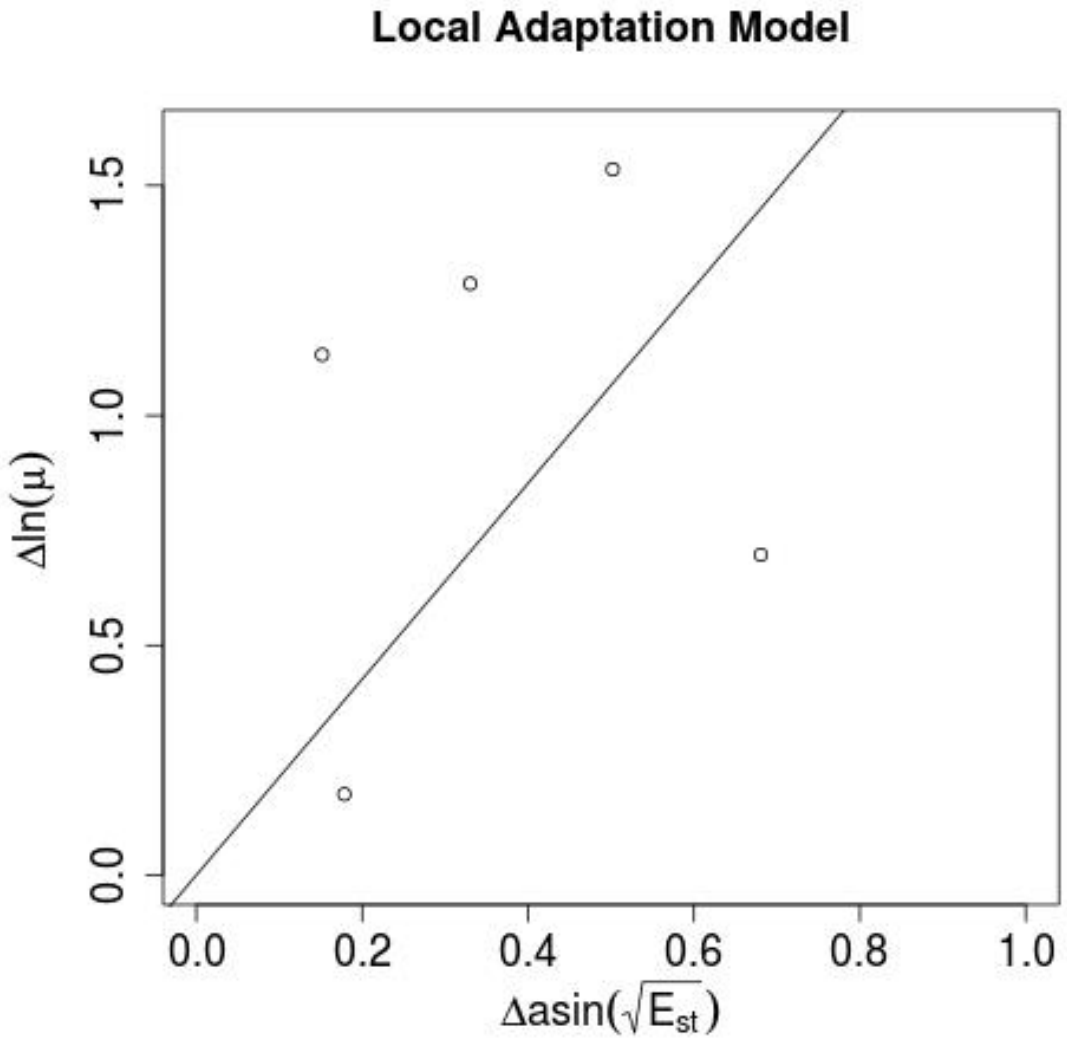

Figure 5.1: Change in survival as a function of change in submergence time, where survival is expressed at the ln, and submergence time is arc-sin square root transformed. The best fit line was constrained through the origin.

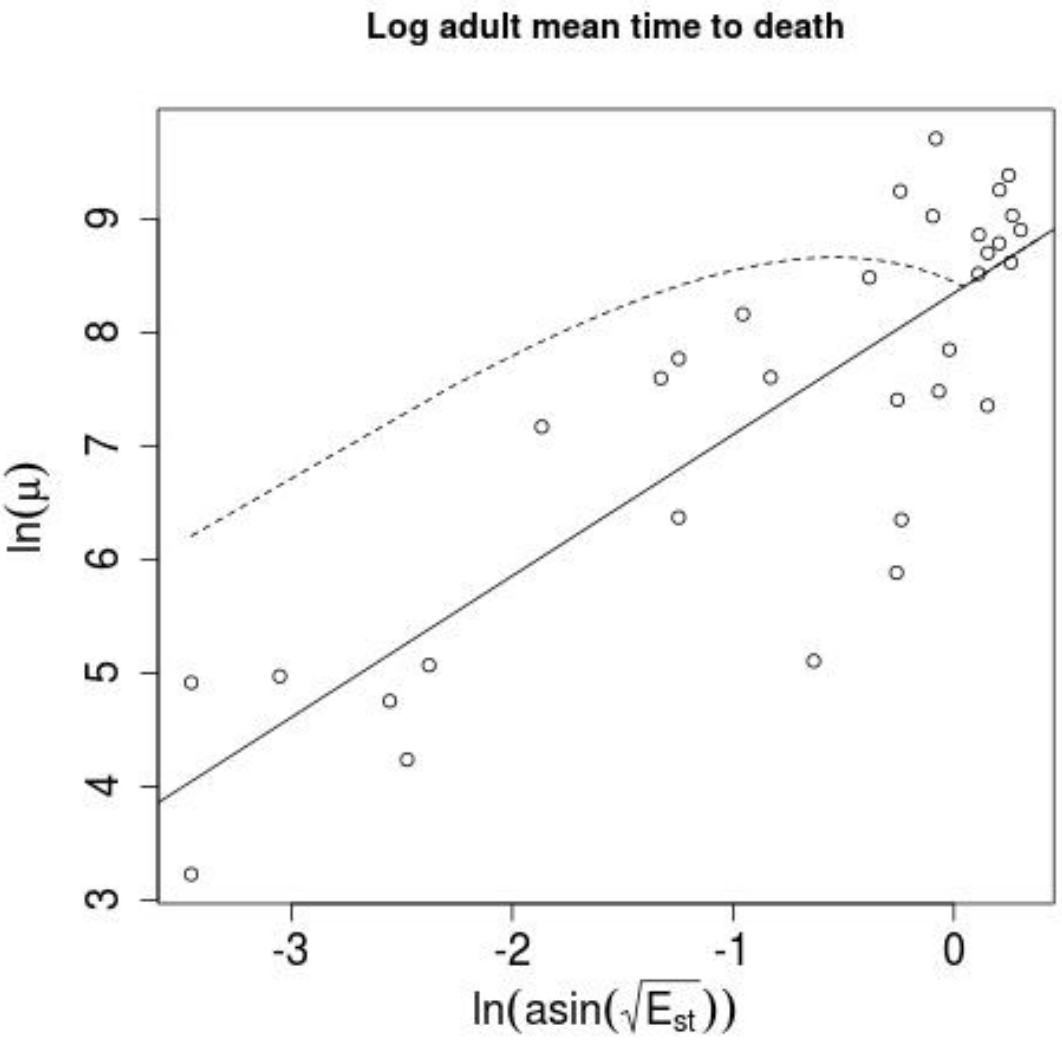

Figure 5.2: The relation between mussel life expectancy μ and submergence time. The dashed line shows the local adaptation correction μ function, circles are means from transplant plots. The correction is used when the new location has a lower submergence time than the origin population (origin submergence time=0.76).

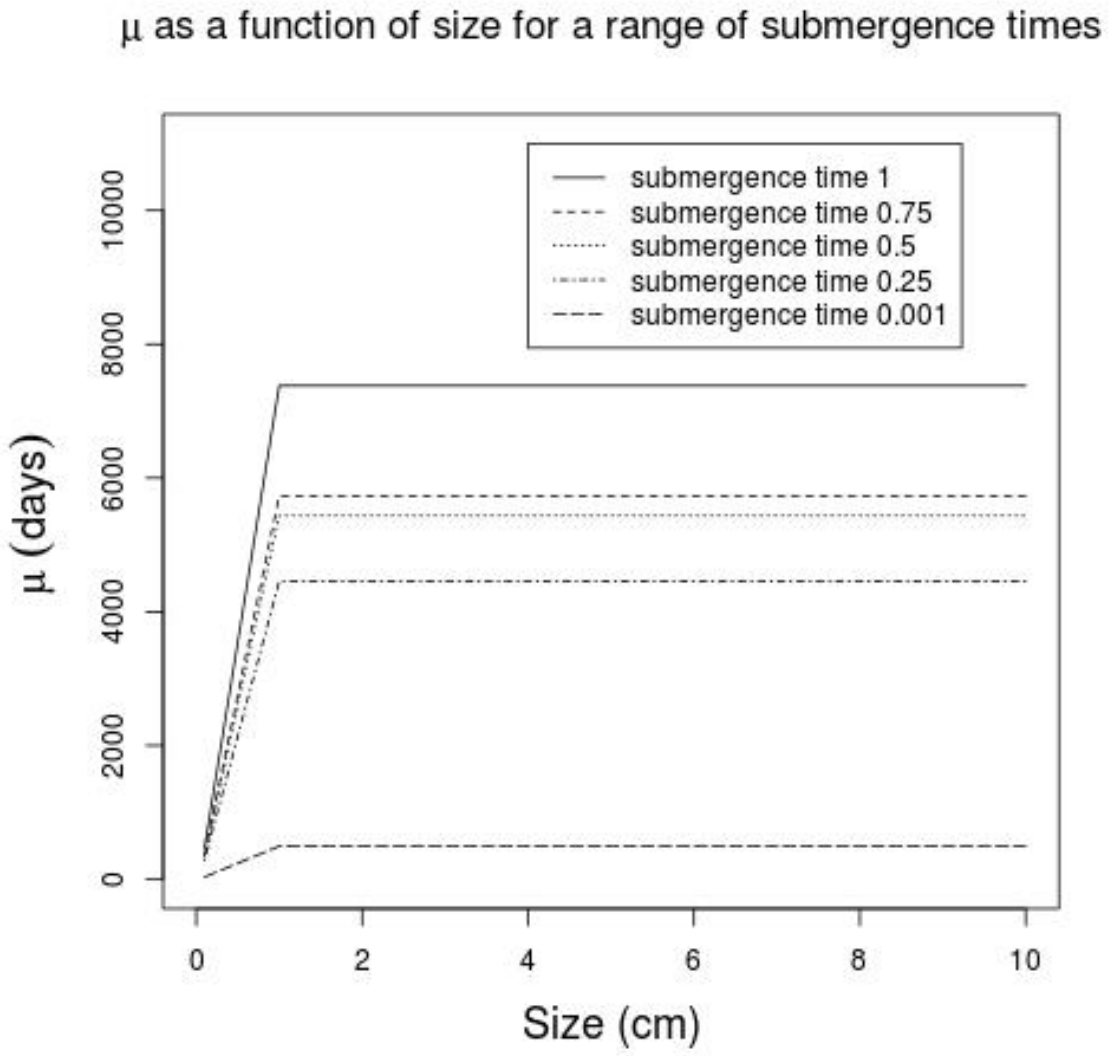

Figure 5.3: Mussel life expectancy (μ, mean time to death), across 5 submergence times as a function of mussel size. Juvenile survival was assumed to increase linearly with size until reaching the constant adult μat a size of 1 cm.

5.2.4 Sensitivity Analysis

To assess the relative importance of growth, survival, and recruitment in determining population density, a sensitivity analysis was performed. The model was simulated with the environmentally dependent parameters of one vital rate set at ± one standard error while the others were held at their estimates, across a range of submergence times. The recruitment function was based on the ANCOVA performed on the fitted values of σ across experimental plots.

The number of iterations was set to the mean age plus one standard deviation of Tatoosh mussels, which was equal to 264 two week periods. The total biomass of mussels at the end of each simulation was calculated using a regression between length and weight found in Suchanek (1979). The difference between total biomass at upper and lower parameter estimates was used as an estimate of the populations sensitivity to variation in each vital rate. Normalized or relative sensitivities were defined as the ratio of the difference in biomass's predicted at upper and lower limits of each vital rate over the largest difference in biomass's predicted across all vital rate model versions for each submergence time.

5.3 Results

5.3.1 IPM

The IPM fit independent size structure data well (see figure 5.4). Recruitment was left as a free parameter, juvenile survival was set to a low level, and all other parameters were empirically estimated or set a priori. The major difference between the predicted and actual size distributions is the stochastic nature of the data vs. the smoothed predictions of the model which assumed a constant rate of recruitment.

σ Realized recruitment

The fitted recruitment rates (σ) required to produce the most realistic predictions (realized recruitment) were one or two orders of magnitude lower than rates measured

Table 5.1: AICc comparison of models predicting ln σ or log realized recruitment, across the Strait of Juan de Fuca. NP=number of fit parameters, LW=likelihood weight.

$\sigma \sim$Explanatory var.	NP	AICc	LW
Intercept	1	73.95	<0.0001
$Subtime$	2	68.85	<0.0001
$Subtime + HP$	3	69.47	<0.0001
$Subtime + Place$	6	-4.76	0.08
$Subtime + Region$	5	-7.22	0.27
$Subtime + Region + HP$	7	-5.64	0.027
$Subtime + Place + HP$	8	-2.55	0.12
$Region$	5	-8.36	0.49

Table 5.2: Linear model of the fitted ln number of recruits needed to settle every two weeks into a 225 cm^2 area to best predict the observed size distribution. A factor aggregating Cape Flattery and Tatoosh is the reference factor and has a coefficient of 0. Adjusted-R^2 =0.92, n=33.

	Estimate	Std. Error	t value	Pr(>|t|)
(Intercept)	0.6872	0.1737	3.96	0.0005
Freshwater Bay	-1.0017	0.5014	-2.00	0.0552
Port Townsend	-3.0275	0.4428	-6.84	0.0000
Coffin Rocks	-8.7814	0.4428	-19.83	0.0000

by Tuffy™. ANCOVA of mean σ values obtained for each plot found that realized recruitment varied only with region and not with environmental gradients (see tables 5.1 and 5.2). The Pearson correlation coefficient for log realized recruitment and log Tuffy™recruitment was low and statistically insignificant (r=-0.03). Fitted recruitment was almost constant across submergence times in contrast to Tuffy™rates (see figures 5.6 and 5.5).

5.3.2 IPM predictions at Coffin Rocks

The model was fit to the four plots at Coffin Rocks assuming a density of one 8 cm mussel per square meter (a conservatively high estimate of density). A recruitment rate of 0.0021-0.00034 recruits per 2 weeks per 225 cm^2 was sufficient to sustain this density across submergence times (see figure 5.7).

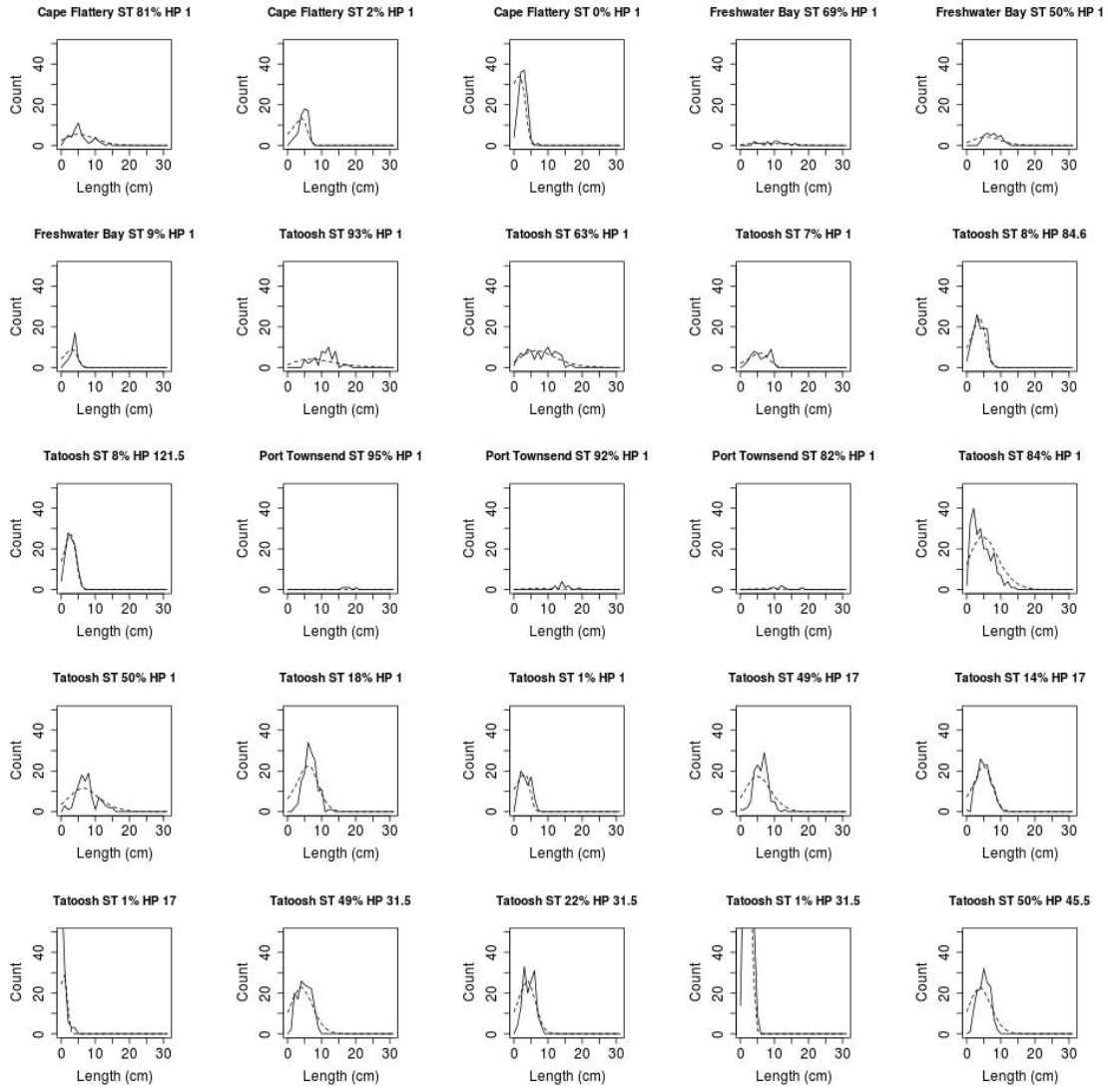

Figure 5.4: Fitted (dashed line) vs actual (solid line) size distributions across a range of locations, submergence times, and horizontal positions in 2010, ST=submergence time, and HP=horizontal position.

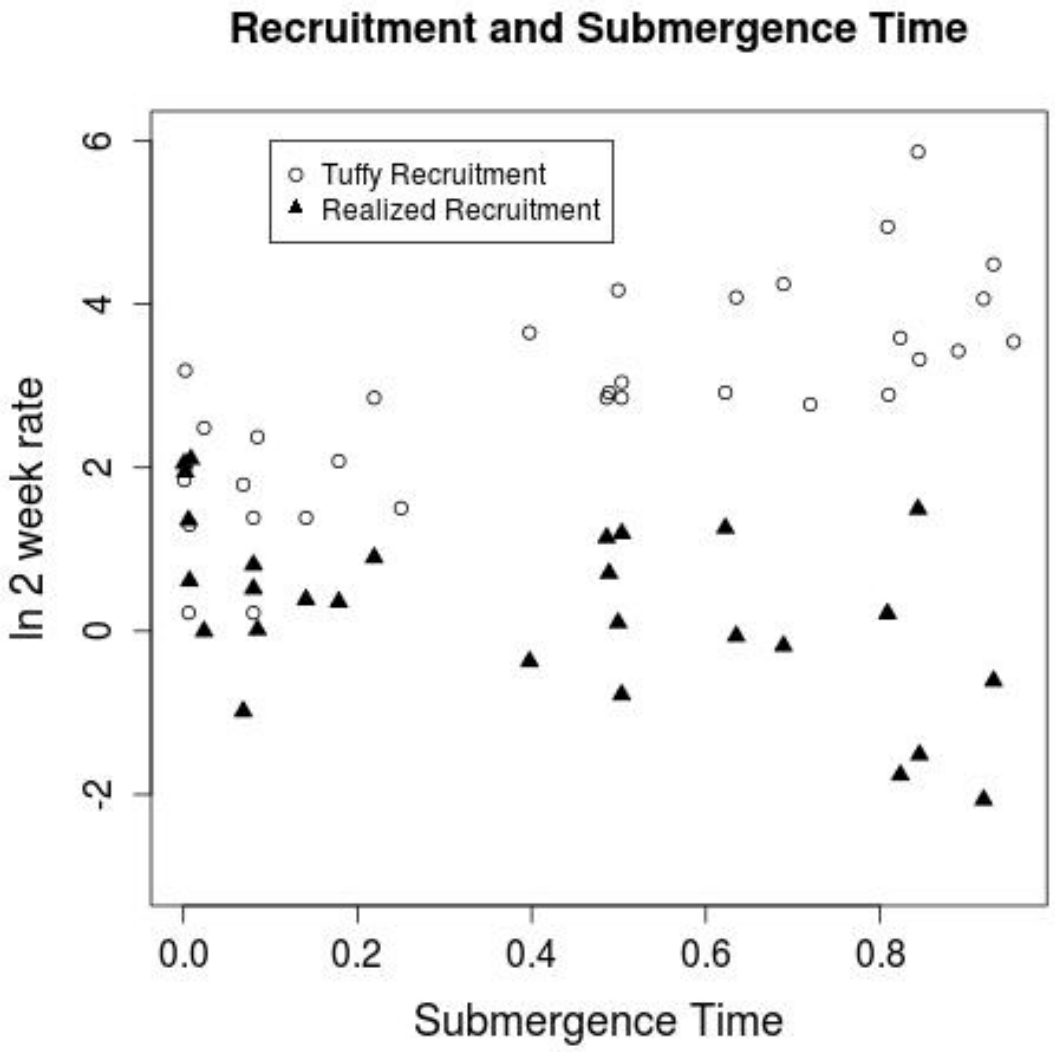

Figure 5.5: Realized recruitment (σ the rate of recruitment required to maintain observed size distribution), and Tuffy™recruitment rates as a function of submergence time.

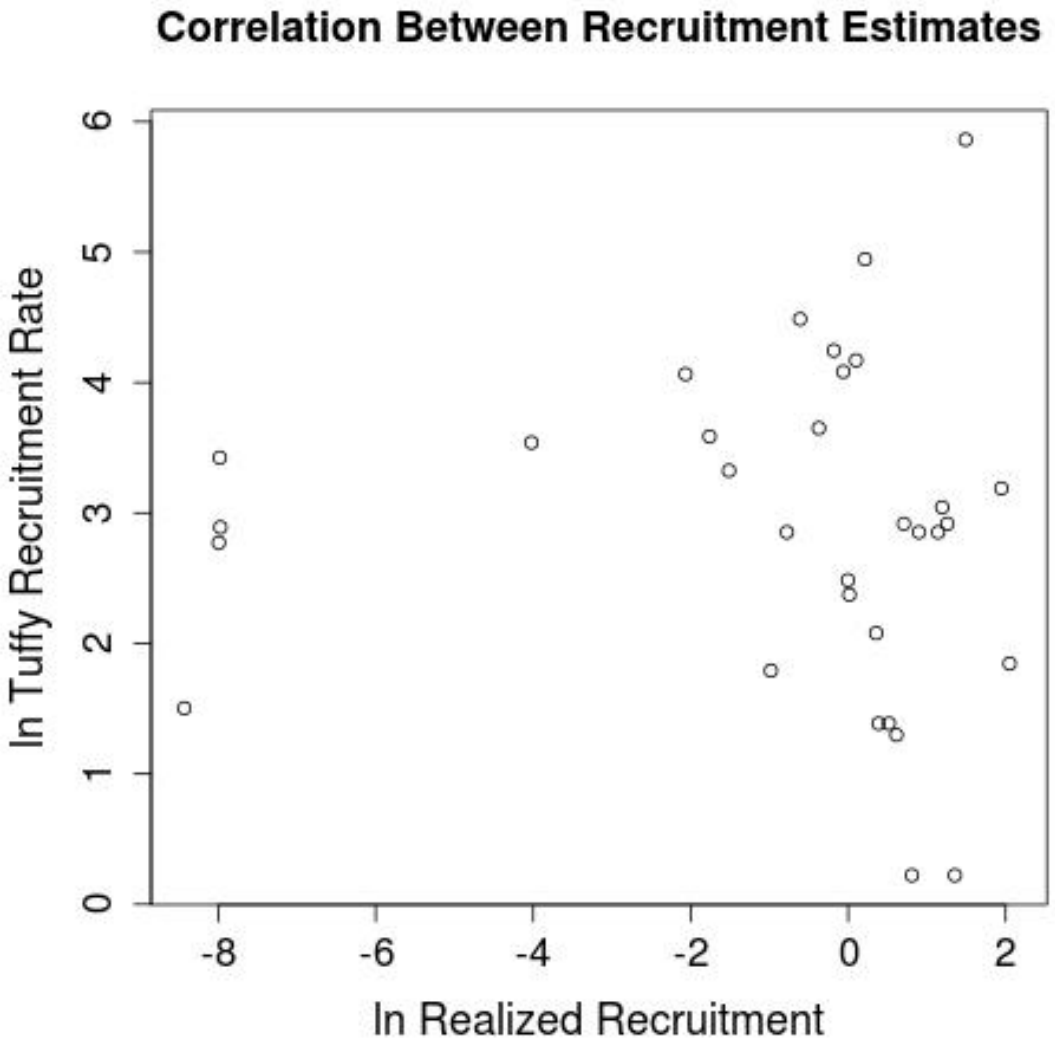

Figure 5.6: Nonsignificant correlation between log Tuffy™and log realized recruitment rate.

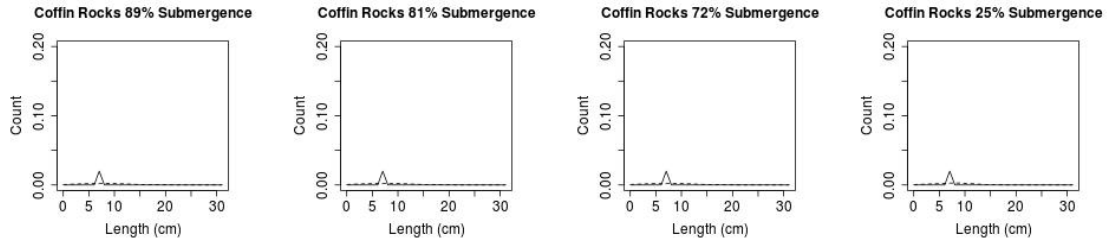

Figure 5.7: Fitted and actual mussel density at Coffin Rocks assuming one 8 cm long individual per square meter (note the truncated y-axis scale compared to figure 5.4).

5.3.3 Sensitivity of IPM

The model is most sensitive to variation in growth (see figure 5.8). Despite the populations sensitivity to the observed variation in growth, even at minimum growth estimates a positive population density is predicted. Recruitment, which can cause changes in biomass about one fifth as large as variation in growth, is the only vital rate which can cause a zero population density given its observed variation. The local maxima in predicted biomass apparent for maximum growth in figure 5.8 is caused by the non-monotonic μ function which was corrected for local adaptation.

Relative sensitivities were defined as the ratio of the difference in biomass predicted at min and max estimates of one vital rate over the maximum difference of biomasses predicted across the min and max of all vital rates. Variation in survival caused approximately one tenth the amount of variation in biomass as observed growth variation, and minimum estimates of survival were insufficient to cause a zero population density. At low submergence times at the upper intertidal limit of the mussel bed the IPM was most sensitive to survival but was still nearly as sensitive to observed variation in growth, suggesting that the repression of survival and growth rates in the high intertidal combine to cause the upper range limit (see figure 5.9).

5.3.4 Simulated Mussel Bed Morphology

The model was simulated across a 25x25 grid of submergence times and horizontal positions to illustrate the vertical and horizontal patterns in mussel mass per unit

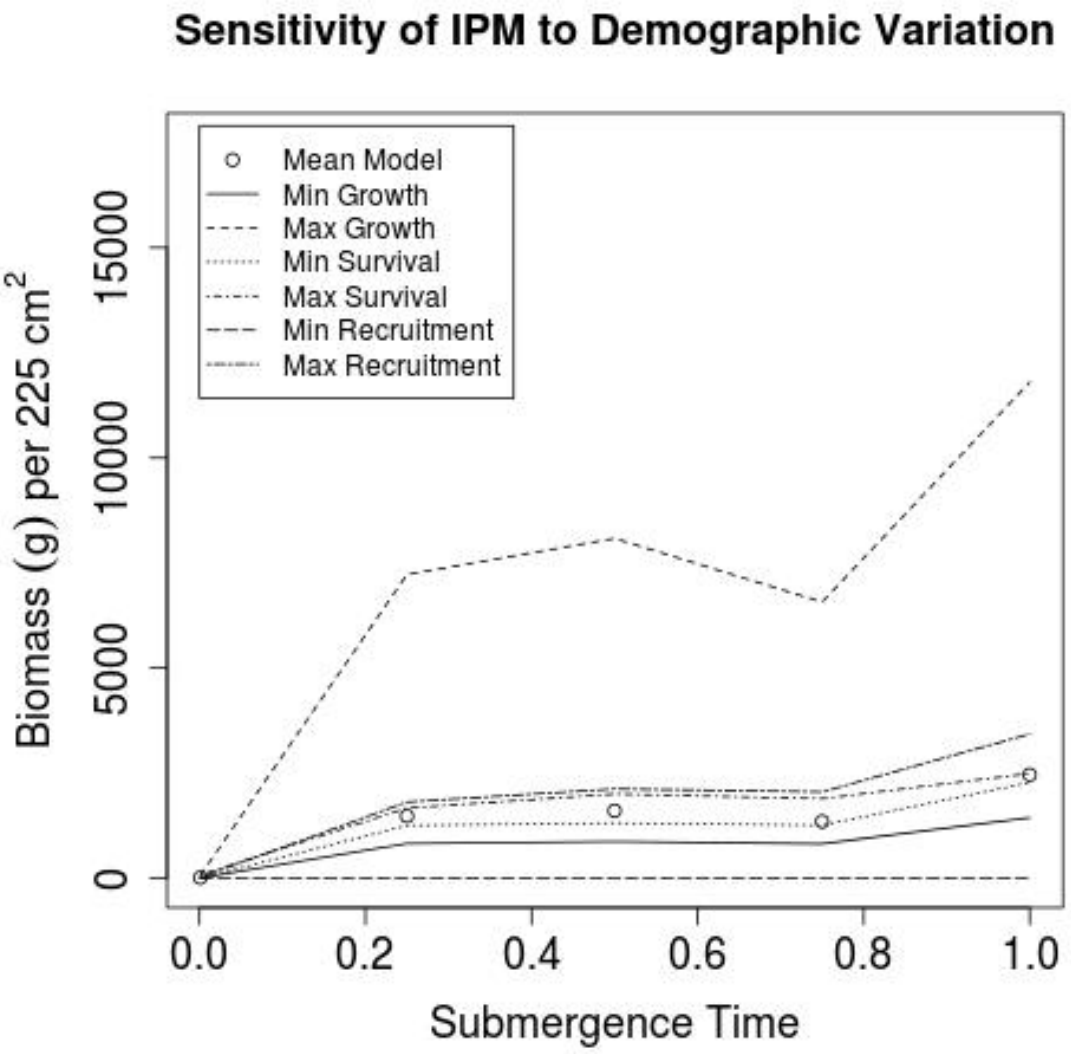

Figure 5.8: The range of biomass per unit area predicted by model versions assuming high and low growth, survival, and recruitment rates across submergence times. High and low estimates were constructed by adding or subtracting one standard deviation from mean coefficient estimates for each vital rate model.

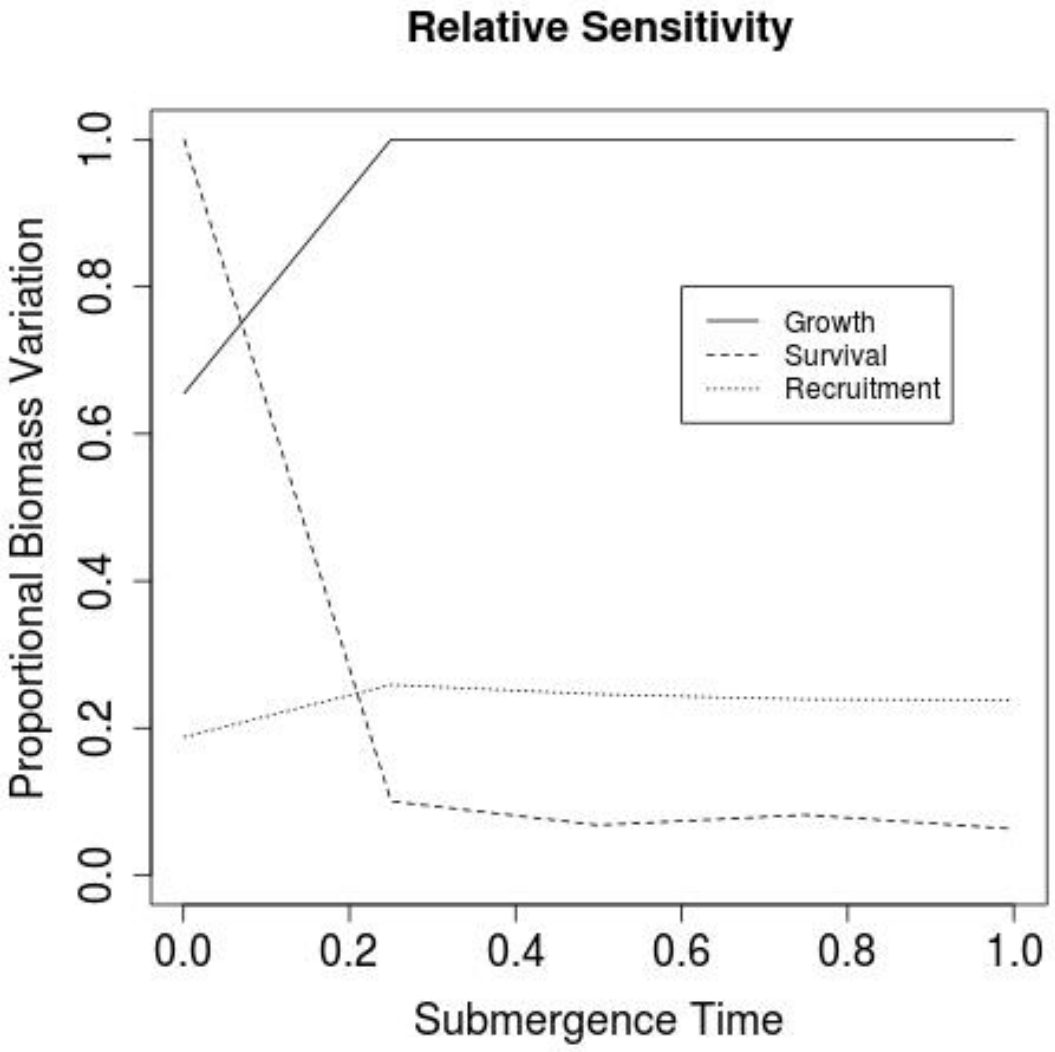

Figure 5.9: The relative sensitivity of the model to variation in each vital rate, where increasing values indicate that variability in a vital rates causes a large proportion of observed variation in biomass per unit area.

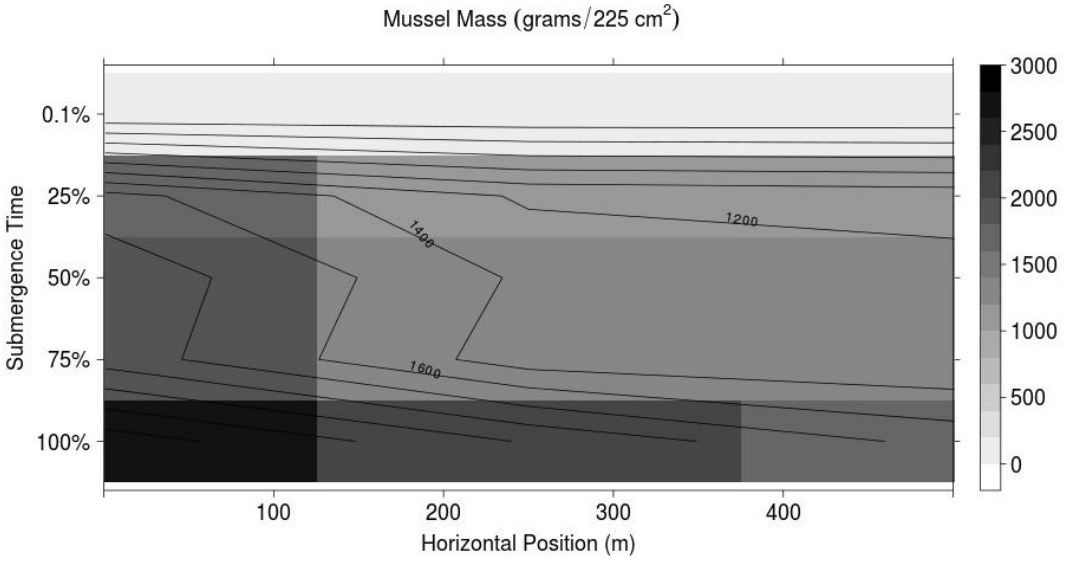

Figure 5.10: The mussel mass per unit area of a simulated mussel bed on Tatoosh or Cape Flattery assuming no disturbance or predation. The graph is oriented similarly to the photograph of Strawberry Point shown in figure 3.5. A horizontal position equal to 1 indicates the end of a wave exposed point.

area. Recruitment was set to the value predicted for Tatoosh/Cape Flattery by the ANCOVA analyzing variation in realized recruitment σ (see figure 5.10). The model predicts the upper intertidal limit of the mussel bed as well as the along shore decline in biomass.

5.4 Discussion

5.4.1 Model Fit

The model produces biologically plausible results across a range of submergence times and locations. The assumption of constant recruitment rate accounts for the much larger stochasticity observed in size structure samples compared to model outputs. If a stochastic rate was simulated the model could produce similar trajectories to those observed. Alternatively the model could also be used to hind-cast recruitment and potentially estimate prior recruitment rates. The IPM predicts the existence of the upper intertidal limit and the decline in the upper limit horizontally along

the shore as a consequence of changes in submergence time, horizontal position, and location which influence growth, survival, and recruitment rates. The lower limit of the mussel bed is not predicted because the model did not include predation. The lower limit is most likely set by the interaction of mussel production rates and the consumption rates of predators such as *Pisaster ochraceous* (Paine 1966; Robles and Desharnais 2002). Recruitment limitation appears most likely to prevent higher densities at Coffin Rocks forming the largest scale distributional limit observed. The lack of recruits could be caused by a lack of transport or by mortality due to low salinity events emanating from Deception Pass. Young (1941) showed that juvenile *Mytilus californianus* are very salinity sensitive.

The results and size structure data show that infrequent and low rates of recruitment are sufficient to maintain one hundred percent cover in the mid intertidal, confirming the theoretical results of Petraitis (1995). For example the size structure at Port Townsend is dominated by small numbers of massive individuals which all likely settled during one season ten or more years ago. (see figure 5.4). These old individuals cover 100% of the surface area. At outer coast locations disturbance may increase the populations sensitivity to recruitment since mortality rates may be higher. However, these populations appear to receive almost constant recruitment resulting in the relatively smooth filled out size distributions observed at high submergence times on Tatoosh (see figure 5.4).

5.4.2 Tuffy™ vs. Realized Recruitment σ

Tuffy's™ when unwrapped represent approximately 920 cm^2 of surface area, they collect tens to hundreds more *Mytilus* recruits than are needed to maintain observed densities in 225 cm^2 core samples. There also appear to be environmental factors affecting Tuffy™ recruitment rates which are not relevant to the determination of realized recruitment σ. Additionally Tuffy™ rates may be elevated by accidental counting of congeners which are common and difficult to identify. The discrepancy between apparent delivery rates at outer coast locations and realized rates may be explained by increased rates of mortality or to misidentification of congeners. The lack of real

data for small juvenile survival was compensated for by setting juvenile survival at a low level, but with an increasing linear rate until 1 cm in length. It may be that very small recruits or juveniles have extraordinarily low survivorship, and that the transition from recruit to the smallest measurable size is non-linear. Further investigation is needed to determine the precise functional form juvenile survivals dependence on size takes, the models relative insensitivity to survival and accurate prediction of upper the upper limit of the mussel bed suggest the assumed linear function is reasonable.In sum Tuffy's™correctly identify the existence of regional variability in recruitment, but translating these values to demographic patterns is uncertain.

5.4.3 Local Adaptation

In the IPM, the survival model incorporated a local adaptation correction since survival rates were calculated using transplanted mussels. In the absence of this correction the model performs well in the low intertidal where most biomass is concentrated and where mussels were transplanted from, but performed poorly in the high intertidal under predicting the upper limit of the mussel bed. This and evidence in Chapter 2 show that mussels are locally adapted at small scales, and that their variation helps enable monopolization of a wide intertidal range.

5.4.4 Sensitivity Analysis

The primary message of the sensitivity analysis was that all three vital rates play important roles in the determination of spatial distribution. Not only is the model differentially sensitive to each vital rate, the importance of each rate is highly variable depending on environmental context. Biomass is most influenced by growth rates, which vary across at least 3 spatial scales, but only extremely low levels of recruitment can cause a zero population density. Survival accounts for more variation in biomass in the high intertidal than growth does, and plays a dominant role in setting the upper intertidal limit of the species, but is much less important at lower tide heights unless mortality from predation is included. This result suggests a nuanced but not overwhelmingly complex determination of spatial distribution. A model including lo-

cal growth and recruitment regimes, location on the submergence time and horizontal position gradients is sufficient to make accurate predictions of mussel size distribution within and at the fringes of the range contingent on the existence of stable debris free sufficiently large rock substrate.

5.4.5 The Complexity of Distributional Limits

The complexity of the processes found to underlie spatial distribution of *Mytilus californianus* suggests that changes in distribution could potentially occur as the result of multiple factors or their interactions. This contrasts with single or simple multi-factor models often used to predict current or future ranges. Not only are mussel population densities determined by local environmental conditions, they are impacted by the regional variation in recruitment and growth rates, and all three vital rates integrate to cause observed densities. More investigations comparing the relative importance of different processes to determination of species distributions are needed to develop generalizations concerning the average complexity of processes underlying species ranges. The present investigation supports the work of theoreticians who have proposed increasingly complex mechanisms which could underlie range limits, and suggests that further testing of models incorporating multiple ecological and evolutionary processes in addition to environmental variables is warranted.

5.4.6 Top Down and Bottom Up Effects as Determinants of Distribution

Mussels grew fastest at Coffin Rocks the site with lowest recruitment and mussel density. At large scales locations with the highest growth rates, had the lowest recruitment rates and population densities (Port Townsend and Coffin Rocks). These patterns were the opposite of what is expected in a "bottom-up" system. Additionally the population appears well buffered against recruitment limitation except at the longitudinal range limit, and requires small numbers of recruits to control the limiting resource space (Dayton 1971). Variation in the bottom up effects of growth and recruitment rates appear unlikely to play dominant roles in determining the presence or

absence of *Mytilus californianus* in Washington State. The high growth and survival rates of adult individuals within and at the edge of the range can compensate for a wide range of recruitment regimes enabling the species to maintain spatial dominance across a wide range of conditions.

5.4.7 Latitudinal Range Limits

Considering the complexity of distributional limits examined in the present investigation it seems likely that the largest scale latitudinal range limits in the species may have similarly complex causes. Changes in temperature, disturbance rate (due to ice scour and/or waves), and predation rates with latitude might combine to cause limits in complex ways via differential effects on multiple vital rates (McCook and Chapman 1997). It is also possible that discontinuities in the availability of suitable rocky substrate at the latitudinal limits prevents expansion of already increasingly marginal populations. More data describing the distribution and density of the species is needed. Development of methods to efficiently collect large scale accurate density data will greatly enhance the potential for understanding these limits.

5.4.8 Conclusion

The spatial distribution of *Mytilus californianus* is a result of the interaction of processes affecting growth, survival, and recruitment rates differently at several spatial scales. The population appears to be well buffered to recruitment limitation within its range and is primarily dependent on the availability of substrate at appropriate submergence times. The utilization of an explicit model defining the demographic dynamics and relative influence of vital rates enabled a detailed dissection of the implications of variation in ecological factors and population density. The method is general and could be applied to many other species. Synthesis regarding the generality of processes causing distributional patterns would be aided by the development of a data set of similarly modeled range limits spanning multiple taxa and geographies.

CHAPTER 6
CONCLUSION

In field guides ranges are usually depicted as shaded regions or solid lines, these metaphorical representations often mask complex spatial and demographic patterns. For example *Mytilus californianus*'s distribution is more accurately described as a discontinuous collection of distant high density populations within which multiple super high density bench sub-populations exist. In the Strait of Juan de Fuca, a few headland complexes probably account for the vast majority of mussel biomass, between these long stretches of beaches are totally devoid of mussels. Within each headland complex mussels are most concentrated on a few super exposed regions where shore angles are shallow enough to provide substantial habitat area. Thus the distribution of *Mytilus californianus* is largely influenced by the geologic processes which generate rocky coasts, and the interaction between shore shape and sea level rise. These processes appear uncoupled from the biological activity of mussels at least over hundreds of years.

At the scale of a single headland or rock bench the mussel bed often exists as a monoculture blanketing the end of the point and tapering away from wave exposure. Within the bed there is a complex demographic mosaic, joinlty determined by variation in growth, survival, and recruitment along environmental gradients, and density dependent disturbance. Mussels can maintain spatial dominance (100% cover) across a wide range of environmental conditions and recruitment regimes depending on disturbance rate. Port Townsend has low recruitment but easily maintains monoclture with a single old size class, on Tatoosh in high disturbance areas it seems unlikely a population could persist with such low or episodic recruitment.

At Coffin Rocks a lack of recruitment, or high predation preempt mussel bed development. However predation seems unlikely because of the presence of more palatable congeners *Mytilus edulis* and the existence of predation vulnerable single

Mytilus californianus in the mid intertidal. The lack of recruits could be due to a lack of transport or to juvenile sensitivity to low salinity water coming from Deception Pass. The local adaptation demonstrated along the tide height gradient throughout the Strait partially determines the width and especially the upper limit of the mussel bed. Thus potentially the distribution of *Mytilus californianus* in the Strait of Juan de Fuca is determined by geology, ecology, evolution, and developmental constraints. All of these figure into why mussels exist where they do, and why they are likely to change in distribution during the next 100 years.

7

APPENDIX

7.1 Appendix A: Comparison of Temperature Sensors

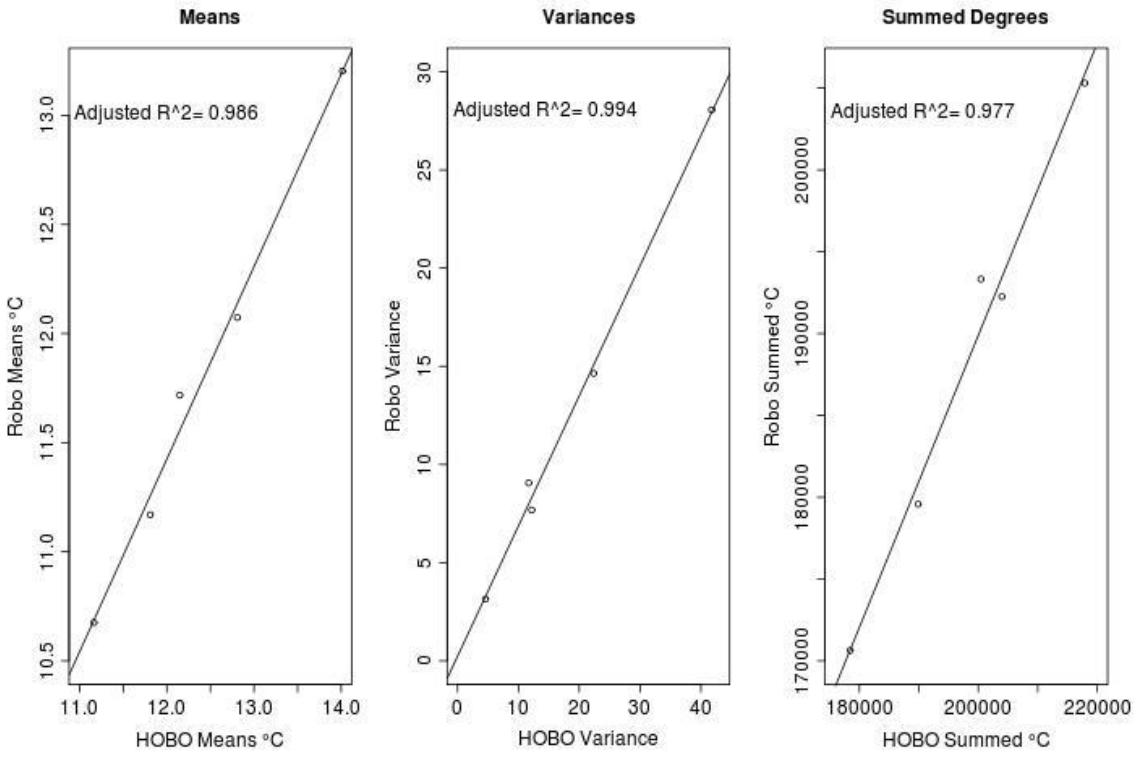

Figure 7.1: Regression between HOBO measured temperatures and Robo mussel temperature statistics. HOBO and Robo mussel pairs were maintained together at multiple tide heights on Tatoosh and at Port Townsend, and were deployed from the beginning of April 2010 to late August 2010.

7.2 Appendix B: Juvenile Mussel Growth

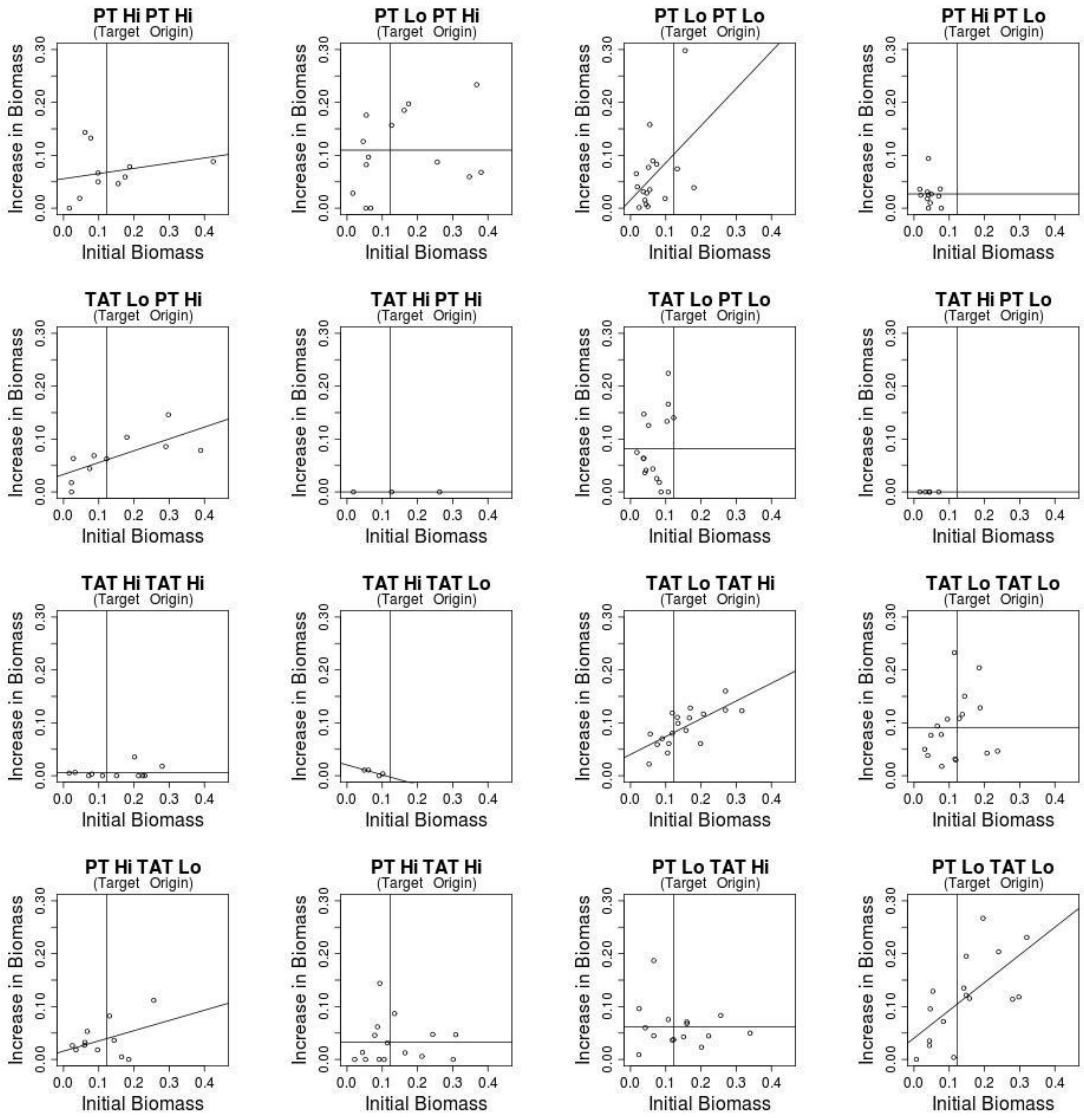

Figure 7.2: Growth of a typical mussel in each treatment. Horizontal lines are regressions and have slopes when AIC comparison supports a linear model with slope, otherwise the mean growth for all individuals in the treatment is used resulting in a horizontal line. Vertical lines show the mean mussel size for the experiment, line intersections indicate where a typical sized mussel growth was calculated to be.

7.3 Appendix C: Size Split Analysis

Table 7.1: Repeated analysis of the common garden linear model for the largest half of individuals in each treatment. TS=%Time Submerged, SD=Summed °C. Adjusted R^2=0.49.

Coefficient	Estimate	Std. Error	t-value	Pr(> |t|)
(intercept)	0.037	0.005	7.148	0.001***
Target SD	-0.019	0.007	-2.739	0.041*
Origin SD	-0.0013	0.007	-0.077	0.941
Target TS	0.0173	0.005	3.237	0.023*
Origin TS	-0.003	0.005	-0.501	0.638
Target SD x Origin SD	0.006	0.005	1.173	0.294
Target SD x Target TS	0.023	0.0011	2.120	0.087
Target SD x Origin TS	0.006	0.005	1.142	0.305
Origin SD x Target TS	0.009	0.005	1.652	0.159
Origin SD x Origin TS	0.011	0.011	0.890	0.414
Target TS x Origin TS	-0.005	0.005	-0.857	0.431

Table 7.2: Repeated analysis of the common garden linear model for the smaller half of individuals in each treatment.TS=%Time Submerged, SD=Summed °C. Adjusted R^2=0.43.

Coefficient	Estimate	Std. Error	t-value	Pr(> |t|)
(intercept)	0.079	0.019	4.24	0.002**
Target SD	-0.082	0.025	-3.282	0.008**
Origin SD	0.029	0.019	1.5	0.165
Target TS	0.026	0.019	1.35	0.207
Target SD x Origin SD	0.073	0.039	1.876	0.090
Target SD x TS	-0.026	0.020	-1.326	0.214

7.4 Appendix D: Coordinate Normalization and Rescale

In order to scale and reorient the Insight3d produced points, I transformed the orientation of the XYZ coordinate system by triangulating three points lying on the surface of the water surrounding the terrace. A second plane normal to the waters surface was then generated using the normal of the sea level plane and one of the sides of the triangle used to define it. Finally the cross product of the normal's of these two planes was taken to generate the normal of a third plane perpendicular to the other two. This procedure defined a natural XYZ coordinate system of three planes perpendicular to each other, with one parallel to the water. The minimum distance from each of the three planes to each vertex included in the set of triangles defining the surface of the terrace was then calculated and defined as the X, Y, or Z coordinate of the point. For example the minimum distance calculated from a point to the plane defined by the new X and Y axes, was defined as the new Z coordinate of the point. The units of the coordinate system were then scaled with reference to distances among multiple reference points measured in situ with a measuring tape.

7.5 Appendix E: Discretization of Triangular Surfaces

In order to discretize the triangles representing the surface of the Strawberry Point the following procedure was followed: 1). The longest side of the triangle was found (Segment AC in fig 3.6). 2).The length of segment BD was calculated and divided by the side length of the square discretization unit (15 cm) giving the number of rows of squares that would fit between the longest side and the opposite point. 3). The endpoints of segments parallel to the longest side joining the two shorter legs of the triangle (segments connected by the filled circles in figure 3.6) were calculated. 4). The position of points along each parallel segment one discretization unit from one another were then calculated. These were used as the center points of squares for which specific tidal heights could be calculated (unfilled circles in fig. 3.6). The imperfect matching between the edges of the squares representing discretization units is negligible in the analysis because the size of the discretization unit becomes small

relative to the lengths of the sides of the triangular surfaces.

7.6 Appendix F: Survival Local Adaptation Model

Table 7.3: Model predicting $\Delta ln(\mu)$ due to transplant to a lower submergence time. Data from chapter 2 juvenile transplant experiments. Adjusted-R^2 =0.60, n=5.

	Estimate	Std. Error	t value	Pr(>|t|)
$\Delta asin(\sqrt{E_{st}})$	2.1306	0.7193	2.96	0.0415

REFERENCES

Addison, Jason A. et al. (2008). "Range-wide genetic homogeneity in the California sea mussel (Mytilus californianus): a comparison of allozymes, nuclear DNA markers, and mitochondrial DNA sequences". In: *Molecular Ecology* 17.19, pp. 4222–4232. ISSN: 1365-294X. DOI: 10.1111/j.1365-294X.2008.03905.x. URL: http://dx.doi.org/10.1111/j.1365-294X.2008.03905.x.

Angert, AL and DW Schemske (2005). "The Evolution of Species' Distributions: Reciprocal Transplants Across The Elevation Ranges of Mimulus cardinalis AND M. Lewisi". In: *Evolution* 59.8, pp. 1671–1684.

Araújo, Miguel B and A Townsend Peterson (2012). "Uses and misuses of bioclimatic envelope modeling". In: *Ecology* 93.7, pp. 1527–1539.

Barton, NH (2001). "Adaptation at the edge of a species' range". In: *Special Publication-British Ecolgical Society* 14, pp. 365–392.

Bayne, B. L. and C. Scullard (May 1977). "Rates of nitrogen excretion by species of Mytilus (Bivalvia: Mollusca)". In: *Journal of the Marine Biological Association of the United Kingdom* 57 (02), pp. 355–369. ISSN: 1469-7769. DOI: 10.1017/S0025315400021809. URL: http://journals.cambridge.org/article_S0025315400021809.

Bayne, B.L. et al. (1976). "The physiological ecology of Mytilus californianus Conrad". In: 22.3, pp. 229–250–. ISSN: 0029-8549. URL: http://dx.doi.org/10.1007/BF00344794.

Beale, Colin M., Jack J. Lennon, and Alessandro Gimona (2008). "Opening the climate envelope reveals no macroscale associations with climate in European birds". In: *Proceedings of the National Academy of Sciences* 105.39, pp. 14908–14912. DOI: 10.1073/pnas.0803506105. eprint: http://www.pnas.org/content/105/39/14908.full.pdf+html. URL: http://www.pnas.org/content/105/39/14908.abstract.

Becker, Bonnie J et al. (2007). "Complex larval connectivity patterns among marine invertebrate populations". In: *Proceedings of the National Academy of Sciences* 104.9, pp. 3267–3272.

Berry, P. M. et al. (2002). "Modelling potential impacts of climate change on the bioclimatic envelope of species in Britain and Ireland". In: *Global Ecology and Biogeography* 11.6, pp. 453–462. ISSN: 1466-8238. DOI: 10.1111/j.1466-8238.2002.00304.x. URL: http://dx.doi.org/10.1111/j.1466-8238.2002.00304.x.

Bird, Eric Charles Frederick and Maurice L Schwartz (2000). *Shore platforms at cape flattery, Washington*. Washington State Department of Natural Resources, Division of Geology and Earth Resources.

Blanchette, CA, B Helmuth, and SD Gaines (2007). "Spatial patterns of growth in the mussel, Mytilus californianus, across a major oceanographic and biogeographic boundary at Point Conception, California, USA". In: *Journal of Experimental Marine Biology and Ecology* 340.2, pp. 126–148.

Blondel, Jacques et al. (1992). "Do harlequin Mediterranean environments function as source sink for Blue Tits Parus caeruleus?" In: *Landscape Ecology* 6 (3). 10.1007/BF00130032, pp. 213–219. ISSN: 0921-2973. URL: http://dx.doi.org/10.1007/BF00130032.

Bridle, Jon R, Sedef Gavaz, and W Jason Kennington (2009). "Testing limits to adaptation along altitudinal gradients in rainforest Drosophila". In: *Proceedings of the Royal Society B: Biological Sciences* 276.1661, pp. 1507–1515.

Brown, James H, George C Stevens, and Dawn M Kaufman (1996). "The geographic range: size, shape, boundaries, and internal structure". In: *Annual review of ecology and systematics*, pp. 597–623.

Brysse, Keynyn et al. (2013). "Climate change prediction: Erring on the side of least drama?" In: *Global Environmental Change* 23.1, pp. 327–337.

Camin, Joseph H and Paul R Ehrlich (1958). "Natural selection in water snakes (Natrix sipedon L.) on islands in Lake Erie". In: *Evolution*, pp. 504–511.

Carson, Henry S et al. (2011). "Evaluating the importance of demographic connectivity in a marine metapopulation". In: *Ecology* 92.10, pp. 1972–1984.

Case, Ted J, Mark L Taper, et al. (2000). "Interspecific competition, environmental gradients, gene flow, and the coevolution of species' borders". In: *The American Naturalist* 155.5, pp. 583–605.

Cazenave, Anny and Robert S Nerem (2004). "Present-day sea level change: Observations and causes". In: *Reviews of Geophysics* 42.3.

Choi, Kwang Hee et al. (2012). "Using cosmogenic 10Be dating to unravel the antiquity of a rocky shore platform on the west coast of Korea". In: *Journal of Coastal Research* 28.3, pp. 641–657.

Church, John A and Neil J White (2006). "A 20th century acceleration in global sea-level rise". In: *Geophysical research letters* 33.1.

Coan, Eugene V, Paul Valentich Scott, and Frank R Bernard (2000). *Bivalve seashells of western North America: marine bivalve mollusks from Arctic Alaska to Baja California*. 2. Santa Barbara Museum of Natural History.

Connell, Joseph H (1961). "The influence of interspecific competition and other factors on the distribution of the barnacle Chthamalus stellatus". In: *Ecology* 42.4, pp. 710–723.

— (1972). "Community interactions on marine rocky intertidal shores". In: *Annual Review of Ecology and Systematics*, pp. 169–192.

Connolly, Sean R, Bruce A Menge, and Joan Roughgarden (2001). "A latitudinal gradient in recruitment of intertidal invertebrates in the northeast Pacific Ocean". In: *Ecology* 82.7, pp. 1799–1813.

Dasgupta, Rajarshi (2010). "Whither shore platforms?" In: *Progress in Physical Geography*.

Day, John W et al. (1995). "Impacts of sea-level rise on deltas in the Gulf of Mexico and the Mediterranean: the importance of pulsing events to sustainability". In: *Estuaries* 18.4, pp. 636–647.

Dayton, Paul K. (Oct. 1971). "Competition, Disturbance, and Community Organization: The Provision and Subsequent Utilization of Space in a Rocky Intertidal Community". In: *Ecological Monographs* 41.4, pp. 351–389. ISSN: 0012-9615. URL: http://dx.doi.org/10.2307/1948498.

Dehnel, Paul A. (1956). "Growth rates influence lattitudinally and vertically separated populations of Mytilus californianus". In: *The Biological Bulletin* 110.1, pp. 43–53. eprint: http://www.biolbull.org/content/110/1/43.full.pdf+html. URL: http://www.biolbull.org/content/110/1/43.abstract.

Denny, Mark W and Steven Dean Gaines (2007). *Encyclopedia of tidepools and rocky shores*. 1. Univ of California Press.

Denny, Mark W et al. (2011). "Spreading the risk: small-scale body temperature variation among intertidal organisms and its implications for species persistence". In: *Journal of Experimental Marine Biology and Ecology* 400.1, pp. 175–190.

Dias, Paula C. and Jacques Blondel (1996). "Local specialization and maladaptation in the Mediterranean blue tit Parus caeruleus". In: *Oecologia* 107 (1). 10.1007/BF00582237, pp. 79–86. ISSN: 0029-8549. URL: http://dx.doi.org/10.1007/BF00582237.

Easterling, Michael R, Stephen P Ellner, and Philip M Dixon (2000). "Size-specific sensitivity: applying a new structured population model". In: *Ecology* 81.3, pp. 694–708.

Emery, KO and GG Kuhn (1982). "Sea cliffs: their processes, profiles, and classification". In: *Geological Society of America Bulletin* 93.7, pp. 644–654.

Filin, Ido, Robert D. Holt, and Michael Barfield (2008). "The Relation of Density Regulation to Habitat Specialization, Evolution of a Species Range, and the Dynamics of Biological Invasions." English. In: *The American Naturalist* 172.2, pp. 233–247. ISSN: 00030147. URL: http://www.jstor.org/stable/10.1086/589459.

Fish, Marianne R et al. (2005). "Predicting the Impact of Sea-Level Rise on Caribbean Sea Turtle Nesting Habitat". In: *Conservation biology* 19.2, pp. 482–491.

Fujii, Toyonobu and Dave Raffaelli (2008). "Sea-level rise, expected environmental changes, and responses of intertidal benthic macrofauna in the Humber estuary, UK". In: *Mar Ecol Prog Ser* 371, pp. 23–35.

Gaines, Steven D and Mark D Bertness (1992). "Dispersal of juveniles and variable recruitment in sessile marine species". In: *Nature* 360.6404, pp. 579–580.

Galbraith, H et al. (2002). "Global climate change and sea level rise: potential losses of intertidal habitat for shorebirds". In: *Waterbirds* 25.2, pp. 173–183.

Goldberg, Emma. and Russell Lande (2006). "Eological and Reproductive Character Displacement of an Environmental Gradient". In: *Evolution* 60.7, pp. 1344–1357. ISSN: 1558-5646. DOI: 10.1111/j.0014-3820.2006.tb01214.x. URL: http://dx.doi.org/10.1111/j.0014-3820.2006.tb01214.x.

Haldane, JBS (1956). "The relation between density regulation and natural selection". In: *Proceedings of the Royal Society of London. Series B, Biological Sciences*, pp. 306–308.

Harley, Christopher DG (2011). "Climate change, keystone predation, and biodiversity loss". In: *Science* 334.6059, pp. 1124–1127.

Harley, Christopher DG and Brian ST Helmuth (2003). "Local-and regional-scale effects of wave exposure, thermal stress, and absolute versus effective shore level on patterns of intertidal zonation". In: *Limnology and Oceanography* 48.4, pp. 1498–1508.

Helmuth, Brian (2002). "How do we Measure the Environment? Linking Intertidal Thermal Physiology and Ecology Through Biophysics". In: *Integrative and Comparative Biology* 42.4, pp. 837–845. DOI: 10.1093/icb/42.4.837. eprint: http://icb.oxfordjournals.org/content/42/4/837.full.pdf+html. URL: http://icb.oxfordjournals.org/content/42/4/837.abstract.

Helmuth, Brian S. T. and Gretchen E. Hofmann (2001). "Microhabitats, Thermal Heterogeneity, and Patterns of Physiological Stress in the Rocky Intertidal Zone". In: *The Biological Bulletin* 201.3, pp. 374–384. eprint: http://www.biolbull.org/content/201/3/374.full.pdf+html. URL: http://www.biolbull.org/content/201/3/374.abstract.

Holt, Robert and Michael Gaines (1992). "Analysis of adaptation in heterogeneous landscapes: Implications for the evolution of fundamental niches". In: *Evolutionary Ecology* 6 (5). 10.1007/BF02270702, pp. 433–447. ISSN: 0269-7653. URL: http://dx.doi.org/10.1007/BF02270702.

Holt, Robert D (2003). "On the evolutionary ecology of species' ranges". In: *Evolutionary Ecology Research* 5.2, pp. 159–178.

Holt, Robert D and Timothy H Keitt (2005). "Species borders: a unifying theme in ecology". In: *Oikos* 108.1, pp. 3–6.

Huntley, B., P. J. Bartlein, and I. C. Prentice (1989). "Climatic Control of the Distribution and Abundance of Beech (Fagus L.) in Europe and North America". English. In: *Journal of Biogeography* 16.6, pp. 551–560. ISSN: 03050270. URL: http://www.jstor.org/stable/2845210.

Huntley, Brian et al. (1995). "Special Paper: Modelling Present and Potential Future Ranges of Some European Higher Plants Using Climate Response Surfaces". English. In: *Journal of Biogeography* 22.6, pp. 967–1001. ISSN: 03050270. URL: http://www.jstor.org/stable/2845830.

IPCC (2007). *Fourth Assessment Report: Climate Change 2007: The AR4 Synthesis Report*. Geneva: IPCC. URL: http://www.ipcc.ch/ipccreports/ar4-wg1.htm.

Jackson, AC and J McIlvenny (2011). "Coastal squeeze on rocky shores in northern Scotland and some possible ecological impacts". In: *Journal of Experimental Marine Biology and Ecology* 400.1, pp. 314–321.

Johnson, Markes E (1988). "Why are ancient rocky shores so uncommon?" In: *The Journal of Geology*, pp. 469–480.

Kirkpatrick, Mark and N.H. Barton (1997). "Evolution of a Species' Range". English. In: *The American Naturalist* 150.1, pp. 1–23. ISSN: 00030147. URL: http://www.jstor.org/stable/10.1086/286054.

Logan, Cheryl A, Laurie E Kost, and George N Somero (2012). "Latitudinal differences in Mytilus californianus thermal physiology". In: *Marine Ecology Progress Series* 450, pp. 93–105.

Long, AJ and I Shennan (1994). "Sea-level changes in Washington and Oregon and the" earthquake deformation cycle"". In: *Journal of Coastal Research*, pp. 825–838.

Martens, P et al. (1999). "Climate change and future populations at risk of malaria". In: *Global Environmental Change* 9, S89–S107.

Mayr, E. (1954). "Evolution as a process". In: ed. by J Huxley, A Hardy, and E Ford. Allen & Unwin. Chap. Change of genetic environmentand evolution, pp. 157–180.

Mazzotti, Stephane, Casey Jones, and Richard E Thomson (2008). "Relative and absolute sea level rise in western Canada and northwestern United States from a combined tide gauge-GPS analysis". In: *Journal of Geophysical Research: Oceans (1978–2012)* 113.C11.

Mbogga, Michael S., Xianli Wang, and Andreas Hamann (2010). "Bioclimate envelope model predictions for natural resource management: dealing with uncertainty". In: *Journal of Applied Ecology* 47.4, pp. 731–740. ISSN: 1365-2664. DOI: 10.1111/j.1365-2664.2010.01830.x. URL: http://dx.doi.org/10.1111/j.1365-2664.2010.01830.x.

McCook, LJ and ARO Chapman (1997). "Patterns and variations in natural succession following massive ice-scour of a rocky intertidal seashore". In: *Journal of Experimental Marine Biology and Ecology* 214.1, pp. 121–147.

Menge, Bruce A (2000). "Top-down and bottom-up community regulation in marine rocky intertidal habitats". In: *Journal of Experimental Marine Biology and Ecology* 250.1, pp. 257–289.

Morris, R.H., D.P. Abbott, and E.C. Haderlie (1980). *Intertidal Invertebrates of California*. Stanford University Press. ISBN: 9780804710459. URL: http://books.google.com/books?id=NAybxQZvWI0C.

Nakaoka, Masahiro (1995). "Size-dependent reproductive traits of Yoldia notabilis (Bivalvia: Protobranchia)". In: *Oceanographic Literature Review* 42.5.

Nicholls, Robert J and Anny Cazenave (2010). "Sea-level rise and its impact on coastal zones". In: *science* 328.5985, pp. 1517–1520.

Nicholls, Robert J et al. (2011). "Sea-level rise and its possible impacts given a beyond 4 C worldin the twenty-first century". In: *Philosophical Transactions of the Royal Society A: Mathematical, Physical and Engineering Sciences* 369.1934, pp. 161–181.

NRC (2012). *Sea-Level Rise for the Coasts of California, Oregon, and Washington: Past, Present, and Future*. Tech. rep. Committee on Sea Level Rise in California, Oregon, et al.

Paine, R. T. (Aug. 1976). "Size-Limited Predation: An Observational and Experimental Approach with the Mytilus-Pisaster Interaction". In: *Ecology* 57.5, pp. 858–873. ISSN: 0012-9658. URL: http://dx.doi.org/10.2307/1941053.

Paine, Robert T. (1966). "Food Web Compexity and Species Diversity". In: *The American Naturalist* 100, pp. 65–75.

Paine, Robert T and Simon A Levin (1981). "Intertidal landscapes: disturbance and the dynamics of pattern". In: *Ecological monographs* 51.2, pp. 145–178.

Paine, R.T. (1974). "Intertidal community structure - Experimental studies on the relationship between a dominant competitor and its principal predator". In: *Oecologia* 15.2. cited By (since 1996) 418, pp. 93–120. URL: http://www.scopus.com/inward/record.url?eid=2-s2.0-34250426091&partnerID=40&md5=43e255188ec4c3b6409d83daa75ec349.

Parmesan, Camille (Nov. 2006). "Ecological and Evolutionary Responses to Recent Climate Change". In: *Annu. Rev. Ecol. Evol. Syst.* 37.1, pp. 637–669. ISSN: 1543-592X. URL: http://dx.doi.org/10.1146/annurev.ecolsys.37.091305.110100.

Parmesan, Camille and Gary Yohe (Jan. 2003). "A globally coherent fingerprint of climate change impacts across natural systems". In: *Nature* 421.6918, pp. 37–42. ISSN: 0028-0836. URL: http://dx.doi.org/10.1038/nature01286.

Parmesan, Camille et al. (2005). "Empirical perspectives on species borders: from traditional biogeography to global change". In: *Oikos* 108.1, pp. 58–75.

Pearson, Richard G. and Terence P. Dawson (2003). "Predicting the impacts of climate change on the distribution of species: are bioclimate envelope models useful?" In: *Global Ecology and Biogeography* 12.5, pp. 361–371. ISSN: 1466-8238. DOI: 10.1046/j.1466-822X.2003.00042.x. URL: http://dx.doi.org/10.1046/j.1466-822X.2003.00042.x.

Peterson, Curt D et al. (2012). "Coseismic subsidence and paleotsunami run-up records from latest Holocene deposits in the Waatch Valley, Neah Bay, Northwest Washington, USA: links to great earthquakes in the northern Cascadia margin". In: *Journal of Coastal Research* 29.1, pp. 157–172.

Petraitis, Peter S (1995). "The role of growth in maintaining spatial dominance by mussels (Mytilus edulis)". In: *Ecology*, pp. 1337–1346.

Pfister, Catherine A. (July 2007). "Intertidal Invertebrates Locally Enhance Primary Production". In: *Ecology* 88.7, pp. 1647–1653. ISSN: 0012-9658. URL: http://dx.doi.org/10.1890/06-1913.1.

Pfister, Catherine A, Jack A Gilbert, and Sean M Gibbons (2014). "The role of macrobiota in structuring microbial communities along rocky shores". In: *PeerJ* 2, e631.

Price, Trevor D and Mark Kirkpatrick (2009). "Evolutionarily stable range limits set by interspecific competition". In: *Proceedings of the Royal Society B: Biological Sciences*, rspb–2008.

Pyenson, Nicholas D and David R Lindberg (2011). "What happened to gray whales during the Pleistocene? The ecological impact of sea-level change on benthic feeding areas in the North Pacific Ocean". In: *PloS one* 6.7, e21295.

Rahmstorf, Stefan et al. (2007). "Recent climate observations compared to projections". In: *Science* 316.5825, pp. 709–709.

Rao, Kandula Pampapathi (1954). "Tidal Rhythmicity of Rate of Water Propulsion in Mytilus, and Its Modifiability by Transplantation". English. In: *Biological Bulletin* 106.3, pp. 353–359. ISSN: 00063185. URL: http://www.jstor.org/stable/1538769.

Roberts, D. A., G. E. Hofmann, and G. N. Somero (1997). "Heat-Shock Protein Expression in Mytilus californianus: Acclimatization (Seasonal and Tidal-Height Comparisons) and Acclimation Effects". In: *The Biological Bulletin* 192.2, pp. 309–320. eprint: http://www.biolbull.org/content/192/2/309.full.pdf+html. URL: http://www.biolbull.org/content/192/2/309.abstract.

Robles, C, D Sweetnam, and J Eminike (1990). "Lobster predation on mussels: shore-level differences in prey vulnerability and predator preference". In: *Ecology*, pp. 1564–1577.

Robles, Carlos (1987). "Predator foraging characteristics and prey population structure on a sheltered shore". In: *Ecology*, pp. 1502–1514.

Robles, Carlos and Robert Desharnais (2002). "History and current development of a paradigm of predation in rocky intertidal communities". In: *Ecology* 83.6, pp. 1521–1536.

Roy, Kaustuv et al. (2009). "A macroevolutionary perspective on species range limits". In: *Proceedings of the Royal Society B: Biological Sciences* 276.1661, pp. 1485–1493.

Sagarin, Raphael D et al. (1999). "Climate-related change in an intertidal community over short and long time scales". In: *Ecological monographs* 69.4, pp. 465–490.

Sanford, Eric and David J. Worth (Nov. 2009). "Genetic differences among populations of a marine snail drive geographic variation in predation". In: *Ecology* 90.11, pp. 3108–3118. ISSN: 0012-9658. URL: http://dx.doi.org/10.1890/08-2055.1.

Sanford, Eric et al. (2003). "Local selection and latitudinal variation in a marine predator-prey interaction". In: *Science* 300.5622, pp. 1135–1137.

Sanford, Eric et al. (Nov. 2006). "Larval Tolerance, Gene Flow, and The Northern Geographic Range Limit of Fiddler Crabs". In: *Ecology* 87.11, pp. 2882–2894. ISSN: 0012-9658. URL: http://dx.doi.org/10.1890/0012-9658(2006)87[2882:LTGFAT]2.0.CO;2.

Schaeffer, Michiel et al. (2012). "Long-term sea-level rise implied by 1.5 [thinsp][deg] C and 2 [thinsp][deg] C warming levels". In: *Nature Climate Change* 2.12, pp. 867–870.

Singh, Gerald G. et al. (May 2013). "Sea Otters Homogenize Mussel Beds and Reduce Habitat Provisioning in a Rocky Intertidal Ecosystem". In: *PLoS ONE* 8.5, e65435–. URL: http://dx.doi.org/10.1371%2Fjournal.pone.0065435.

Somero, George N. (2002). "Thermal Physiology and Vertical Zonation of Intertidal Animals: Optima, Limits, and Costs of Living". In: *Integrative and Comparative Biology* 42.4, pp. 780–789. DOI: 10.1093/icb/42.4.780. eprint: http://icb.oxfordjournals.org/content/42/4/780.full.pdf+html. URL: http://icb.oxfordjournals.org/content/42/4/780.abstract.

Soot-Ryen, T. (1955). *A report on the family Mytillidae (Pelecypoda)*. Tech. rep. 20. Hancock Pacific Expedition.

Sotka, Erik E. et al. (2004). "Strong genetic clines and geographical variation in gene flow in the rocky intertidal barnacle Balanus glandula". In: *Molecular Ecology* 13.8, pp. 2143–2156. ISSN: 1365-294X. DOI: 10.1111/j.1365-294X.2004.02225.x. URL: http://dx.doi.org/10.1111/j.1365-294X.2004.02225.x.

Stephenson, WJ (2000). "Shore platforms: a neglected coastal feature?" In: *Progress in Physical Geography* 24.3, pp. 311–327.

Stephenson, WJ et al. (2010). "Decadal scale micro erosion rates on shore platforms". In: *Geomorphology* 114.1, pp. 22–29.

Strathmann, M.F. (1987). *Reproduction and Development of Marine Invertebrates of the Northern Pacific Coast: Data and Methods for the Study of Eggs, Embryos, and Larvae*. University of Washington Press. ISBN: 9780295965239. URL: http://books.google.com/books?id=Hw9-QgAACAAJ.

Suchanek Thomas, H. (1979). "The Mytilus californianus community: Studies on the composition, structure, organization, and dynamicsof a mussel bed". PhD thesis. University of Washington.

Suchanek, ThomasH. (1981). "The role of disturbance in the evolution of life history strategies in the intertidal mussels Mytilus edulis and Mytilus californianus". In: 50.2, pp. 143–152. ISSN: 0029-8549. URL: http://dx.doi.org/10.1007/BF00348028.

Trenhaile, Alan S (2001). "Modeling the effect of weathering on the evolution and morphology of shore platforms". In: *Journal of Coastal Research*, pp. 398–406.

Trenhaile, AS (1980). "Shore platforms: a neglected coastal feature". In: *Progress in physical geography* 4.1, pp. 1–23.

U.S. Climate Change Science Program; National Research Council, Committee on Strategic Advice on the (2009). *Restructuring Federal Climate Research to Meet the Challenges of Climate Change*. The National Academies Press. ISBN: 9780309131735. URL: http://www.nap.edu/openbook.php?record_id=12595.

Vaselli, Stefano et al. (2008). "Assessing the consequences of sea level rise: effects of changes in the slope of the substratum on sessile assemblages of rocky seashores". In: *Marine Ecology Progress Series* 368.1, pp. 9–22.

Vermeer, Martin and Stefan Rahmstorf (2009). "Global sea level linked to global temperature". In: *Proceedings of the National Academy of Sciences* 106.51, pp. 21527–21532.

Walther, Gian-Reto et al. (Mar. 2002). "Ecological responses to recent climate change". In: *Nature* 416.6879, pp. 389–395. ISSN: 0028-0836. URL: http://dx.doi.org/10.1038/416389a.

Wethey, David S (1983). "Geographic limits and local zonation: the barnacles Semibalanus (Balanus) and Chthamalus in New England". In: *The Biological Bulletin* 165.1, pp. 330–341.

Wootton, J T (2001). "Prediction in complex communities: analysis of empirically derived Markov models". In: *Ecology* 82.2, pp. 580–598.

Wootton, J Timothy (1993). "Indirect effects and habitat use in an intertidal community: interaction chains and interaction modifications". In: *American Naturalist*, pp. 71–89.

Wootton, J. Timothy (Jan. 1994). "Predicting Direct and Indirect Effects: An Integrated Approach Using Experiments and Path Analysis". In: *Ecology* 75.1, pp. 151–165. ISSN: 0012-9658. URL: http://dx.doi.org/10.2307/1939391.

Wootton, J Timothy (2010). "Experimental species removal alters ecological dynamics in a natural ecosystem". In: *Ecology* 91.1, pp. 42–48.

Wootton, J Timothy and James D Forester (2013). "Complex Population Dynamics in Mussels Arising from Density-Linked Stochasticity". In: *PloS one* 8.9, e75700.

Young, RT (1941). "The distribution of the mussel (Mytilus californianus) in relation to the salinity of its environment". In: *Ecology* 22.4, pp. 379–386.